TECHNICAL REPORT WC/96/37
Overseas Geology Series

Assessment of contamination by metals and selected organic compounds in coastal sediments and waters of Mombasa, Kenya.

T M Williams[1], J Rees[1], K K Kairu[2] & A C Yobe[2]
1: British Geological Survey, Keyworth, Nottingham, UK.
2: Kenya Marine and Fisheries Research Institute, Mombasa, Kenya.

Natural Environment Research Council

International Division
British Geological Survey
Keyworth
Nottingham
United Kingdom NG12 5GG

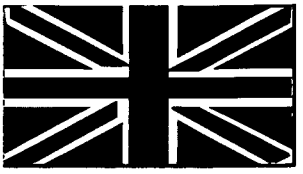

ODA

BRITISH GEOLOGICAL SURVEY

TECHNICAL REPORT WC/96/37
Overseas Geology Series

Assessment of contamination by metals and selected organic compounds in coastal sediments and waters of Mombasa, Kenya.

T M Williams[1], J Rees[1], K K Kairu[2] & A C Yobe[2]
1: British Geological Survey, Keyworth, Nottingham, UK.
2: Kenya Marine and Fisheries Research Institute, Mombasa, Kenya

A report prepared for the Overseas Development Administration, Natural Resources Division, Environment Research Programme (ERP) under ODA-BGS contract R6191: Land-Ocean Contamination Study (LOCS).

ODA classification
Subsector: Environment Research Programme
Project title: Land-Ocean Contamination Study (LOCS).
Project Reference: R6191.

Bibliographic reference: T M Williams, J Rees, K K Kairu & A C Yobe: 1996. Assessment of contamination by metals and selected organic compounds in coastal sediments and waters of Mombasa, Kenya.

Key words: Pollution, metals, hydrocarbons, organochlorines, sediments, water, suspended particulates.

Cover illustration: Aerial view of Mombasa north coast between Nyali and Mtwapa.

CONTENTS

SUMMARY

In 1995 a coastal-zone pollution monitoring programme for developing countries, the Land-Ocean Contamination Study (LOCS), was initiated by the British Geological Survey (BGS) under funding from the UK Overseas Development Administration (ODA) Natural Resources Division (NRD). The central objectives of LOCS are (i) the provision of data regarding the sources, transport pathways and fates of contaminant metals and selected organic compounds along urbanised coastal margins, and (ii) promotion of the use of such data in integrated coastal-zone management (CZM).

A systematic geochemical and hydrochemical survey of the inshore waters of Mombasa, Kenya was carried out under the ODA-LOCS programme in liaison with the Kenya Marine and Fisheries Research Institute (KMFRI) during the period September 1995 to February 1996. The survey included an assessment of heavy metal, alkane, polycyclic aromatic hydrocarbon (PAH) and organochlorine concentrations in water, suspended particulate matter (SPM) and sediment at 48 localities within the inshore lagoonal waters, and the reef-fronted coastline extending to Mtwapa Creek some 13 km to the north. Oceanographic and sedimentological data of relevance to the interpretation of contaminant distributions and transport pathways were also collected and form the subject of an independent report (Rees et al., 1996).

The fundamental hydrochemical properties (e.g. pH, salinity, dissolved oxygen) of individual creek and back-reef water bodies are readily differentiable, reflecting variations of residence-time, evaporative influence and freshwater influx. All are characterised by concentrations of Cu, Cd and Cr within the global background range for marine waters. The concentration of Pb is, however, systematically elevated. Anomalous concentrations of Zn and Cd prevail along the reef-front between Nyali and Mtwapa, although precise source has not been ascertained.

Concentrations of several potentially toxic trace elements (e.g. Cr, As, Ni, Cu & V) are enriched in suspended particulate matter (SPM) in Tudor Creek, relative to SPM in other inshore and reef-front waters. A spatial correlation between these metals and Mn is evident. Such trends are inconsistent with an anthropogenic control, and are almost certainly attributable to the dominance of mangrove-derived particulate matter in the overall SPM assemblage in Tudor Creek.

Several heavy metals attain high concentrations in surficial sediments around Mombasa. With the exception of Pb, Zn and Cu, the signatures are almost entirely related to lithology. Localised enrichment of Pb, Zn and Cu is evident in close proximity to several known point-sources including sewage outfalls to the east of Mombasa Island, Likoni and Kilindini docks. Temporal flux variations, typically involving increased trace metal deposition towards the sediment-water interface, are apparent from downcore concentration profiles through the sediments of Makupa Creek, Port Kilindini and Tudor Creek. Following normalisation against Al_2O_3 or TiO_2, however, no clear anthropogenic control can be identified.

Sedimentary partitioning data for sediments from Makupa Creek indicate that labile geochemical fractions (e.g. reducible oxides) are significant as carriers of Mn, Pb, Cu and Co. Detrital silicates and sulphides form the principal carriers of Fe, Al, V, Co, Cr and Ni. The available partitioning data and complementary data for intersitial pore-waters suggest that the post-depositional alteration of labile phases predominantly results in the immobilisation of metals as sulphides. Under such circumstances, the sediment reservoir can be considered to constitute a relatively long-term contaminant sink.

The concentrations of n-alkanes, PAHs and organochlorines recorded in Mombasa sediments are very low (often falling below analytical detection limits). Alkanes and PAHs frequently remain as residues at sites of crude oil spillage. Their low concentrations in the sediments of Port Reitz and Makupa Creek, both known to have been impacted by spills during the last decade, signify high rates of biodegradation facilitated by conducive climatic and biochemical factors.

The geochemical, oceanographic and sedimentological data collated under the LOCS programme for Mombasa provide a valuable baseline against which to evaluate the effects of future urban and industrial development. In an attempt to maximise the utility of the survey outputs in practical CZM and planning, a GIS has been developed allowing interrogation of pollution data in conjunction with pre-existing information concerning land- and marine resource use.

1: INTRODUCTION

Estuarine and coastal sites form important focal points for urban and industrial development worldwide, offering favourable conditions for trade and transportation, marine fisheries exploitation and domestic or industrial effluent disposal. Such diverse activities are, however, often poorly compatible and problems of coastal-zone pollution are becoming increasingly prevalent, with potentially severe environmental and socio-economic implications. The consequences of nearshore contamination are particularly acute in the many developing countries of Africa, Asia, the Caribbean and Latin America which are reliant on the coastal zone for the provision of domestic food supplies, or for foreign exchange generation through fisheries exports and tourism. With continued urban and industrial growth along the seaboards of such countries, the implementation of strategies to assess the sources, fates and impacts of land-derived contaminants (at both national and trans-boundary scales) may be vital to underpin sustainable long-term development.

In 1995, the British Geological Survey (BGS) initiated a coastal-zone pollution monitoring programme for developing countries, the Land-Ocean Contamination Study (LOCS), under funding from the UK Overseas Development Administration (ODA), Natural Resources Division (NRD). The central objective of LOCS is the provision of contaminant monitoring, impact amelioration and integrated coastal-zone management protocols to meet the specific social, technical and economic requirements of the targeted study regions. The LOCS project structure comprises three discrete phases of field activity, the first focusing on the reef fringed coastal margins of East Africa, the second on the more heavily industrialised setting of Jakarta Bay, Indonesia, and the third on lagoonal coasts of Latin America. This report outlines the methodology, preliminary results and implications of a geochemical survey of waters around Mombasa, Kenya, executed by BGS in liaison with the Kenya Marine and Fisheries Research Institute (KMFRI) during the period September 1995 - January 1996 as a component of Phase One of the project.

2: REGIONAL SETTING

2.1: Physiography and climate

The administrative district of Mombasa occupies an area of approximately 275 km^2 on the Indian Ocean coast of Kenya, centred on latitude 4.05°S and longditude 39.65°E (Fig. 1). The district comprises the island settlement of Mombasa (now connected to the mainland by the c. 1 km Makupa causeway) and a series of mainly urban or industrial settlements to the north-east, west and south-west, the combined population of which exceeds 500,000. To the south-west and west of Mombasa Island, the Port Kilindini and Port Reitz creek complexes extend inland

for some 15 km. To the north-east and north, the island is bounded by Mombasa Harbour and the Tudor Creek complex. Fluvial inputs to these systems are provided by the Mwache, Shimba, Kombeni and Tsalu rivers, the annual discharges from which range between 10 - 50 x 10^6 m^3. The open coastline north and south of Mombasa is fringed by a multiple reef (typically 1-1.5 km offshore) which extends virtually unbroken for a distance of 60 km between Mtwapa and Gazi.

Figure 1: Physiography of Mombasa, showing principal rivers and inshore water bodies.

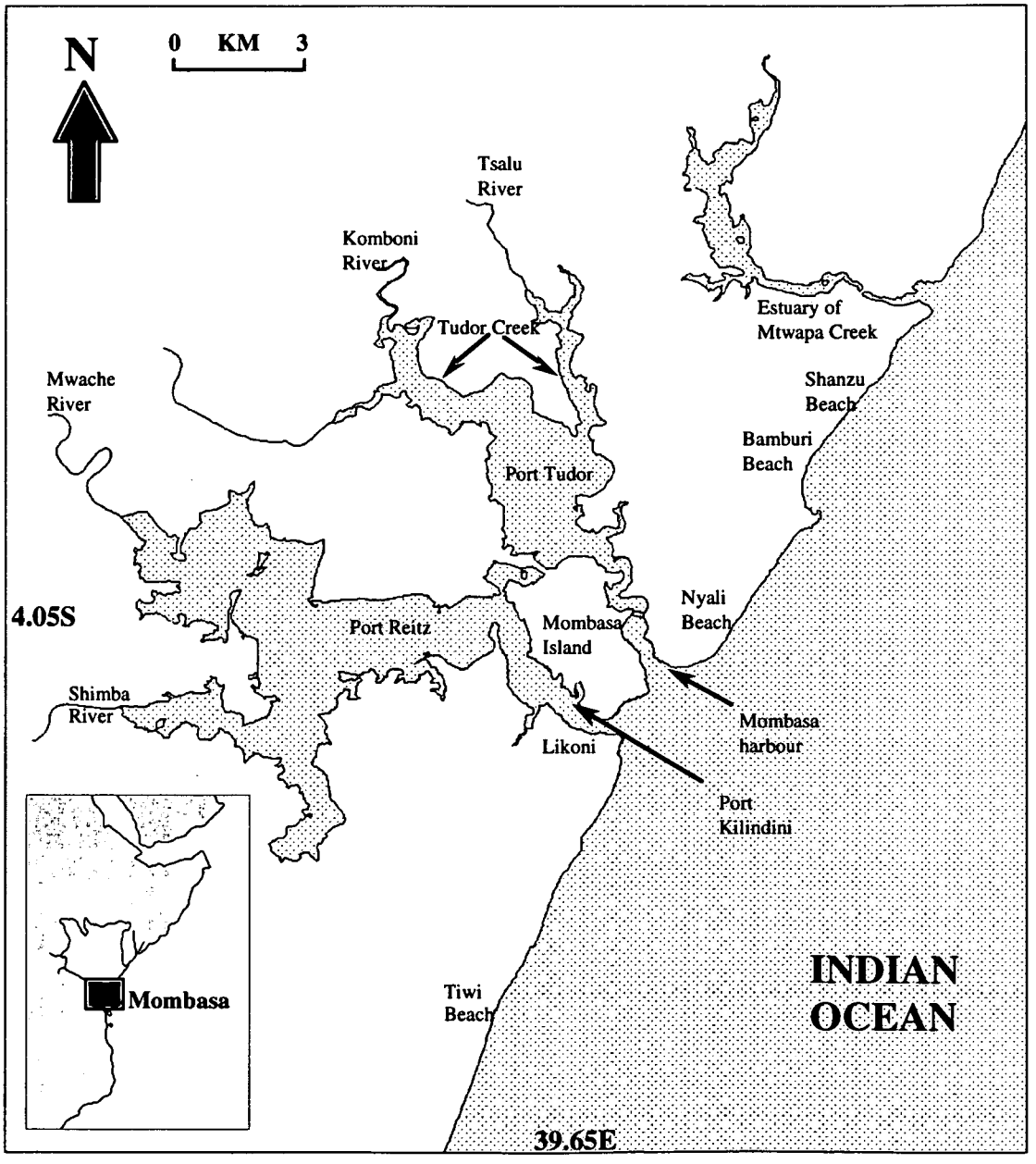

The rainfall regime of the Kenya coast is influenced by two seasonal wind regimes, the South-East Monsoon from April-October and the North-East Monsoon from November-March (Fig. 2). An average annual precipitation of 1100 mm is substantially concentrated into two periods referred to as the 'short' (October-November) and 'long' (March-May) rains. Average daily temperatures range from 23°C in June-July to 31°C in December-January, with a mean relative humidity of 67%.

Figure 2: Seasonal wind roses showing monsoon orientations in the vicinity of Mombasa (from Norconsult, 1975). Wind speeds are expressed in m/s. The mean (green) and peak (red) velocities are shown for the dominant wind direction in each monsoon season.

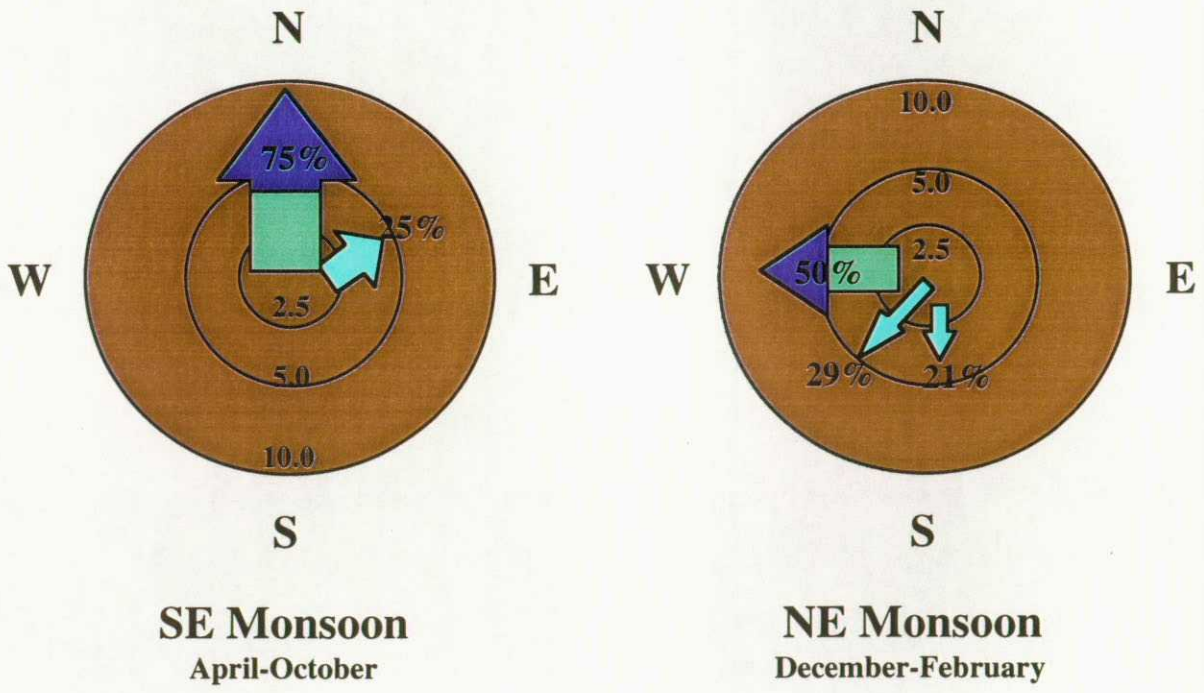

2.2: Geology

The hinterland to the west of Mombasa is formed of sedimentary lithologies of Upper Palaeozoic to Cenozoic age, striking parallel to the coast (SW-NE) and younging eastwards (Figure 3). The upper sectors of the catchments that drain into the inshore waters of Mombasa are hosted by the Taru, Maji ya Chumvi, Mariakani and Mazeras formations of the Karoo system (Upper Carboniferous to Lower Jurassic). This lies unconformably on the Archean

Figure 3: Simplified geology of the Mombasa area.

(Post-Karoo sediments include the Kambe and Mtomkuu formations. Karoo sediments include all other units overlying the basement).

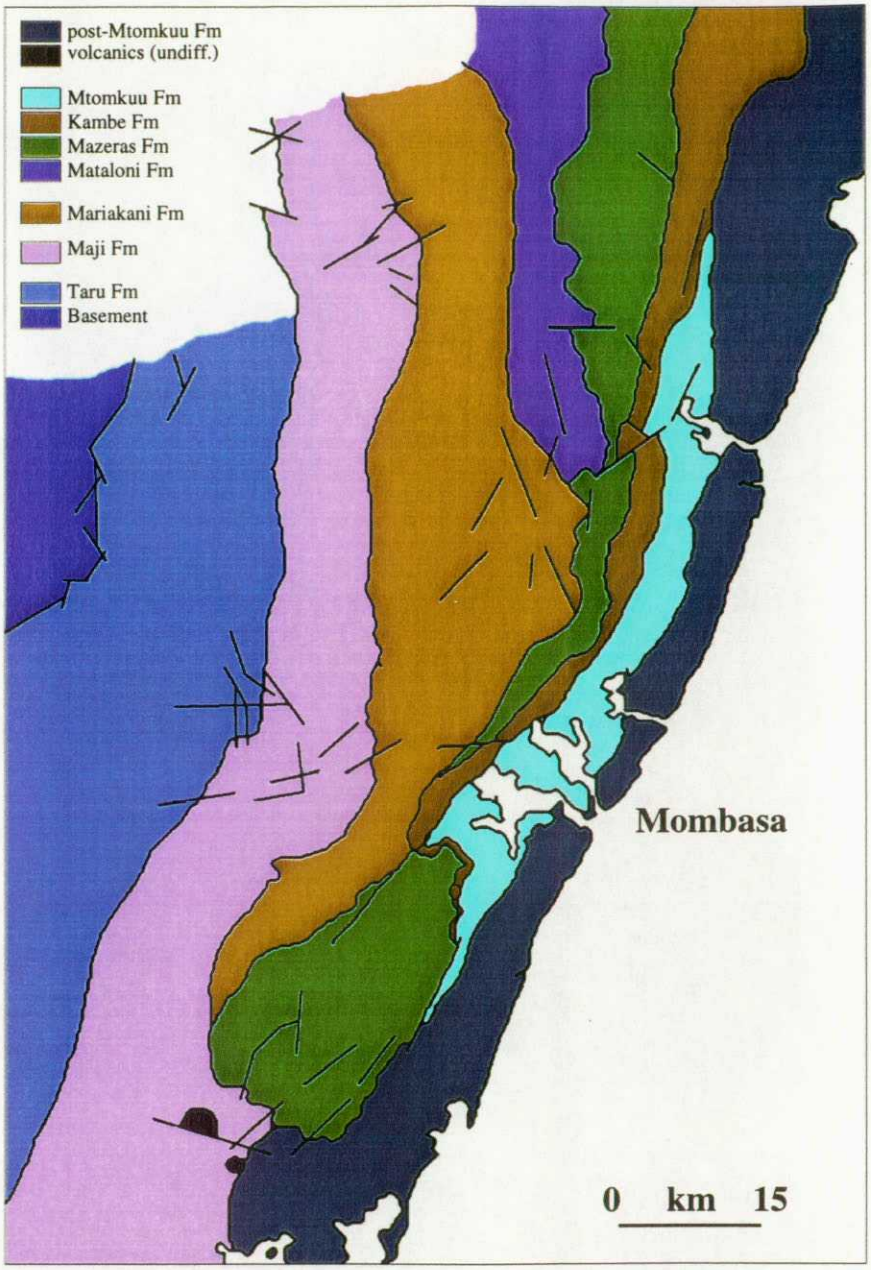

basement. The formations comprise sandstones, sandy shales and conglomerates deposited in fluviatile, lacustrine, deltaic and aeolian environments.

The tidal reaches of the Port Reitz and Port Tudor creek systems are predominantly confined within Upper Jurassic marine shales, sandstones and limestones of the Mtomkuu Formation (Rais-Assa 1988). Shales of this formation are widely exposed around the creek margins, and form shale-gravels where broken-up underwater. The underlying Middle to Upper Jurassic

marine shales, sandstones, limestones and conglomerates of the Kambe Formation (Rais-Assa 1988) are resistant to incision and form a broad ridge to the north-west of the creeks.

The position, orientation and morphology of the Port Tudor, Kilindini and Port Reitz creek complexes is largely controlled by the solid geology of the area. Both are hosted in depressions within Jurassic rocks on the landward-side of topographically proud Pleistocene reef limestones and back-reef deposits (Caswell, 1953, 1956; Carruthers 1985). The Pleistocene rocks are breached by the narrow channels of Mombasa Harbour and Port Kilindini, which link the inshore waters to the coast. Locally, the Pleistocene rocks unconformably overlie the Magarini Sands of Pliocene age. Outcrops of these friable orange-brown sands cap Jurassic outcrops north of Port Reitz (in the vicinity of Moi International Airport), and between the River Majera and the Pleistocene coastal sequence to the south of Port Reitz.

Late Pleistocene and Holocene reef flats dominate the intertidal and marginal supra-tidal zone along the open-coastlines north and south of Mombasa. Mangrove muds with intermittent peaty horizons occur widely in the upper tidal reaches of Tudor Creek, Port Kilindini and Port Reitz.

2.3: Physical oceanography

2.3.1: Bathymetry:

The physical oceanographic characteristics of the study area, including current orientation and residence-time models for the principal creek systems of Mombasa, have been outlined by Norconsult (1975) and Rees et al. (1996). Bathymetric data for the inland creek systems (Figure 4) show a prevalence of narrow scoured seaward entrances up to 50 m deep, with broad and shallow (2-5 m) upper reaches. Depth/area curves for Port Reitz (including Kilindini) and Port Tudor produced by Norconsult (1975) indicate that the surface areas of the two systems are 45 km^2 and 20 km^2 respectively, of which at least 50% is characterised by water depths of <10 m. Water volumes within the two systems have been estimated at 240 x 10^6 m^3 and 86 x 10^6 m^3 respectively (Norconsult, 1975). The bathymetric data for the nearshore waters indicate the presence of a virtually continuous shallow lagoon (<5 m) up to 2 km wide, underlain by Pleistocene reef flats and bounded on the seaward side by the present-day reef front. Offshore of the reef, water depths increase rapidly to >200 m.

2.3.2: Tides:

Mombasa tidal cycles are semi-diurnal with an average range of 2.3 m. Tidal ranges within the creek systems of Port Tudor and Kilindini have been reported to be closely analogous (Norconsult, 1975).

Figure 4: Bathymetry of inshore and nearshore waters in the vicinity of Mombasa.

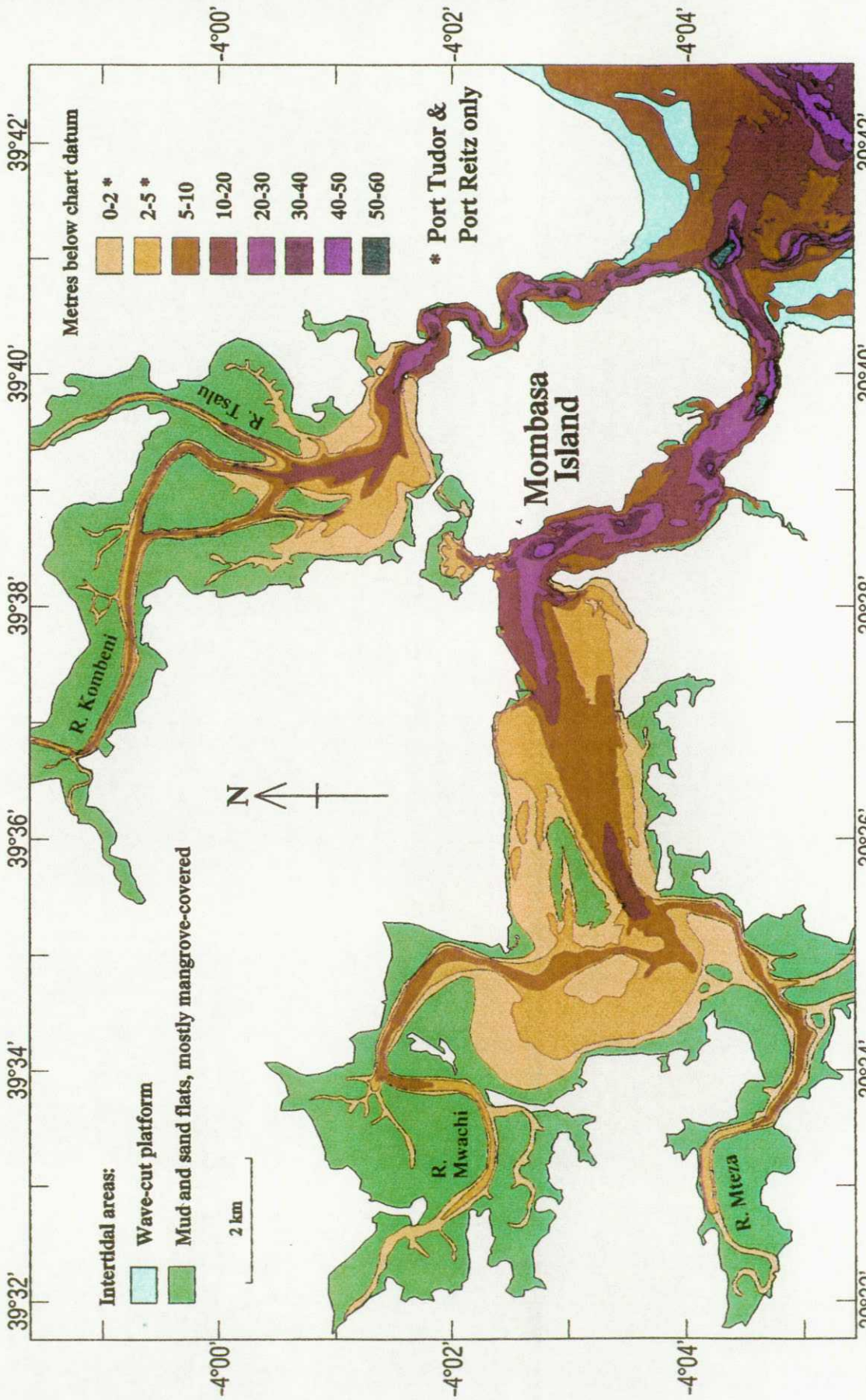

2.3.3: Ocean currents:

Surface ocean currents vary in accordance with the seasonal monsoons. In the eastern Indian Ocean, the NE Monsoon period (November - March) is characterised by two west-trending currents (focused on 2-8° N and 10-20°S), between which flows the easterly Equatorial Counter-Current. In the vicinity of Mombasa, water flowing to the Counter-Current runs northward along the coast (Fig. 5a) during this period, although southward flows prevail along the coast north of Malindi. With the onset of the SE Monsoon (May - September), the Equatorial Counter-Current disappears and all surface currents parallel to the Kenya coast trend northward (Fig. 5b).

Figure 5: Oceanic surface currents in the Indian Ocean a) November-March, b) May-September

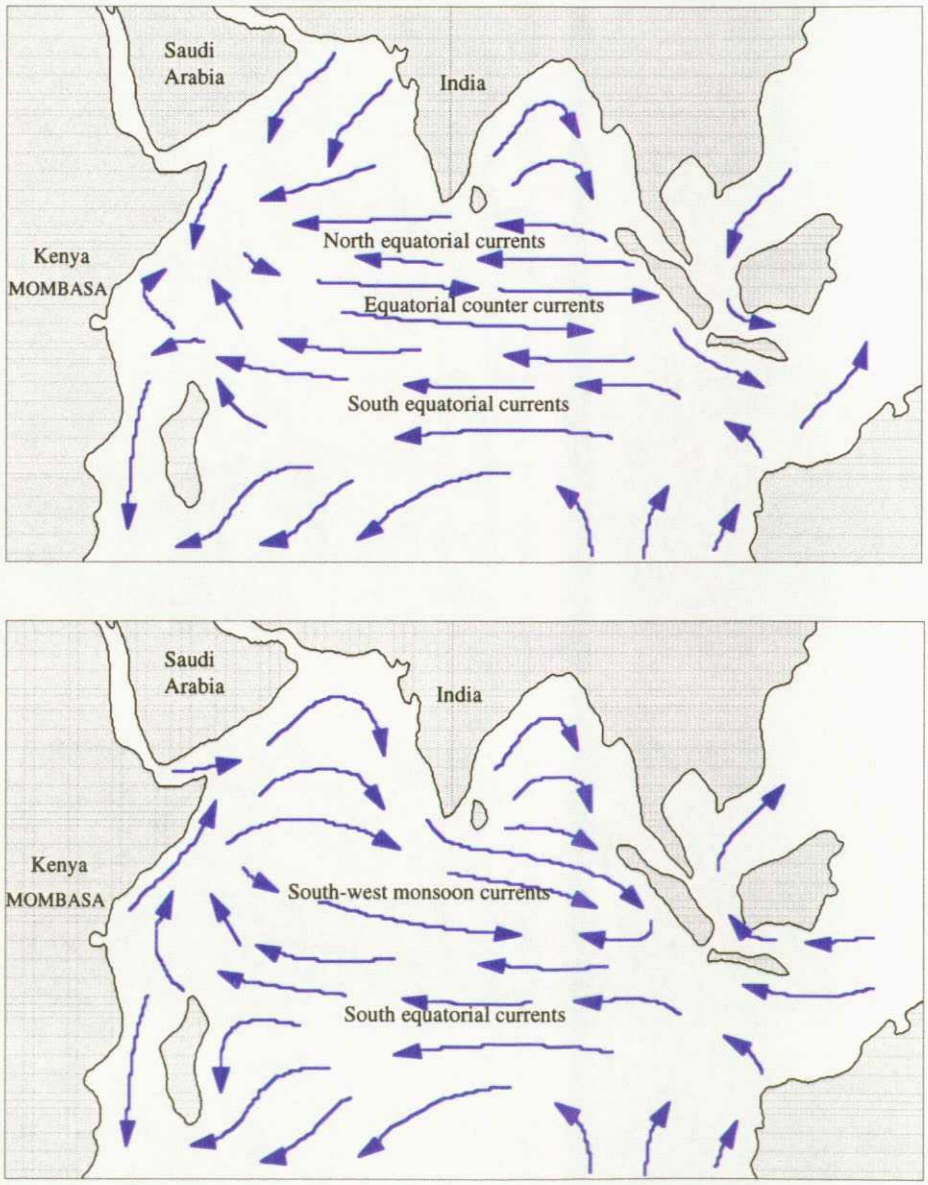

2.3.4: Nearshore currents:

Nearshore currents in the vicinity of Mombasa are largely accordant with ocean current movements, with minor modifications induced by local reef configurations, bed morphologies, winds and tides (Norconsult, 1975). Predominantly northerly nearshore currents with velocities of 0.3 - 0.5 m/s prevail throughout most of the NE Monsoon, although a southerly current develops during a 2-3 week period prior to the monsoon interchange in February or March. The northerly currents continue to prevail during the SE Monsoon, with velocities generally accelerated by south-easterly winds. Persistent modification of this northerly nearshore current trend has, however, been recorded at the entrances to Mombasa Harbour and the Kilindini/Port Reitz creek complex (Norconsult, 1975) due to the influence of tidal currents of 0.25-0.5 m/s running perpendicular to the open coastline (Fig. 6).

Figure 6: Current drogue study of Mombasa Harbour and Kilindini entrances: flood tide (blue) & ebb tide (red). All transport times are given in hours.

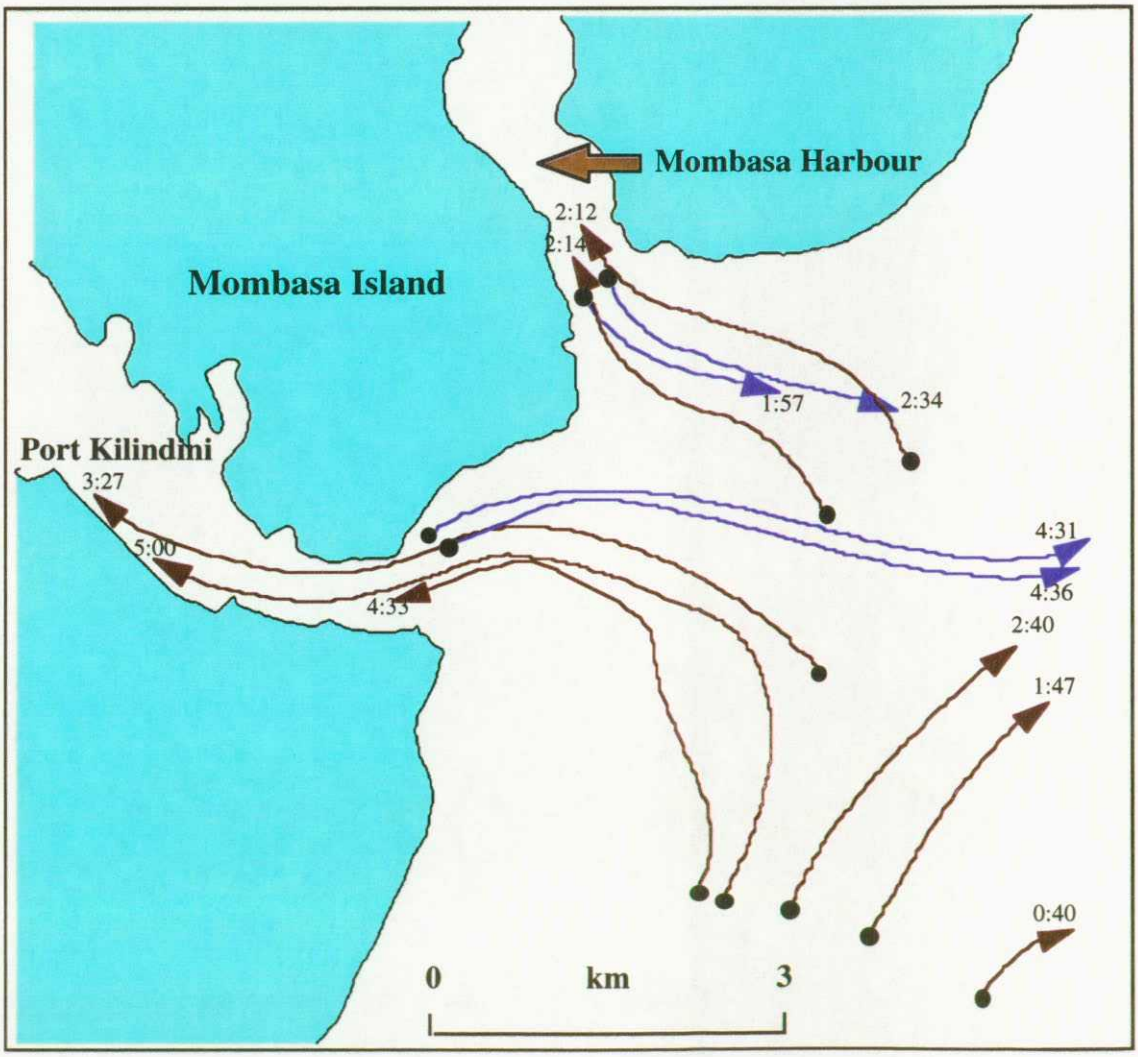

2.3.5: Back-reef lagoonal currents:

Tidal movements in the lagoonal systems constitute the principal determinant of current directions and velocities. High velocity currents are generated in the vicinity of reef channels during the initial stages of the flood tide (producing onshore currents) and the latter stages of the ebb tide (producing offshore currents). Longshore currents produced by wave action in the lagoons may attain velocities of 0.5 m/s (Norconsult, 1975).

2.3.6: Inshore tidal currents:

A large tidal prism accumulates in the shallow waters of the Port Tudor and Kilindini/Port Reitz creek systems during each flood tide, resulting in the generation of strong tidal currents in the seaward openings to these inshore waters. Data derived from drogue studies of Port Kilindini and Port Tudor (Norconsult, 1975) indicate typical current strengths of 0.3-0.6 m/s throughout the tidal cycle, except for periods of around 1 hr at maximum flood and maximum ebb, when velocities increase to around 1 m/s. Current velocities vary little with depth. Opposing flood and ebb tide current velocities are maximised along the eastern margin of Port Kilindini (adjacent to the loading berths), the northern shoreline of Port Reitz, and along a central scour channel in Port Tudor. The large tidal excursion inferred from the Norconsult (1975) drogue studies suggests an almost complete exchange of water in the major creeks with each tidal cycle. Substantially longer residence times may, however, prevail in the landward parts of certain systems. For example, hydrodynamic models for Tudor Creek (incorporating pressure, current, bathymetric and salinity data) have produced residence-time estimations of up to 14 days (Nguli, 1994; Odido, 1994).

2.4: Industrial activity

A synopsis of industrial activity within Mombasa District has been provided by Munga et al. (1994) in a document prepared for the WHO. Most industrial activities are concentrated within designated industrial areas on the western side of Mombasa Island and the northern margin of Port Reitz. A summary of industrial plant registered with the Kenya Mininstry of Industry is given in Table 1, and the locations of plant in each activity class are shown in Figure 7.

2.5: Marine contaminant sources and waste management.

The relatively large urban population of Mombasa, coupled with it's broad industrial base, maritime activity and increasingly intensive agricultural development of the Mwache and Kombeni catchments, provide a diversity of contaminant sources which may potentially affect the quality of inshore and nearshore waters. The municipal sewage treatment system serves approximately 17% of the population, with plant located on Mombasa Island at Kizingo and on the mainland near Kipevu oil terminal. These installations discharge treated residues into Tudor

Creek and lower Port Reitz respectively. Both plant are currently operating at low efficiency with the result that large volumes of raw sewage are discharged (Munga et al., 1994). The remaining 83% of the population utilise pit latrines or septic tank facilities for sewage disposal, with sludges dumped at Kibarani landfill (adjacent to Makupa Creek) or other unspecified areas of mangrove (Munga et al., 1994). Beach hotels along the coastal strips to the north and south of Mombasa (with a current capacity of approximately 10,000 beds) typically utilise septic tanks, with overflows discharging directly into the sea. Sewage constitutes the dominant source of N and P to the inshore waters of Mombasa, exceeding industrial emissions by at least a factor of three (Table 2).

Municipal refuse is currently dumped at Kibarani landfill. Leachate migration from the site is unconfined and discharges directly into Makupa Creek. There is no specified treatment procedure for waste from ships using Kenya Port Authority berths, although some solid (often toxic) waste products are reportedly discarded at Kibarani.

Data produced by Munga et al (1994) indicate that industrial wastes are the dominant contributor to BOD in the inshore waters of Mombasa (72% total, Table 2). Textiles and brewing activities exert a disproportionate influence. A major component of the total heavy metal load is derived from steel-rolling and galvanising activities (>3 t/yr), the non-ferrous metal industry (0.1 t/yr) and power generation (0.1 t/yr). Petroleum refining activities provide the principal source of phenols.

Table 1: Industrial activities in Mombasa District, classified according to Kenya Government Ministry of Industry criteria (from Munga et al., 1994).

INDUSTRY	PLANT NO.	ANN. INPUT	ANN PRODUCTION
Fish processing	2	-	1,694 ton
Slaughter house	1	28762 ton	-
Milk processing	1	-	67,251 ton
Vegetable/animal oil	9	-	48,064 ton
Grain mills	8	-	12,613,618 ton
Bakeries	8	-	50,004 ton
Soft drink manufact.	2	-	1,484 cu m
Brewing	1	-	45,041 cu m
Soap manufacture	2	-	1,250 ton
Textiles	22	-	50,000 ton
Plastics	8	-	150,000 ton
Oil refining	1	2,000,000 ton	-
Glass manufacture	2	-	5,000 ton
Ferrous metals	7	-	30,464 ton
Non ferrous metals	12	-	69,123 ton
Power generation	2	-	100.292 MW

Figure 7: Location of industrial plant (classified by activity) in Mombasa District (source - UNEP EAF6 Kenya Coast database).

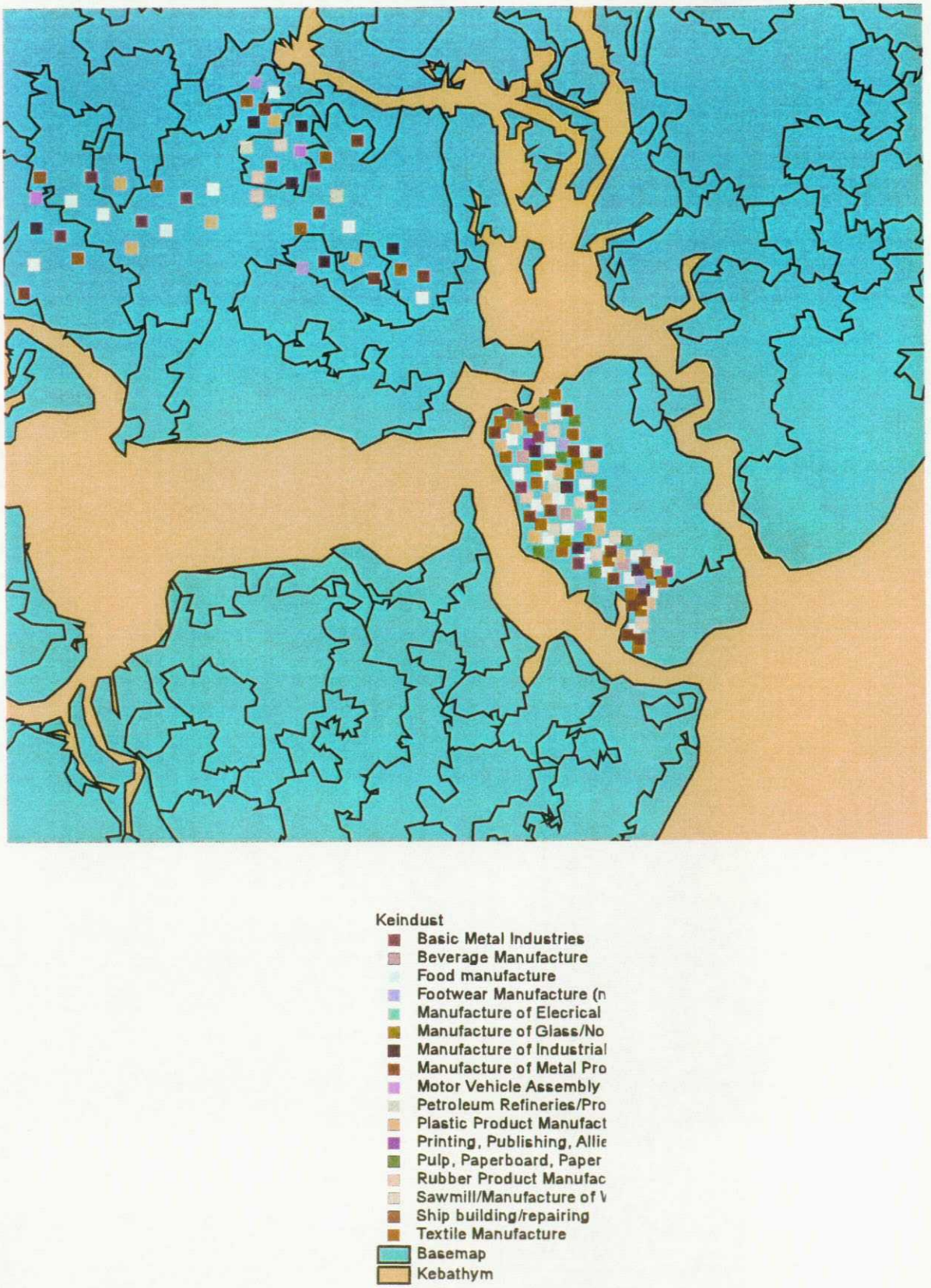

Agrochemicals are used widely in the Mwachi and Kombeni basins, providing a potentially significant flux of nutrients and toxic organic residues (and the dominant source of organochlorines) to the inshore waters. Data compiled by the District Agricultural Office in 1992 indicate that approximately 7000 kg of fertilizers, 300 kg of fungicides, 325 kg of insecticides and 250 kg of nematicides are used in the area annually.

Table 2: Summary of estimated pollution loads (tons/yr) to marine waters in Mombasa District, classified by generic source type (blanks indicate that inputs cannot be quantified on the basis of existing data).

Source	BOD	SS	Oil	N	P	Metals	Phenols
Domestic sewage	3909	3550	-	138	34	-	-
Beach hotels	143	126	-	26	3	-	-
Storm water runoff	679	9252	-	123	12	-	-
Solid waste (municipal)	1575	-	-	-	-	-	-
Industrial waste	16249	21837	103	45	6	Cr - 0.25, Cu - 0.001 Fe - 2.9 Ni - 0.005 Zn - 0.11	0.01
Ship waste (solid and liquid)	11	11	-	2	0	-	-
Livestock waste	73	493	-	75	56	-	-

3: BGS - KMFRI INVESTIGATION

3.1: Water quality assessment.

3.1.1: Sampling and analytical methods.:

Water quality assessments were undertaken at 35 stations within the inshore waters of Port Tudor, Port Kilindini and Port Reitz, and at 4 stations along the northern Mombasa coastline between Nyali and Mtwapa Creek (Fig 8). All stations were initially sampled during the period 8th-25th September 1995. Selected re-sampling of stations was carried out in January 1996 to provide an indication of temporal variability. Sampling of each individual creek was carried out under a range of flood- and ebb tide conditions. All systematic contrasts of hydrogeochemical signature noted between the respective water bodies are therefore considered to be largely independent of tidal condition.

At all stations, measurements were made of water temperature, dissolved oxygen (DO), O_2-saturation, pH, Eh, turbidity, conductivity and salinity using a pHOX™ model 902 sonde and

datalogger. Calibration of the component electrodes and sensors in the sonde was carried out using the following reagents:- (a) 2% sodium sulphite (zero DO), (b) buffer solutions of pH 4.0 and pH 10.0, (c) potassium ferro- and ferricyanide redox standards of 125 and 350 mV, (d) potassium chloride conductivity standards of 100, 1000 and 50000 µS, and (e) polymeric turbidity solutions of 1, 100 and 1000 FTU.

Water samples for chemical analysis were recovered from the mid-water column using a 2.5 l acrylic Kemmerer sampler, activated by a 250 g messenger (Fig. 9). Immediately following collection, each sample was decanted into an acid-washed PTFE reservoir, from which a volume of 0.5 l was pressure-filtered (at 20-40 psi) through a 0.45 µm x 50 mm diameter cellulose acetate membrane (Sartorius™) into an HNO_3-washed HDPE bottle (Nalgene™). Samples were acidified with 1% v/v HNO_3 (ARISTAR) within 8 hours of collection. Analyses for a suite of 6 heavy metals (Pb, Zn, Cu, Cd, Cr & Ni) were carried out by anodic stripping voltammetry (ASV) at the UK Environment Agency (formerly NRA) laboratories, Llanelli, Wales. The practical analytical detection limits for the six analysed elements in seawater by this method are 0.024 µg/l Pb, 0.042 µg/l Cd, 0.05 µg/l Cu, 0.1 µg/l Zn, 0.35 µg/l Cr and 0.058 µg/l Ni.

Figure 8: Mombasa stations selected for sampling of water, suspended particulate matter and sediment under the LOCS programme.

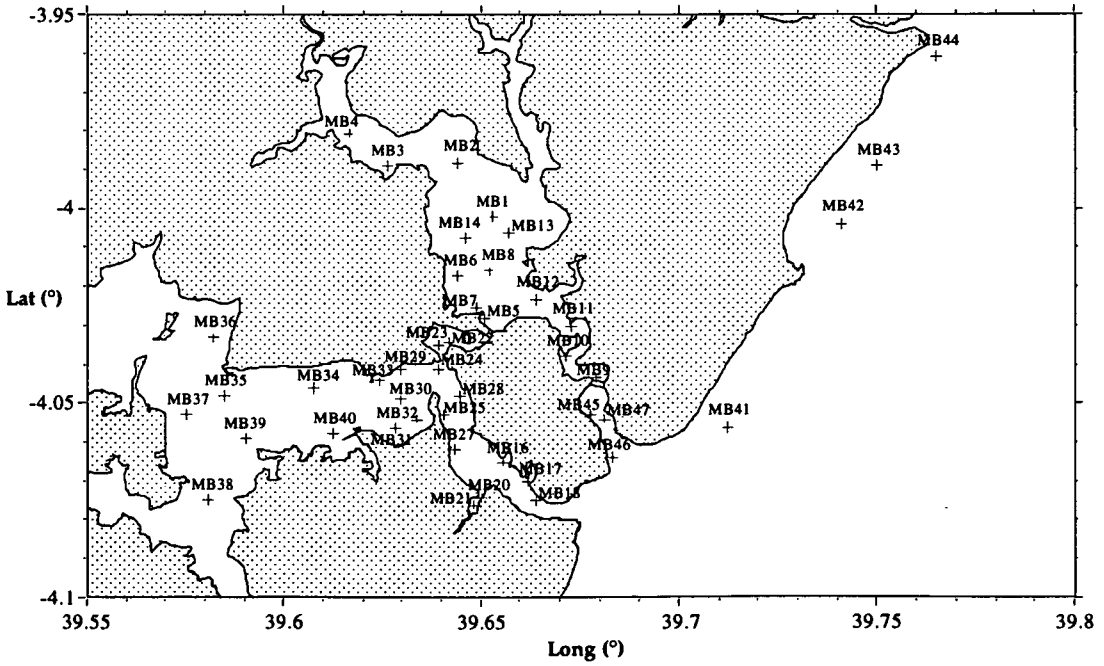

3.1.2: Results:

3.1.2.1: Physico-chemical parameters: The geographic coordinates, basic physico-chemical characteristics and trace metal content of the Mombasa seawater suite are given in Table 3, with summary statistics provided in Table 4. Dissolved O_2, pH and salinity vary significantly between the principal inshore water systems (Figs. 10-11), reflecting differences of residence time and/or freshwater-seawater mixing. Relatively low values (DO <70% sat., pH <7.7, salinity <34.0 g/l) consistent with the influence of a terrestrial runoff component (possibly coupled with a residence-time of several tidal-cycles) prevail in the upper reaches of Tudor Creek (sites MB1-MB4). Values for these parameters increase progressively through the mid- and lower reaches of Port Tudor (sites MB5-MB13), approaching typical pure seawater levels (exemplified on Figs. 10 - 11 by the 'reef front' suite) throughout much of Port Kilindini and Port Reitz. These physico-chemical trends concur with modelled hydrodynamic data for the inshore waters of Mombasa (Rees et al., 1996), which suggest substantial flushing of the Port Kilindini and lower Port Reitz systems during each tidal cycle. The position of the Makupa Creek waters on the horizontal axis of the DO vs. salinity plot suggests a similarly short (single tidal cycle) residence time. Disproportionately low DO values in this lagoon reflect the eutrophicating effect of solid waste and leachate from the Kibarani disposal site.

Figure 9: Kemmerer messenger sampler and filtration equipment used in the hydrochemical survey of Mombasa.

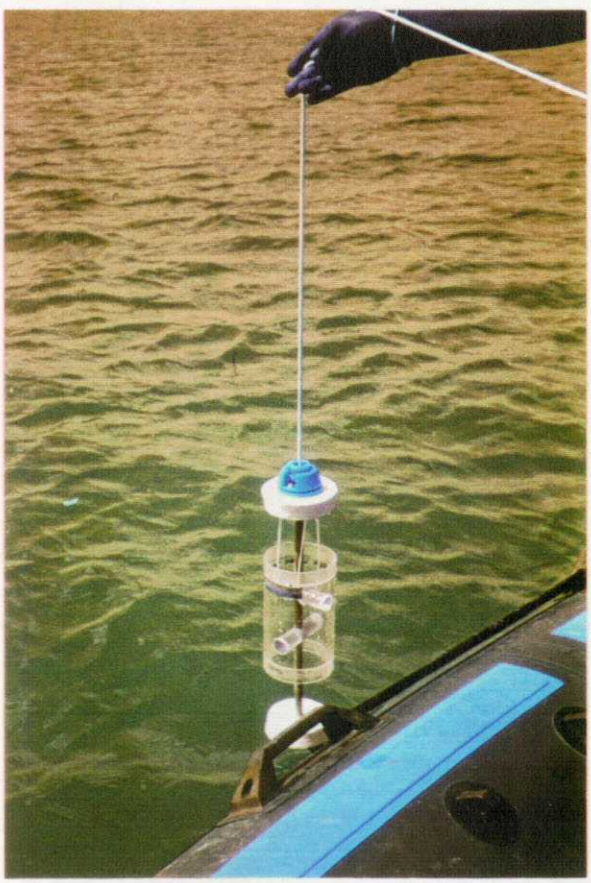

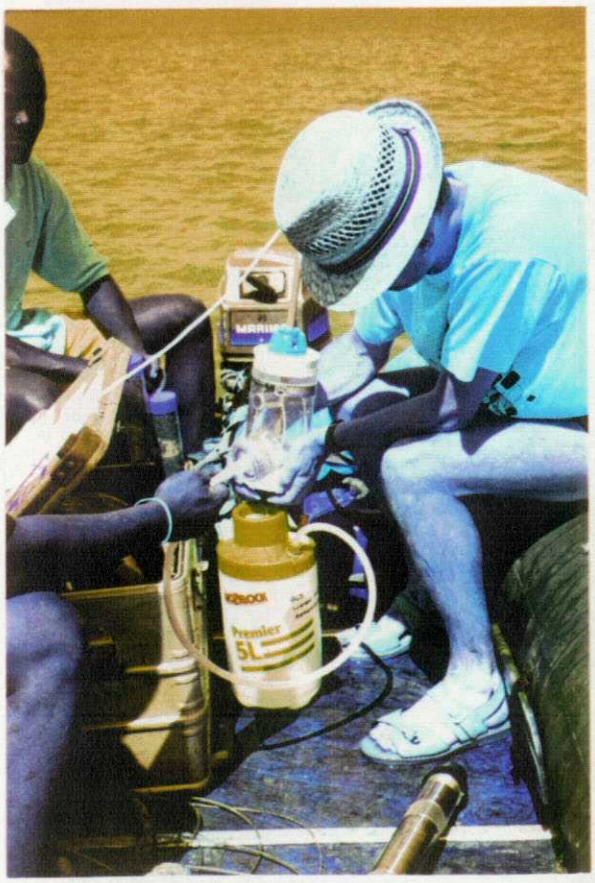

Table 3: Physico-chemical data for Mombasa sea-water samples. Absent data fields indicate that parameters were not determined. All trace metal data are expressed in µg/l.

Lab_Ref	Sample_ No.	Long (°)	Lat (°)	pH	Eh (mV)	DO (mg/l)	DO (% sat)	Temp (°C)	Cond (µS)	Salinity	Turb (FTU)	Pb	Cd	Cu	Zn	Cr	Ni
E386793	MB1	39.653	-4.002	7.70		3.4	63	27.4	51200	33.6	30	.571	.042	20.500	8.120	.350	.179
E386794	MB2	39.644	-3.988	7.60		3.3	63	27.4	51000	33.4	44	.472	.042	6.210	12.600	.350	.595
E386795	MB3	39.626	-3.989	7.50		3.4	54	27.6	50700	33.2	49	.460	.042	5.850	9.570	.380	.610
E386796	MB4	39.612	-3.981	7.50		3.7	70	27.9	50500	33.1	60	.460	.042	2.640	7.800	.350	.565
E386797	MB5	39.651	-4.028	8.00	190	4.2	80	27.5	52400	34.4	39	.658	.042	2.380	10.000	.350	.512
E386798	MB6	39.644	-4.017	7.80	196	3.8	74	27.6	52200	34.3	50	.409	.042	3.040	12.600	.350	.653
E386799	MB7	39.649	-4.025	7.90	190	4.0	78	27.4	52200	34.4	48	.536	.042	2.760	7.740	.350	.409
E386800	MB8	39.652	-4.016	7.90	173	4.1	79	27.0	52600	34.6	52	1.090	.042	2.810	8.120	.350	.327
E386801	MB9	39.678	-4.044	8.00		3.9	76	26.5	52900	34.8	92	1.880	.042	3.880	18.000	.680	.169
E386802	MB10	39.671	-4.038	8.00		4.1	78	26.8	53000	34.8	71	.923	.042	3.170	6.780	.350	.426
E386803	MB11	39.673	-4.029	7.90		3.9	75	26.9	52900	34.7	67	.599	.042	2.860	18.900	.470	.414
E386804	MB12	39.664	-4.023	7.80		3.6	68	27.0	52400	34.5	72	.534	.042	3.110	8.620	.350	.292
	MB13	39.657	-4.006	7.60		3.9	75	27.8	51900	34.1	96						
	MB14	39.646	-4.007	7.70		3.6	71	27.6	52100	34.2	89						
E386805	MB15											.024	.042	.051	2.000	.350	.058
E386806	MB16	39.656	-4.065	8.20	126	4.5	86	26.4	53400	35.2	41	.888	.042	3.170	9.900	.350	.280
E386807	MB17	39.662	-4.070	8.20	85	4.5	85	26.2	53500	35.3	41	.830	.042	4.270	15.600	.350	.207
E386808	MB18	39.664	-4.075	8.20	90	4.6	90	26.7	53500	35.3	44	.444	.042	1.840	10.700	.450	.275
E386809	MB19			8.20	86	4.9	92	26.5	53500	35.4	44	.483	.042	1.670	9.930	.350	.325
E386810	MB21	39.648	-4.076	8.20		4.7	92	26.9	53500	35.2	45	.950	.042	1.990	6.780	.350	.252
E386811	MB22	39.642	-4.035	8.00	120	3.3	65	27.5	53000	35.0	54	.806	.042	2.740	10.200	.350	.975
E386812	MB23	39.639	-4.035	8.10	67	4.1	80	28.1	53400	35.2	74	.698	.042	2.200	7.600	.350	.858
E386813	MB24	39.639	-4.040	8.10	93	4.1	80	27.1	53600	35.4	60	1.970	.042	1.940	5.220	.350	.156
E386814	MB25	39.640	-4.053	8.10		4.6	88	26.8	53600	35.3	74	.677	.042	2.020	4.100	.350	.190
E386815	MB26											.127	.042	.051	2.000	.350	.058
E386816	MB27	39.643	-4.062	8.10	90	4.4	85	26.6	53600	35.4	69	1.290	.049	1.910	9.120	.350	.395
E386817	MB28	39.645	-4.048	8.10	88	4.4	86	26.9	53600	35.3	71	.594	.042	2.190	5.110	.350	.286
E386818	MB29	39.630	-4.041	8.00	67	4.4	85	27.4	53400	35.2	84	1.120	.042	1.640	6.050	.410	.277
	MB30	39.630	-4.049	8.10		4.4	85	26.9	53500	35.3	76						
E386819	MB33	39.624	-4.044	8.10	90	4.2	82	26.8	53500	35.3	73	.794	.042	2.620	5.580	.390	.237
E386820	MB34	39.608	-4.046	8.00	90	4.4	86	27.4	53400	35.2	73	.623	.042	3.250	13.200	.350	.362
E386821	MB35	39.585	-4.048	7.90		4.4	85	27.4	53400	35.2	75	.494	.042	2.890	4.920	.350	.241
E386822	MB36	39.582	-4.033	7.80		4.0	79	27.6	53200	35.0	82	1.410	.042	3.950	5.720	.350	.282
E386823	MB38	39.581	-4.075	7.70		3.4	69	27.5	53000	35.0	79	.648	.042	4.480	3.100	.350	.419
E386824	MB39	39.590	-4.059	7.95		4.1	81	27.5	53500	35.3	78	.517	.042	2.210	9.520	.350	.228
E386825	MB41	39.712	-4.056	8.30		6.1	116	26.4	53700	35.4	51	1.340	.576	1.680	67.100	.350	.326
E386826	MB42	39.741	-4.004	8.20		5.0	98	25.7	53800	35.5	53	1.080	.676	3.680	69.600	.420	.124
E386827	MB43	39.750	-3.989	8.30		5.6	105	25.9	53800	35.5	50	1.290	.173	2.880	24.000	.350	.214
E386828	MB44	39.765	-3.961	8.20		5.1	96	25.7	53900	35.5	51	1.420	.540	2.640	49.900	.360	.149
E386829	MB45	39.677	-4.053	8.10		5.2	102	28.4	53300	35.1	56	1.400	.042	1.760	7.800	.350	.260
E386830	MB46	39.682	-4.064	8.20		5.4	105	26.9	53600	35.4	51	1.230	.042	1.260	5.030	.350	.441
E386831	MB47	39.681	-4.053	8.20		4.8	92	26.4	53500	35.4	49	.728	.042	1.470	11.400	.350	.464
E386832	MB48											.181	.042	.051	2.000	.350	.058

Table 4: Descriptive statistics for Mombasa seawaters. All trace metal data are reported as µg/l.

	Mean	Std. Dev.	Count	Minimum	Maximum	# Missing	Variance	Range	Geom. Mean	Harm. Mean	Median	Mode
Pb	.780	.461	42	.024	1.970	3	.213	1.946	.594	.295	.667	•
Cd	.085	.146	42	.042	.676	3	.021	.634	.053	.046	.042	.042
Cu	2.909	3.095	42	.051	20.500	3	9.577	20.449	1.851	.511	2.630	.051
Zn	12.286	14.969	42	2.000	69.600	3	224.060	67.600	8.248	6.045	8.120	2.000
Cr	.368	.056	42	.350	.680	3	.003	.330	.365	.363	.350	.350
Ni	.338	.197	42	.058	.975	3	.039	.917	.284	.224	.284	.058
pH	7.986	.219	40	7.500	8.300	5	.048	.800	7.983	7.980	8.000	8.200
DO (mg/l)	4.287	.642	40	3.300	6.100	5	.412	2.800	4.242	4.199	4.200	4.400
DO (% sat)	82.475	12.645	40	54.000	116.000	5	159.897	62	81.529	80.574	81.500	85.000
Temp (°C)	27.050	.623	40	25.700	28.400	5	.389	2.700	27.043	27.036	27.000	27.400
Cond (µS)	52967.500	880.672	40	50500.000	53900.000	5	775583.333	3400	52960.246	52952.875	53400.000	53500.000
Salinity	34.885	.654	40	33.100	35.500	5	.427	2.400	34.879	34.873	35.200	35.300
Turb (FTU)	61.425	16.488	40	30.000	96.000	5	271.840	66.000	59.244	57.067	58.000	•
V_p	1.042	.903	37	.080	4.540	8	.816	4.460	.727	.460	.760	•
Cr_p	.771	.613	37	-.070	2.920	8	.375	2.990	•	•	.550	•
Mn_p	6.606	4.344	37	.600	22.640	8	18.867	22.040	5.097	3.266	5.700	4.310
Co_p	.127	.104	37	.010	.540	8	.011	.530	.090	.053	.100	.070
Ni_p	1.120	1.721	37	-.070	9.290	8	2.961	9.360	•	•	.510	.220
Cu_p	1.214	.847	37	.150	3.080	8	.717	2.930	.901	.620	1.110	•
Zn_p	10.995	21.766	37	1.110	113.510	8	473.740	112.400	5.309	3.661	5.360	6.820
As_p	.132	.096	37	-.025	.422	8	.009	.447	•	•	.115	•
Mo_p	.035	.026	37	.003	.089	8	.001	.086	.024	.015	.025	•
Cd_p	.014	.021	37	-.004	.103	8	4.397E-4	.107	•	•	.007	0.000
Pb_p	.675	.637	37	.080	3.720	8	.406	3.640	.498	.362	.640	.310
Th_p	.466	2.211	37	.010	13.540	8	4.888	13.530	.083	.043	.090	•
U_p	.029	.028	37	.001	.165	8	.001	.164	.021	.012	.023	.014

Figure 10: Relationship between DO saturation (%) and pH in Mombasa waters.

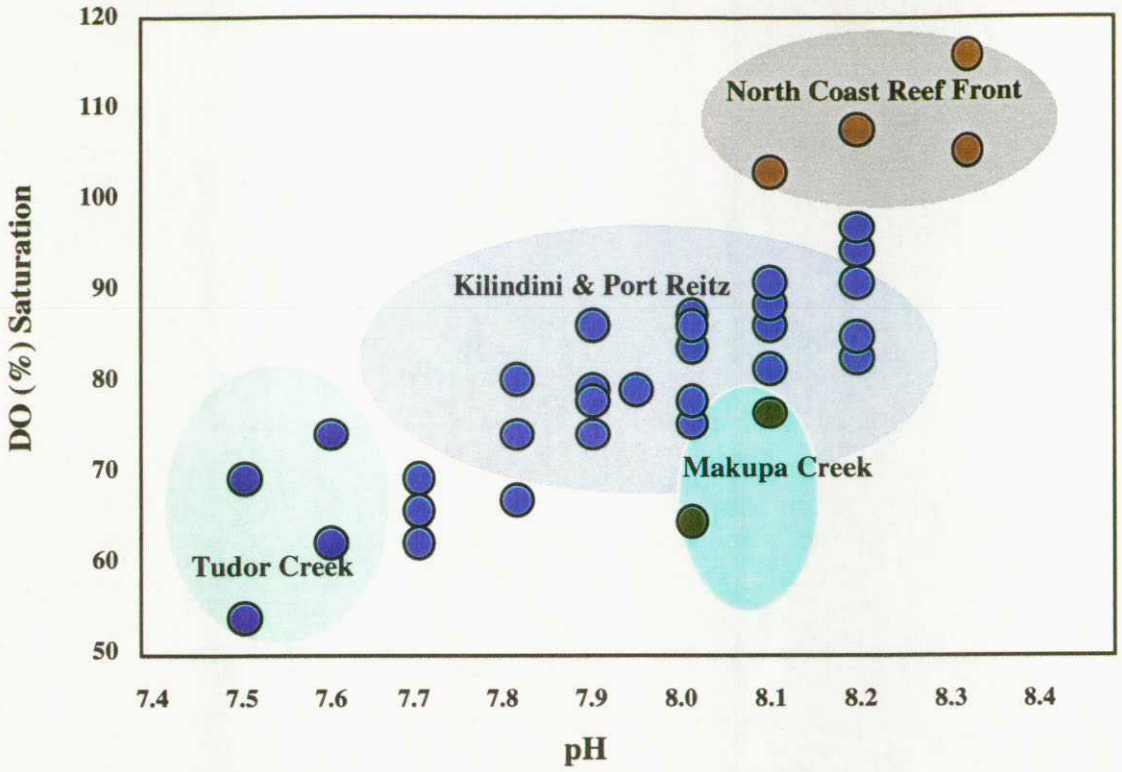

Figure 11: Relationship between DO saturation & salinity in Mombasa waters.

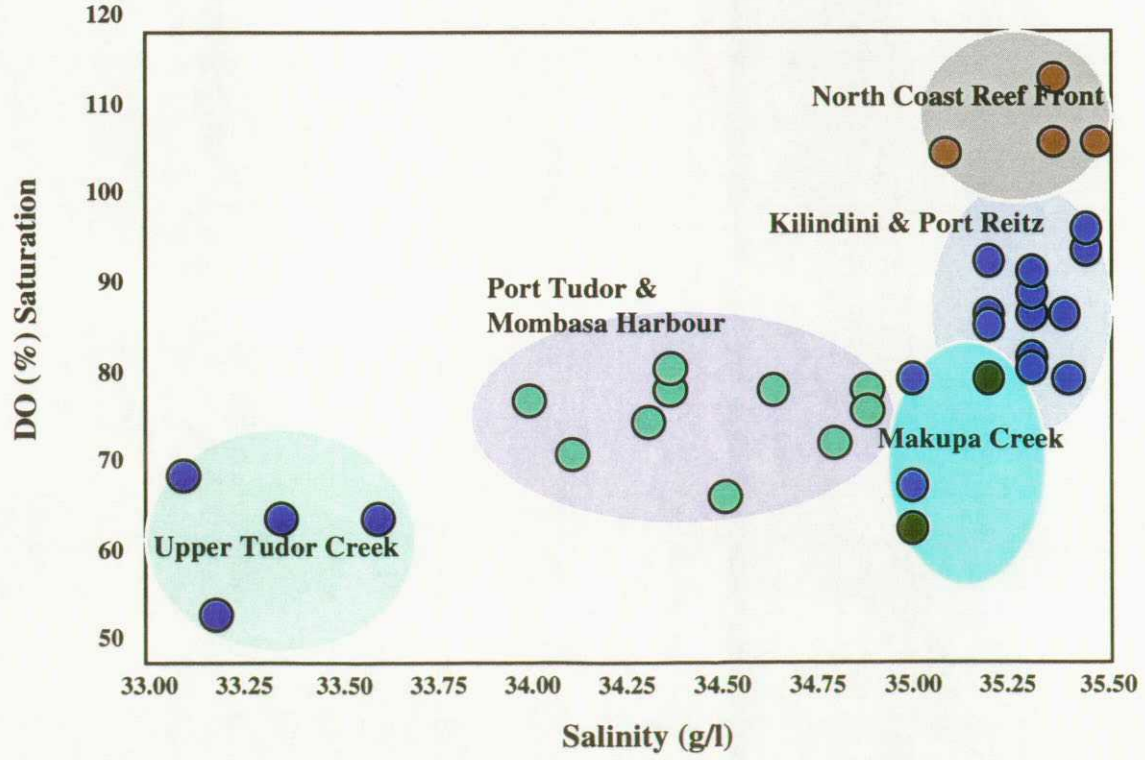

The turbidity of the inshore and reef-front waters was consistently low (<100 FTU) during both the September 1995 and January 1996 field campaigns. The very low values (<50 FTU) recorded in the zone of mixing in the upper reaches of Tudor Creek (sites MB1-MB3) suggest that the flux of Fe and dissolved humic organic matter in terrestrial runoff (and consequent flocculation of these components) is negligible. Although probably subject to marked seasonal variation, the limited presence of flocculated particulates may significantly influence dissolved trace metal mobility by restricting particulate scavenging and sedimentation. Locally elevated turbidities (>80 FTU) in shallow water (<3 m) at the confluence of the two major inland arms of Tudor Creek (sites MB13 and MB14) result from localised eddying and entrainment of bottom sediment. A turbidity value of 84 FTU was recorded close to the discharge outlet of a sewage plant near Kipevu oil terminal on the northern shore of Port Reitz (MB29).

3.1.2.2: Trace metals: Spatial variations in the concentration of the six analysed metals in the Mombasa water suite are shown in Figures 12-17. With the exception of Pb, for which relatively high values of up to 1.9 µg/l were recorded, the median metal concentrations for all elements (Cd <0.042 µg/l, Cu 2.63 µg/l, Zn 8.1 µg/l, Cr <0.35 µg/l, Ni 0.28 µg/l) lie within the global background range for marine waters (e.g. Crecelius, 1969). The spatial covariability of dissolved metals is limited (Table 5), with the exception of Zn and Cd (Pearson R coeff. = 0.967) which display coincident enrichment in the reef-front waters between Nyali and Mtwapa (sites MB41 - MB44).

Table 5: Pearson correlation matrix for hydrochemical parameters determined in filtered water from Mombasa.

	Pb	Cd	Cu	Zn	Cr	Ni	pH	DO (% sat)	Salinity
Pb	1.000	.308	-.194	.286	.309	-.413	.422	.426	.444
Cd	.308	1.000	-.060	.967	.034	-.284	.358	.507	.282
Cu	-.194	-.060	1.000	-.048	-.007	-.104	-.443	-.459	-.510
Zn	.286	.967	-.048	1.000	.152	-.238	.355	.483	.235
Cr	.309	.034	-.007	.152	1.00	-.220	.024	-.078	.009
Ni	-.413	-.284	-.104	-.238	-.220	1.000	-.361	-.435	-.382
pH	.422	.358	-.443	.355	.024	-.361	1.000	.840	.885
DO%	.426	.507	-.459	.483	-.078	-.435	.840	1.000	.744
Temp	-.292	-.561	.131	-.582	-.210	.532	-.622	-.489	-.512
Cond	.458	.297	-.511	.251	.027	-.400	.886	.751	.996
Sal	.444	.282	-.510	.235	.009	-.382	.885	.744	1.000
Turb	.242	-.156	-.301	-.193	.368	-.068	-.123	-.100	.219

Statistical analysis (ANOVA and Tukey HSD) of metal data for six discrete sectors of the study area:- (A) upper Tudor Creek, (B) Port Tudor & Mombasa Harbour, (C) Port Kilindini, (D) Makupa Creek, (E) Port Reitz and (F) the North Coast reef front, has highlighted significant

differences of hydrochemical signature, variably controlled by freshwater inputs, point-source anthropogenic contamination and hydrodynamic factors. Upper Tudor Creek is discriminated by anomalous Cu concentrations (max. 20.5 µg/l) and, to a lesser extent, Ni enrichment.

Figures 12-13: Distribution of Cu and Zn (µg/l) in 0.45 µm-filtered mid-water column samples from Mombasa.

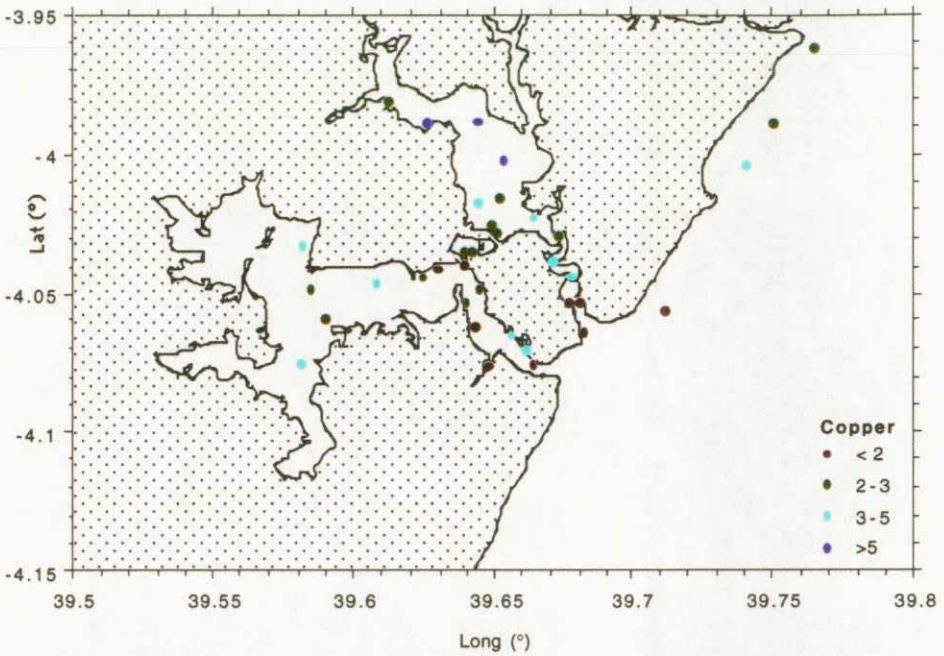

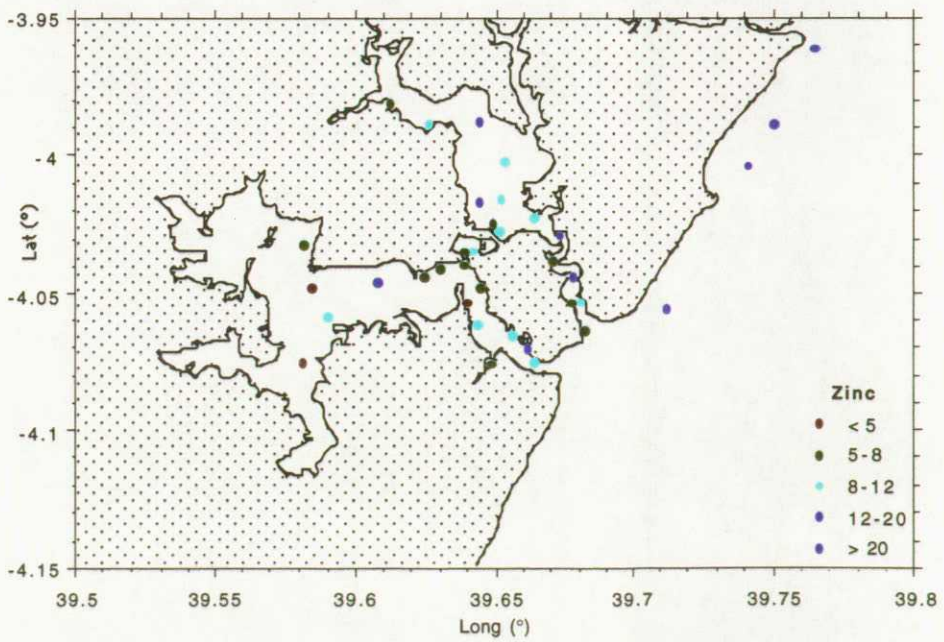

Figures 14-15: Distribution of Pb and Cd (µg/l) in 0.45 µm-filtered mid-water column samples from Mombasa.

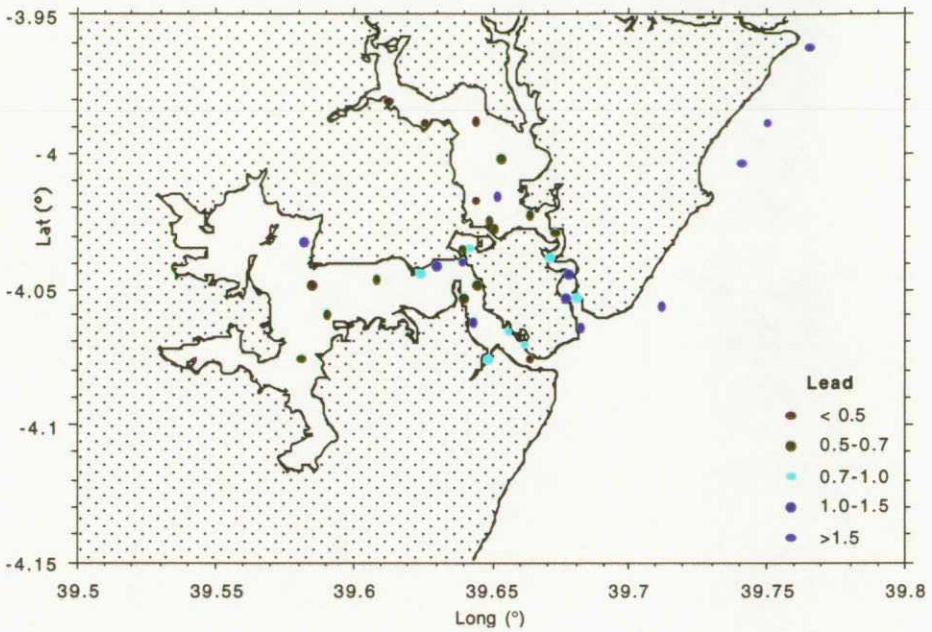

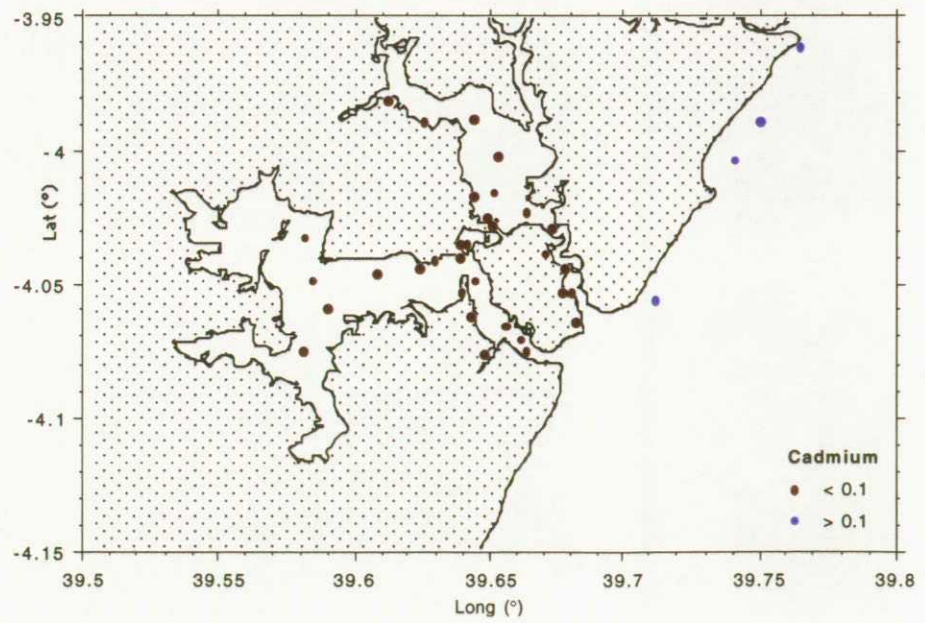

Figures 16-17: Distribution of Ni and Cr (µg/l) in 0.45 µm-filtered mid-water column samples from Mombasa.

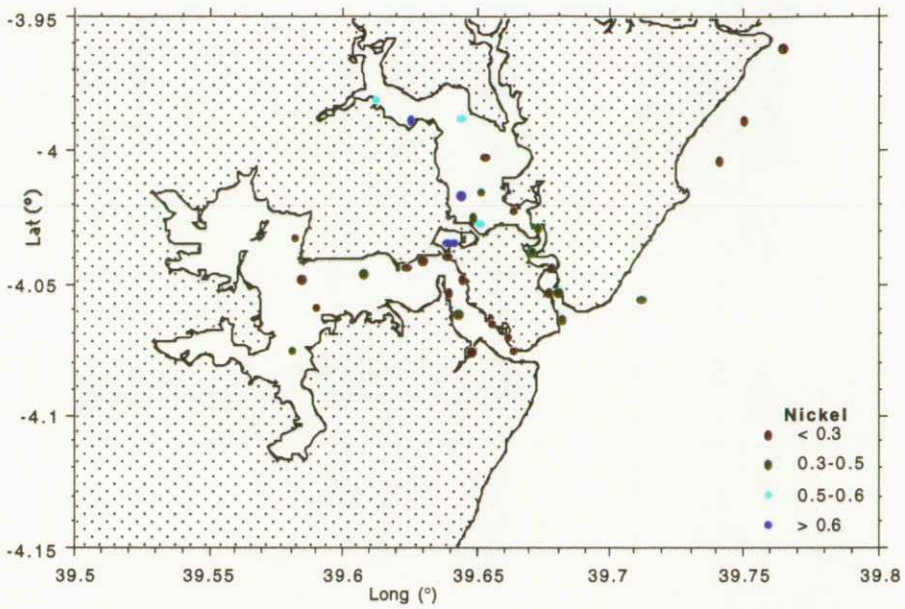

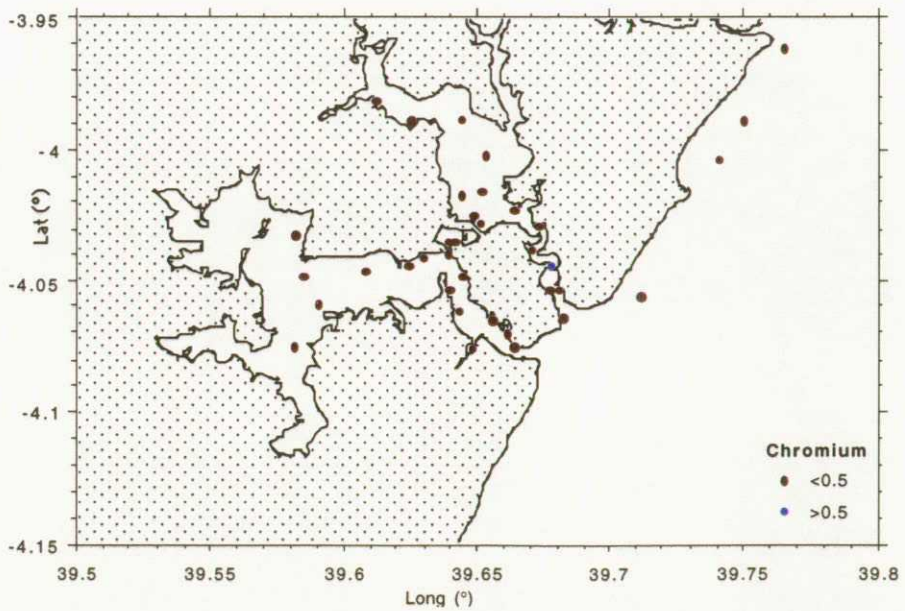

This trend does not, in itself, infer a higher Cu flux than that prevailing in other inshore water areas, as the observed concentrations are likely to be accentuated by ineffective circulation and hence extended water residence in the uppermost reaches of the creek. A general tendency for Cu enrichment in all areas of freshwater-seawater mixing (Cu vs. salinity: R = -0.51, Table 5; also Fig. 18) does, however, suggest that the Cu concentration of terrestrial runoff into Tudor

Creek may exceed that of incoming seawater. No anthropogenic contaminant source is implicated.

Makupa Creek waters (MB22-MB23) are distinguished from all other components of the inshore and reef-front suite by substantial enrichment of Ni (max. 0.975 µg/l. Modelled hydrodynamic data (Rees et al., 1996) and physico-chemical inferences regarding residence-time (see section 3.1.2.1 above) suggest that comprehensive flushing of this lagoonal system occurs over as few as two tidal cycles. This hydrochemical anomaly must unequivocally be controlled by an elevated Ni flux, probably carried in leachate from the Kibarani landfill.

The reef-front waters extending between Nyali and Mtwapa (MB41-MB44) are clearly differentiated from all inshore samples, displaying enrichment of Zn, Cd and Pb. Concentrations of Zn in the range 24-69 µg/l exceed the median for the total Mombasa suite by at least a factor of 3 (Fig. 18). In the case of Cd, samples MB41-MB44 provided the only instances in which the analytical detection limit (0.042 µg/l) was significantly exceeded (range:-0.173 - 0.676 µg/l). No identifiable source of metals along this coastline has been identified, and further investigation of the controls on Pb, Zn and Cd enrichment is currently in progress.

Figure 18: Relationship between dissolved metals (Cu, Zn and Ni) and DO in Mombasa waters.

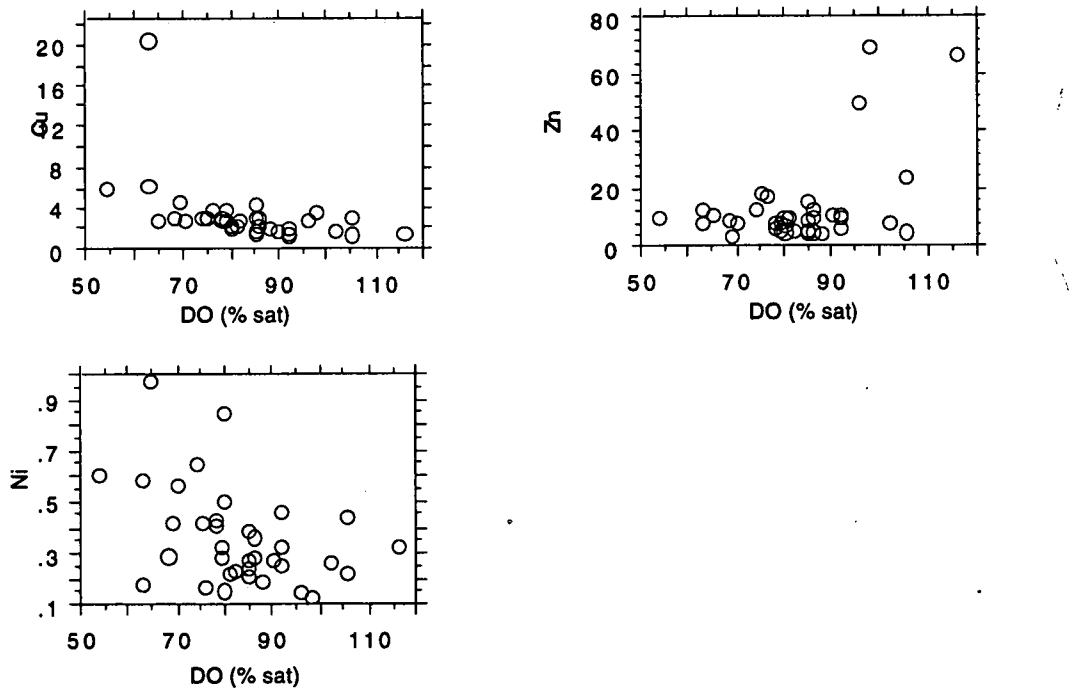

3.2: Suspended particulate matter.

3.2.1: Sampling and analytical methods.:

Suspended particulate matter (SPM) was collected at all inshore and reef-front water sampling stations included in the LOCS survey. All SPM samples were obtained from the mid-water column during the filtration of waters collected for dissolved metal analysis (see section 3.1.1 above). The simultaneous collection of SPM and filtered water from a single sample in this manner is considered most appropriate for the study of biogeochemical interactions between particulate and dissolved phases. At each sampling station, a known volume of water (typically 1 litre) was pressure-pumped through a pre-loaded 50 mm diameter filtration cartridge, housing a 0.45 μm cellulose acetate membrane (Sartorius™). The pump reservoir pressure was kept as low as possible throughout filtration to minimise the rupturing of algal cells, and attendant loss of metals into the dissolved phase. On completion of the exercise, the filter cartridge was opened and the membrane transferred into a Sterilin storage tube.

On return to the laboratory, each cellulose acetate filter was weighed to assess the approximate mass of SPM residue held upon it. Each was then placed in a sealed PTFE bomb and digested in 5 ml HNO_3 + 2 ml $HClO_4$ + 2 ml HF until a particulate-free solution remained. The solutions were subsequently diluted to an appropriate volume and analysed for 13 trace elements (V, Cr, Mn, Co, Ni, Cu, Zn, As, Mo, Cd, Pb, Th and U) by ICP-MS. A suite of pristine (ie. unused) membranes, and a variety of acid reagent mixtures were also prepared and analysed using identical methods to establish their respective trace metal contents. 'Blank' corrections were then applied to the trace metal data generated for all Mombasa SPM samples to account for any filter/reagent contamination.

3.2.2: Results:

3.2.2.1: Contribution of SPM to the water column trace-metal load. The trace metal loads held by SPM, expressed as concentration per litre of seawater for each Mombasa sampling station, are given in Table 6. For the six metals also analysed in filtered waters, the presentation of SPM data in this manner facilitates direct assessment of the relative importance of particulate and solute phases as contaminant carriers in the water column.

The mass-balances for Ni and Cr are dominated by particulate carriers at over 60% of sampling stations, with median SPM values of 0.51 μg/l and 0.55 μg/l respectively, compared to 0.28 μg/l and <0.35 μg/l respectively in solution. The SPM contribution to the total Ni load exceeds that of dissolved phases by an order of magnitude at Makupa Creek site MB22. The dominance of SPM with respect to Cr is maximised in Tudor Creek, where particulate/dissolved ratios of 8 are recorded (site MB4). In the Mombasa area as a whole, the SPM contribution to total water

Table 6: Trace element loading of mid-water column suspended particulate matter (SPM), expressed as µg per litre of sea water.

Sample_No.	V	Cr	Mn	Co	Ni	Cu	Zn	As	Mo	Cd	Pb	Th	U
MB1	1.23	.78	5.16	.14	1.35	2.21	3.03	.115	.034	.005	.48	.09	.026
MB2	2.40	1.54	10.12	.27	2.35	2.78	5.27	.180	.089	.006	.79	.16	.044
MB3	2.62	1.72	12.18	.32	3.52	1.53	6.73	.171	.063	.011	.73	.17	.049
MB4	4.54	2.92	22.64	.54	1.56	2.83	8.85	.327	.085	.044	1.11	.29	.077
MB5	.85	.59	5.50	.11	.65	1.25	5.36	.094	.032	.103	.68	.06	.020
MB6	1.90	1.10	8.80	.19	1.25	1.25	3.97	.247	.056	.007	.65	.13	.042
MB7	2.11	1.32	10.05	.23	1.00	2.29	6.96	.243	.065	.017	1.00	.15	.045
MB8	2.05	1.36	9.72	.24	1.77	1.46	8.10	.291	.069	.030	.67	.14	.046
MB9	1.13	.70	7.03	.14	1.54	1.71	8.36	.166	.047	.011	.71	.11	.034
MB10	1.50	1.42	8.26	.18	1.59	2.28	6.27	.163	.072	.004	.66	.12	.042
MB11	2.04	1.43	11.86	.25	1.10	3.08	8.45	.256	.069	.009	.92	.16	.053
MB12	1.81	1.18	9.46	.21	4.92	2.51	6.82	.212	.071	.025	.90	.12	.041
MB16	.76	.48	5.51	.09	1.02	1.31	5.88	.118	.042	.008	.57	.07	.028
MB17	.49	.36	4.52	.07	.51	.82	3.74	.060	.032	.008	.64	.06	.020
MB18	.87	.84	5.86	.09	.81	1.66	8.47	.130	.036	.007	.48	.11	.027
MB19	.64	.44	4.31	.06	.86	.88	4.51	.046	.041	.006	.25	.06	.023
MB21	.53	.39	4.17	.07	.33	.72	2.72	.087	.023	.005	.49	.06	.017
MB22	.59	.45	4.98	.05	9.29	2.24	5.41	.123	.054	.006	.74	.04	.021
MB23	.64	.41	5.70	.07	.43	.51	6.82	.220	.063	.016	.57	.19	.030
MB24	.65	.46	5.40	.09	.35	.40	2.21	.048	.010	0.000	.24	.06	.014
MB25	.25	.16	2.19	.04	.12	.15	1.14	.044	.004	.001	.08	.03	.007
MB27	.59	.51	5.19	.09	.45	1.38	3.73	.089	.017	0.000	.31	.07	.014
MB28	.44	.48	5.38	.10	.28	.31	3.58	.167	.008	0.000	.25	.07	.014
MB29	.82	1.42	6.69	.11	1.95	.56	4.45	.088	.015	.002	.31	.08	.019
MB30	.21	.10	2.05	.02	.05	.61	1.26	.052	.004	0.000	.14	.01	.005
MB33	.50	.33	4.31	.07	.09	.16	1.95	-.002	.008	-.003	.75	13.54	.165
MB34	1.06	.67	9.40	.14	.22	.39	2.12	.088	.012	0.000	.28	.13	.025
MB35	.74	.55	6.49	.11	.34	.26	1.86	.091	.018	-.004	.23	.09	.018
MB36	.84	.49	8.00	.11	.22	.29	2.07	.028	.012	-.002	.21	.10	.022
MB38	1.35	.85	7.17	.16	.37	.69	2.65	.074	.022	0.000	.31	.11	.029
MB41	.17	.26	1.79	.04	.17	1.70	51.23	.068	.013	.021	1.31	.01	.008
MB42	1.13	1.72	15.16	.15	.64	1.38	113.51	.422	.025	.061	3.72	.10	.023
MB43	.08	.06	.62	.01	-.01	.24	15.99	.061	.018	.014	.64	.01	.004
MB44	.41	.65	5.89	.07	.22	.95	69.52	.188	.019	.046	1.91	.47	.017
MB45	.38	.30	1.56	.04	.17	1.11	6.86	.115	.021	.027	.98	.04	.014
MB46	.13	.14	.60	.01	.02	.36	5.87	-.025	.003	.013	.17	.01	.001
MB47	.12	-.07	.71	.01	-.07	.64	1.11	.043	.006	.002	.10	.01	.004

column budgets for Ni and Cr vary independently of turbidity (ie. the volume or mass of SPM present), suggesting that partitioning is actively regulated by in-situ exchange processes in the water column. The presence of certain metals in hydroxy-complexes (notably Cr) with a propensity for incorporation into colloids, may constitute one such process.

A contrasting trend is displayed by Cu, the mass-balance for which is dominated by dissolved phases at most sites (SPM median = 1.1 µg/l, water median = 2.63 µg/l). There is also limited evidence (notably at stations MB41-MB44) of a dominance of Cd in the dissolved phase. The partitioning patterns for Zn and Pb are less clearly defined.

The partitioning of individual metals between particulate and aqueous phases in the water column is a function of (i) the physical form in which the respective metals are introduced (via anthropogenic pathways or terrestrial runoff), (ii) biogeochemical regulation (notably the selective removal of metals from solution by primary producers), (iii) the solubility products and stabilities of the principal metal species, and (iv) the composition and surface charge properties of SPM (ie. sorption surfaces). For most Mombasa stations, the presence of a brown SPM residue, soluble only on the addition of HF during the digestion procedure, suggests that the SPM matrix is largely inorganic. This may provide a partial explanation for the limited affinity of Cu to particulate matter. While no empirical speciation data are available, the principal dissolved metal species are likely to be uncomplexed divalent cations (Zn^{2+}, Ni^{2+}, Cu^{2+}, Cd^{2+}, Pb^{2+}), chloride complexes (notably of Cd and Pb) and hydroxy complexes of Cr, Cu and Pb, the solubility products of which are unlikely to be influential.

3.2.2.2: Spatial covariation of metals in SPM and solution. The extent of spatial covariation between dissolved and particulate loadings of selected metals in inshore waters of Mombasa is illustrated in Figure 19. Low Pearson R coefficients (<0.3) have been calculated for particulate vs. dissolved Ni, Pb and Cu. Higher coefficients for Cd and Zn are produced if the entire dataset is used (R = 0.80 and 0.84 respectively), but these values fall to insignificant levels if the enriched North Coast reef-front suite is excluded.

3.2.2.3: Mass-specific trace element concentrations. The dry weights of SPM residues for the Mombasa sample suite were found to lie within the range 10-14 mg. Errors in the derivation of weights for some samples were, however, suspected due to the variable dessication of filter membranes during drying. Consequently, SPM metal concentrations (Table 7) have been calculated indirectly using the following procedure:-

$$\mathbf{M2\ mg/kg} = \frac{\mathbf{M1\ \mu g/l \times W \times D \times LT}}{\mathbf{T}}$$

where M2 = the mass specific metal concentration in SPM, M1 = the SPM metal load per litre of seawater, W = the weight of the smallest SPM sample collected (10 mg), D = the SPM dilution factor in seawater for the smallest SPM sample analysed ie. 100,000), LT = the lowest recorded turbidity value (30 FTU) and T = the turbidity of the sample yielding metal load M2. The calculation method assumes a linear relationship between SPM mass and water turbidity.

Figure 19: Relationship between dissolved and particulate metal loadings of selected trace metals in Mombasa waters.

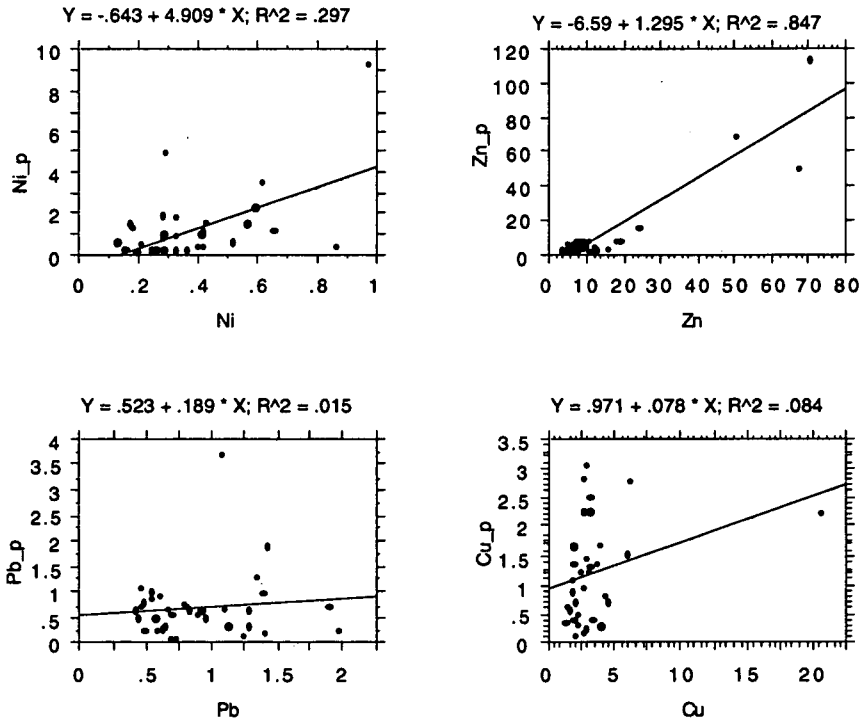

Descriptive statistics for the Mombasa SPM suite are given in Table 8. Median elemental abundances decline in the order:- Mn > Zn > Cu > Ni > V > Pb > Cr > As > Co > Th > Mo > U >Cd. Spatial abundance variations (Figs. 20-27) form a coherent trend, As, Mo and most first-row transition elements (Mn, V, Cr, Co, Ni) showing systematic enrichment in the upper sector of Tudor Creek relative to all other inshore waters. The principal exception (with respect to the first-row transition group) is Zn which, although enriched in Tudor Creek relative to Port Reitz and Kilindini, attains highest concentrations (> 6000 mg/kg) along the North Coast reef-front. Constrasts of SPM metal concentration between individual inshore water bodies are summarised in Figure 28, in which representative trace element values for SPM from Tudor Creek, Mombasa Harbour, Kilindini, Makupa Creek, Port Reitz and the North Coast reef-front are plotted on a single spidergram. Notable features include the relative enrichment of Ni in SPM

Table 7: Mass specific concentration of selected trace elements (mg/kg) in SPM from the inshore waters of Mombasa.

Sample_No.	V_p/n*	Cr_p/n*	Mn_p/n*	Co_p/n*	Ni_p/n*	Cu_p/n*	Zn_p/n*	As_p/n*	Mo_p/n*	Cd_p/n*	Pb_p/n*	Th_p/n*	U_p/n*
MB1	123	78.3	516.1	14.117	135	221.1	303	11.5	3.4	.50	48	9.1	2.6
MB2	163.6	105	690	18.409	160.2	189.5	359	12.2	6	.40	53	10.9	3
MB3	160.4	105.3	745.7	19.592	215.5	93.6	412	10.4	3.8	.67	44	10.4	3
MB4	227	146	113	27	78	141.5	442	16.3	4.2	2.2	55	14.5	3.8
MB5	65.3	45.3	423	8.462	50	96.1	412	7.2	2.4	7.9	52	4.6	1.5
MB6	114	66	528	11.400	75	75	238	14.8	3.3	.42	39	7.8	2.5
MB7	131.8	82.5	628.1	14.375	62.5	143.1	435	15.1	4	1.1	62	9.3	2.8
MB8	118.2	78	560.7	13.846	102.1	84.2	467	16.7	3.9	1.7	38	8.1	2.6
MB9	36.8	22.8	229.2	4.565	50.2	55.7	272	5.4	1.5	.35	23	3.5	1.1
MB10	63.3	60	349	7.606	67.1	96.3	264	6.8	3	.16	27	5.1	1.7
MB11	91.3	64	531	11.194	49.2	137.9	378	11.4	3.1	.40	41	7.1	2.3
MB12	75.4	49.1	394.1	8.750	205	104.5	284	8.8	2.9	1.04	37	5	1.7
MB16	55.6	35.1	403.1	6.585	74.6	95.8	430	8.6	3.1	.58	41	5.1	2.1
MB17	35.8	26.3	330.7	5.122	37.3	60	273	4.3	2.3	.58	46	4.3	1.4
MB18	59.3	57.2	399.5	6.136	55.2	113.1	577	8.8	2.4	.47	32	7.5	1.8
MB19	43.6	30	293.8	4.091	58.6	60	307	3.1	2.7	.40	17	4.1	1.5
MB21	35.3	26	278	4.667	22	48	181	5.8	1.5	.33	32	4	1.1
MB22	32.7	25	276.6	2.778	516.1	124.4	300	6.8	3	.33	41	2.2	1.1
MB23	25.9	16.6	231	2.838	17.4	20.6	276	8.9	2.5	.64	23	7.7	1.2
MB24	32.5	23	270	4.500	17.5	20	110	2.4	.5	.01	12	3	.70
MB25	10.1	6.4	88.7	1.622	4.8	6	46	1.7	.16	.04	3	1.2	.28
MB27	25.6	22.1	225.6	3.913	19.5	60	162	3.8	.73	.01	13	3	.60
MB28	18.5	20.2	227.3	4.225	11.8	13	151	7.1	.33	.01	10	2.9	.59
MB29	29.2	50.7	238.9	3.929	69.6	20	158	3.1	.53	.07	11	2.8	.67
MB30	8.2	3.9	80.9	.789	1.9	24	49	2.0	.15	.01	5	.39	.19
MB33	20.5	13.5	177.1	2.877	3.1	6.5	80	0.01	.32	.01	30	556.4	6.7
MB34	43.5	27.5	386.3	5.753	9.	16	87	3.6	.49	.01	11	5.3	1.1
MB35	29.6	22	259.6	4.400	13.6	10.4	74	3.6	.72	.01	9	3.6	.72
MB36	30.7	17.9	292.6	4.024	8	10.6	75	1	.43	.01	7	3.6	.80
MB38	51.2	32.2	272.2	6.076	14	26.2	100	2.8	.83	.01	11	4.1	1.1
MB41	10	15.2	105.2	2.353	10	100	3013	4	.76	1.2	77	.58	.47
MB42	63.9	97.3	858.1	8.491	36.2	78.1	6425	23.8	1.4	3.4	210	5.6	1.3
MB43	4.8	3.6	37.2	.600	0.6	14.4	959	3.1	1.1	.84	38	.60	.24
MB44	24.1	38.2	346.4	4.118	12.9	55.8	4089	11	1.1	2.7	112	27.6	1
MB45	20.3	16	83.5	2.143	9.1	59.4	367	6.1	1.1	1.4	52	2.1	.75
MB46	7.6	8.2	35.2	.588	1.1	21.1	345	1.4	.17	.76	10	.58	.05
MB47	7.3	4.2	43.4	.612	0.6	39.1	67	2	.36	.12	6	.61	.24

Table 8: Descriptive statistics for (turbidity-normalised) trace element data for Mombasa SPM samples.

	V_p/n*	Cr_p/n*	Mn_p/n*	Co_p/n*	Ni_p/n*	Cu_p/n*	Zn_p/n*	As_p/n*	Mo_p/n*	Cd_p/n*	Pb_p/n*	Th_p/n*	U_p/n*
Mean	56.687	41.444	350.519	6.822	61.345	68.710	621.137	7.163	1.922	.827	37.657	20.407	1.539
Count	37	37	37	37	37	37	37	37	37	37	37	37	37
Minimum	4.800	-4.286	35.294	.588	-4.286	6.081	46.216	-1.471	.158	-.160	3.243	.395	.059
Maximum	227.000	146.000	1132.000	27.000	516.111	221.000	6425.094	23.887	6.068	7.923	210.566	556.438	6.781
# Missing	8	8	8	8	8	8	8	8	8	8	8	8	8
Median	35.854	27.534	292.683	4.565	36.226	60.000	284.167	6.161	1.533	.409	32.727	4.390	1.167

Table 9: Pearson correlation matrix for trace elements determined in Mombasa SPM samples.

	V_p/n*	Cr_p/n*	Mn_p/n*	Co_p/n*	Ni_p/n*	Cu_p/n*	Zn_p/n*	As_p/n*	Mo_p/n*	Cd_p/n*	Pb_p/n*	Th_p/n*	U_p/n*
V_p/n*	1.000	.940	.906	.992	.355	.723	-.043	.702	.839	.195	.247	-.089	.607
Cr_p/n*	.940	1.000	.958	.947	.333	.705	.216	.808	.773	.284	.470	-.107	.550
Mn_p/n*	.906	.958	1.000	.921	.304	.630	.262	.827	.725	.322	.515	-.090	.549
Co_p/n*	.992	.947	.921	1.000	.316	.696	-.003	.702	.800	.223	.273	-.083	.598
Ni_p/n*	.355	.333	.304	.316	1.000	.523	-.087	.270	.538	2.077E-4	.095	-.098	.208
Cu_p/n*	.723	.705	.630	.696	.523	1.000	.097	.618	.818	.237	.372	-.175	.412
Zn_p/n*	-.043	.216	.262	-.003	-.087	.097	1.000	.498	-.068	.423	.909	-.054	-.091
As_p/n*	.702	.808	.827	.702	.270	.618	.498	1.000	.674	.395	.719	-.194	.362
Mo_p/n*	.839	.773	.725	.800	.538	.818	-.068	.674	1.000	.193	.247	-.155	.531
Cd_p/n*	.195	.284	.322	.223	2.077E-4	.237	.423	.395	.193	1.000	.535	-.097	.053
Pb_p/n*	.247	.470	.515	.273	.095	.372	.909	.719	.247	.535	1.000	-.007	.169
Th_p/n*	-.089	-.107	-.090	-.083	-.098	-.175	-.054	-.194	-.155	-.097	-.007	1.000	.709
U_p/n*	.607	.550	.549	.598	.208	.412	-.091	.362	.531	.053	.169	.709	1.000

37 observations were used in this computation.
8 cases were omitted due to missing values.

Figures 20-21: Mass-specific concentration of Cr and As in SPM from Mombasa.

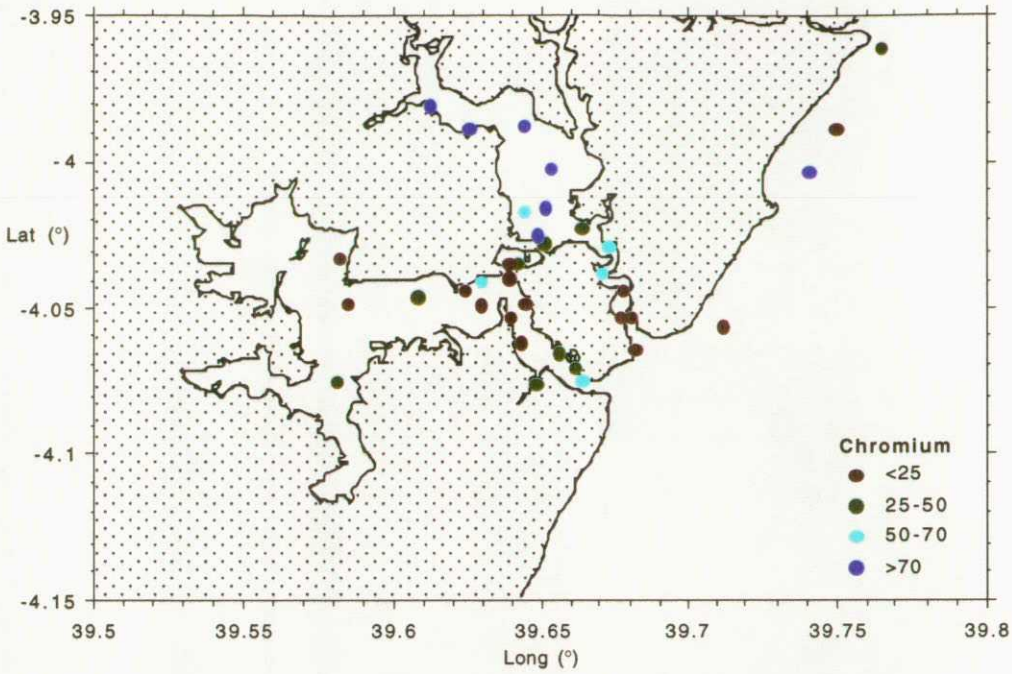

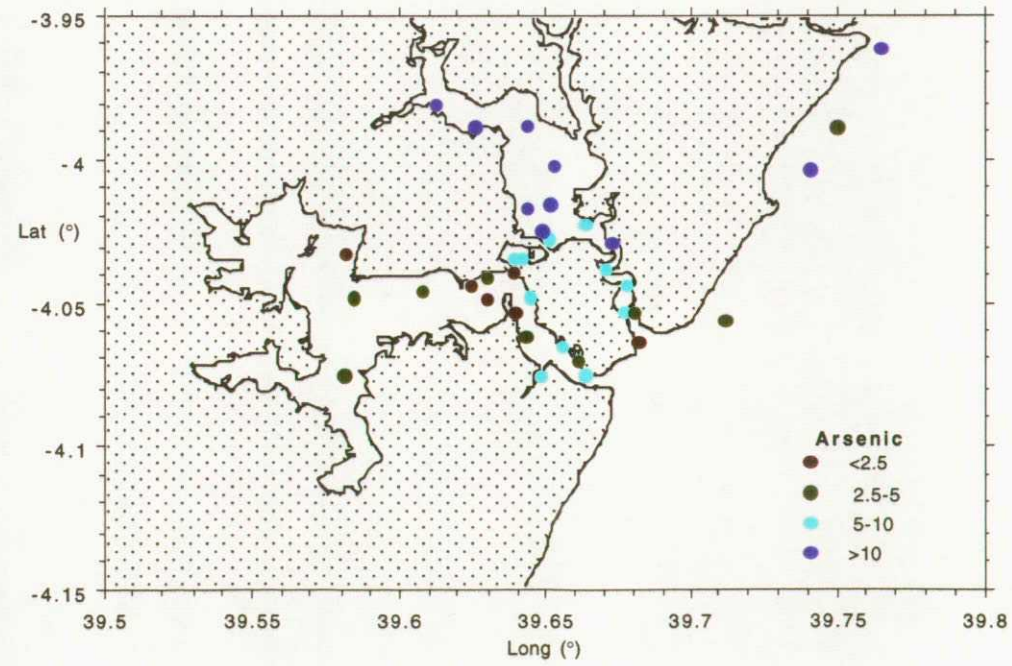

Figures 22-23: Mass-specific concentration of Co and Ni in SPM from Mombasa.

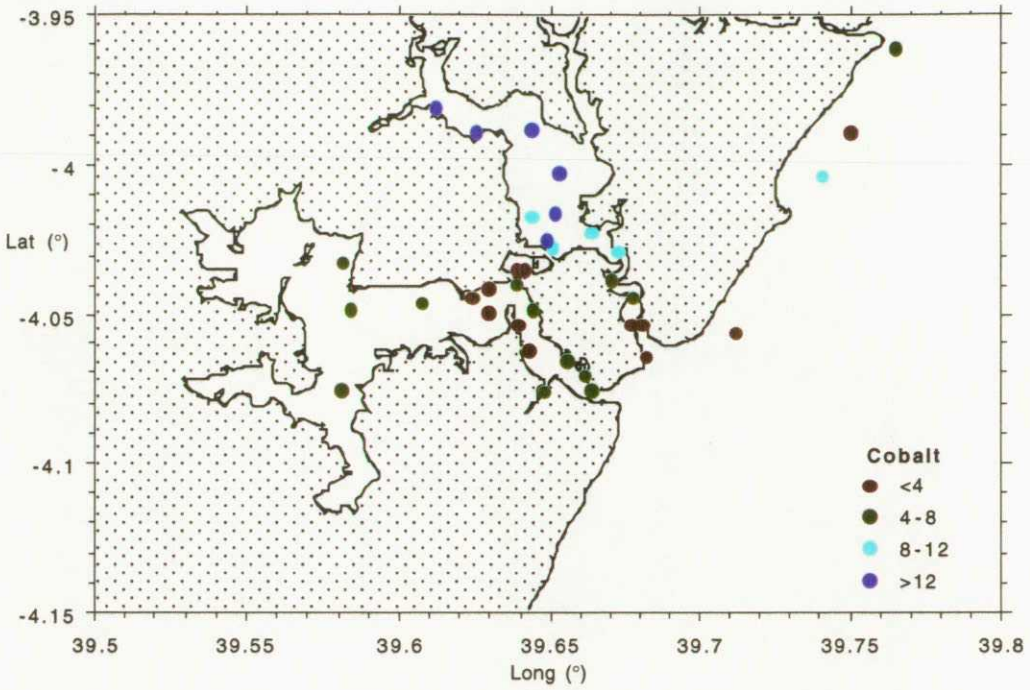

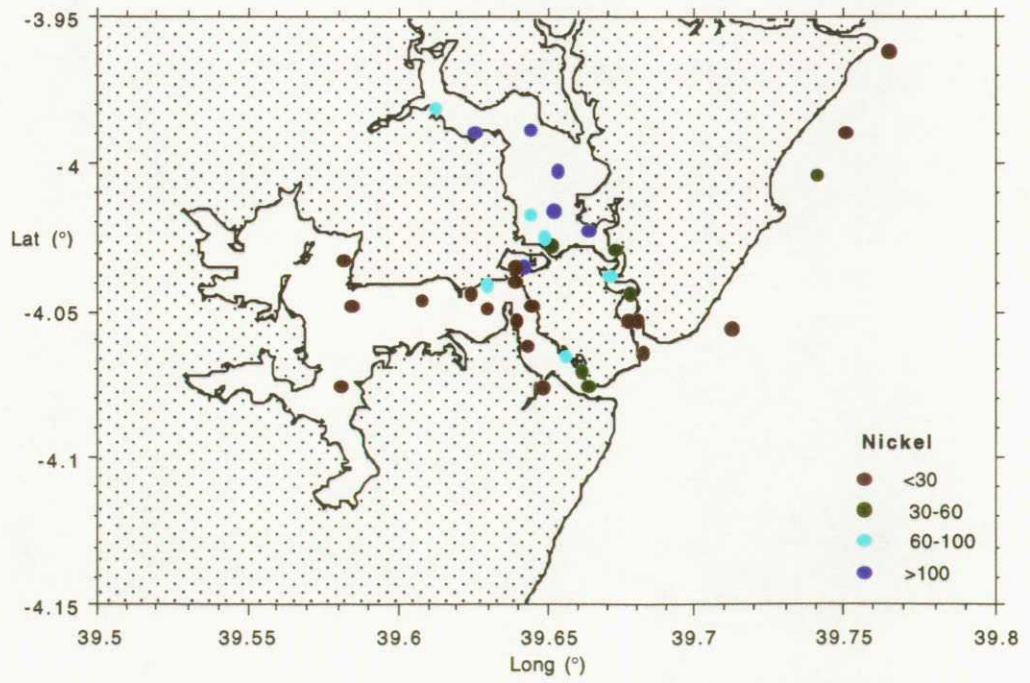

Figures 24-25: Mass-specific concentration of Mn and Cu in SPM from Mombasa.

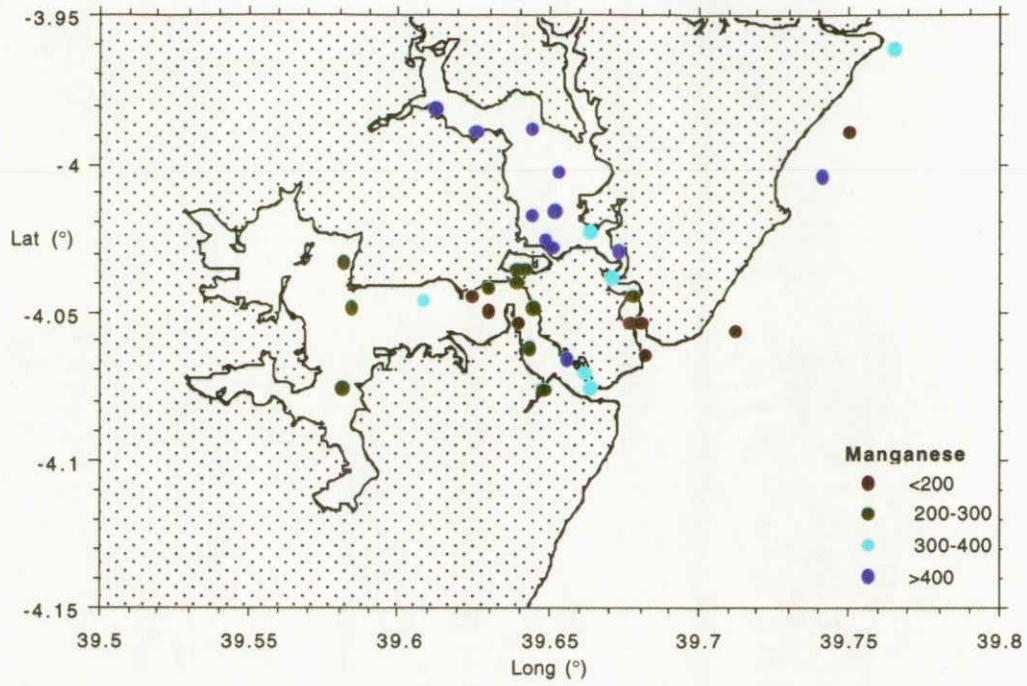

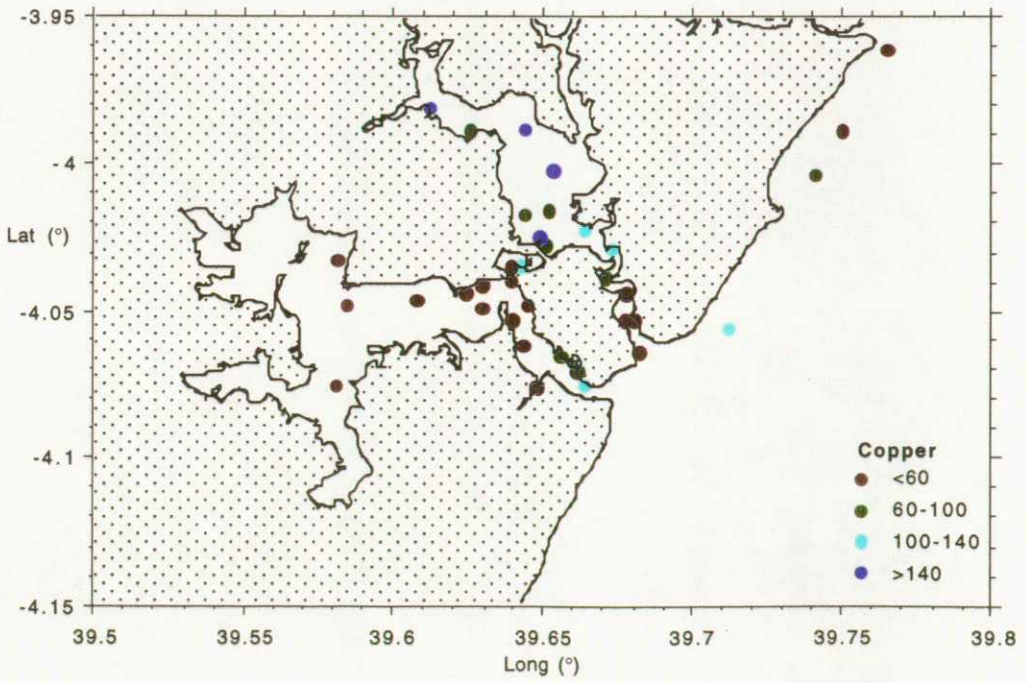

Figures 26-27: Mass-specific concentration of Zn and V in SPM from Mombasa.

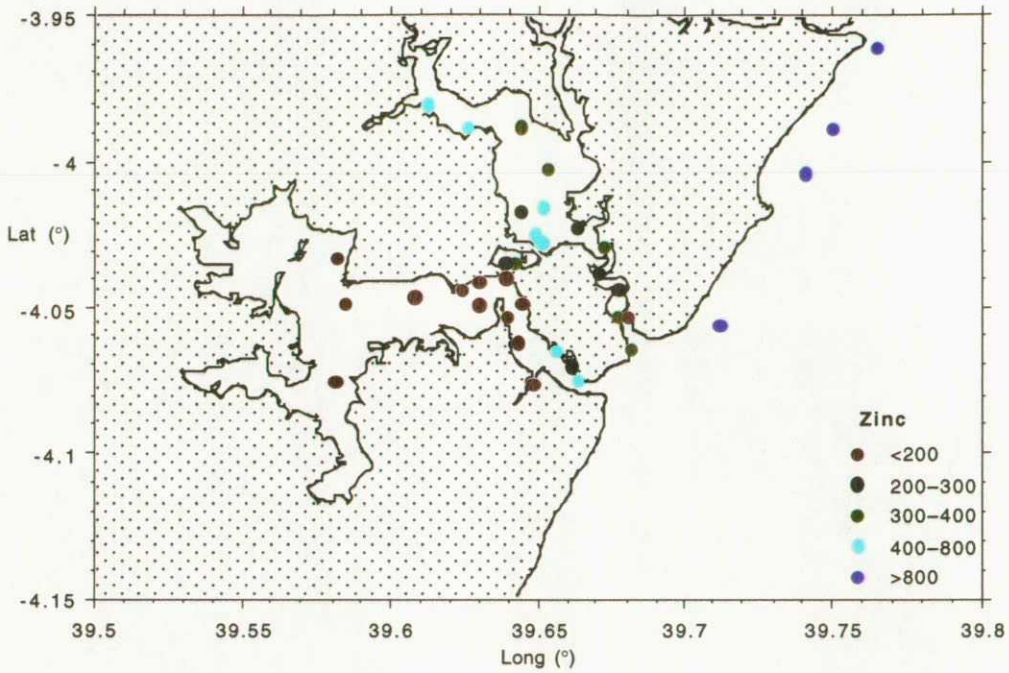

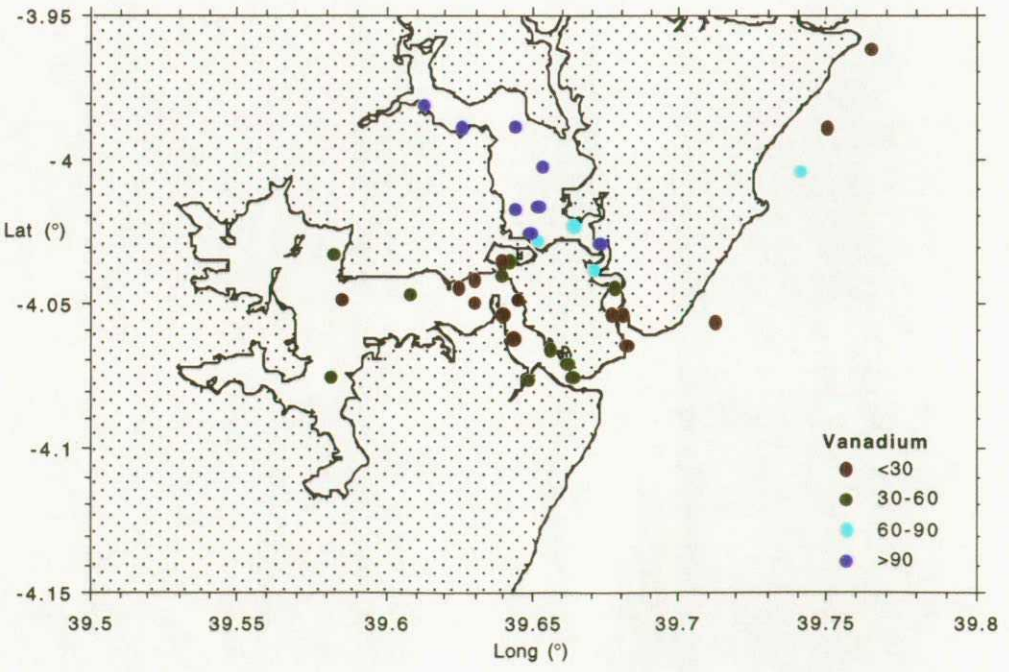

from Makupa Creek (max. 516 mg/kg), enrichment of Pb in reef-front samples (max. 112 mg/kg) and low concentrations of Ni, Cu, Zn, As, Mo, Cd and Pb in Port Reitz. Pearson correlation coefficients for the 13 analysed trace elements (Table 9) confirm the close interrelationship of Mn, V, Cr, Co and As (R >0.8 using Mn as the 'x' variable) graphically portrayed in Figs. 20-27. Weaker, yet analogous affinities are displayed by Cu, Mo and Ni. A second statistically covariant group comprises Zn, Pb and Cd.

Figure 28: Geochemical signatures of SPM in selected inshore waters around Mombasa. Arithmetic means have been utilised in the production of spidergrams for Tudor Creek (n = 4), Mombasa Harbour (n = 6), Kilindini (n = 4), Port Reitz (n = 4) and the North Coast reef front (n = 4). Makupa Creek is represented by a single sample (MB22).

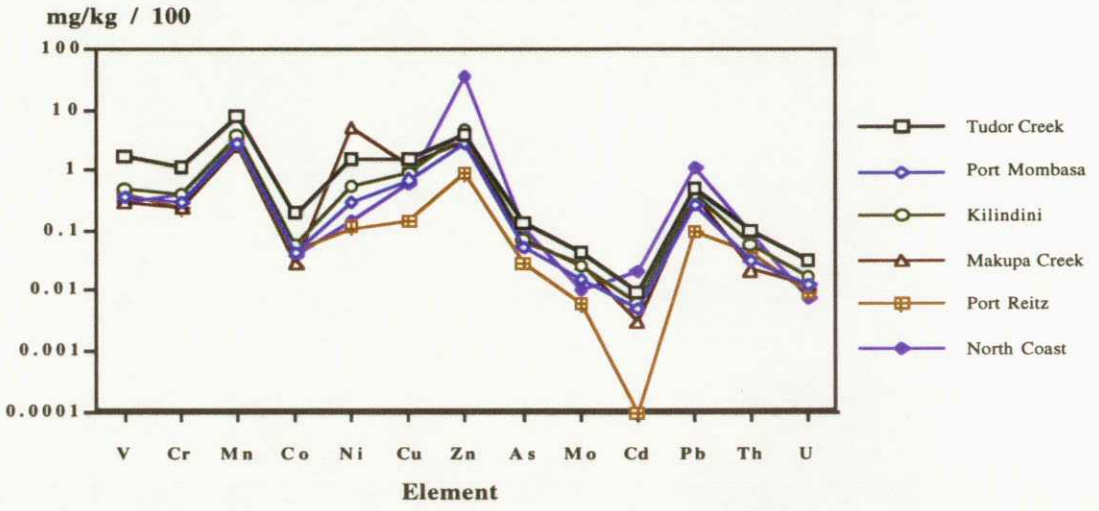

The observed patterns of trace element enrichment in SPM are unrelated to urban settlement or industrial activity. Detrital rather than anthropogenic inputs are thus considered likely to dominate the total particulate metal flux to the inshore waters. The prevalence of Cu, Ni, Cr, V, Co and As in Port Kilindini and Port Reitz (which host all major shipping, petrochemicals and sewage installations) at concentrations up to an order of magnitude lower than in the (unindustrialised) catchment of Tudor Creek reflects fundamental contrasts of SPM source and composition, compounded by differing surface chemistries and water column behaviour.

The contribution of mangrove-derived detritus to total the SPM budgets of the respective inshore water bodies is critical. Fine-grained mangrove muds are routinely enriched in a wide range of trace metals (up to 1% Mn, 1000 mg/kg Zn and 500 mg/kg of most other first-row transition elements) relative to other coastal and intertidal sediments (eg. Badarudeen et al., 1996). Such enrichment reflects the presence of a ubiquitous hydrous Fe/Mn oxide coating on

the fine-grained superficial material, the ability of which to concentrate elements such as Co, Zn, Ni, V and As by surface adsorption has been well documented (e.g. Balistrieri and Murray, 1986, Williams, 1992). In the inshore lagoonal systems of Mombasa, scavenging of trace metals (resulting in strong statistical covariation with Mn, as indicated in Table 9) occurs initially in the mangrove environment, and may continue following the outwash of Fe/Mn oxide-rich particulates into the water column. In the latter environment, the capacity of SPM to accumulate metals will be significantly influenced by residence time (ie. the time available for the operation of surface exhange and sorption/desorption processes). High levels of trace metal enrichment in hydrous-oxide-bearing SPM from the uppermost reaches of Tudor Creek may therefore be anticipated relative to SPM from lower Tudor Creek, Port Kilindini, lower Port Reitz, Makupa Creek or the North Coast reef-front, on account of the longer residence time prevailing in the former area (see section 3.1.2.1).

X-ray fluorescence analyses of the <63 μm fraction of mangrove muds from the Mombasa hinterland have confirmed the presence of concentrations of Mn, Zn, Ni, Cr, V and Co which lie within 20% of the mean for SPM from upper Tudor Creek sites MB1-MB4, suggesting that wave-erosion of mangrove flats constitutes the principal source of particulate matter in these waters. With the exception of the north-western sector of Port Reitz, the margins of the inland lagoons to the west and south-west of Mombasa Island (Kilindini, Makupa, Port Reitz) are less dominated by mangroves than the catchment of Tudor Creek. Their significance as a source of SPM may thus be correspondingly lower. In Port Reitz, the terrestrial component of SPM mainly comprises clastic detritus derived from the erosion of Jurassic shales. A substantial marine inorganic/algal component may also be supplied by each flood-tide. Although also supplied to Port Tudor, the influence of this algal component on the geochemical signature of the SPM is less pronounced in this area, due to the higher clastic loading.

3.3: Sediment geochemistry.

3.3.1: Sampling and analysis:

Sediment samples were collected from a total of 47 stations within the inshore and reef-front waters of Mombasa during September 1995 (see Fig. 8 for locations), with selected sites (MB1, MB5, MB20, MB23, MB27, MB29) re-sampled in January 1996. During the 1995 survey, a 20 kg Wildco™ gravity corer of 0.5 m length (Fig. 29) was used at all sites with silty or clay-rich sediments. A 1.1 m pneumatic piston corer (Fig. 30) was used during the 1996 survey. This system facilitated core recovery with minimal disturbance of the interfacial layer, and was utilised specifically at sites considered (on the basis of data from the 1995 campaign) to have potential for the retention of sedimentary pollution chronologies. Approximately 8 sampling sites in the lower reaches of Mombasa Harbour, Port Kilindini and along the Nyali-Mtwapa reef-front were dominated by quartzo-feldspthic or carbonate sand sediments, into which the

gravity and piston corers failed to penetrate. In these instances, samples of the uppermost 5-10 cm of sediment were obtained using a Van-veen grab sampler of stainless steel construction.

Figure 29: Wildco gravity corer used for sampling of stratified mud and silt lithologies in the inshore waters of Mombasa in 1995.

Figure 30: Pneumatic piston corer, used for sampling of stratified mud and silt lithologies in the inshore waters of Mombasa in 1996.

All sample cores were retained upright in sealed perspex tubes during transport to the laboratory, and were sub-sampled at 2-5 cm resolution on extrusion within 24 hours of collection. Core sub-samples and grab samples were transported to the UK in air-tight securitainers or polythene bags. Further sub-sampling was then undertaken to produce aliquots for bulk geochemistry, solid-phase speciation and sediment grain size analyses.

The concentrations of 10 major oxides and 13 minor or trace elements were determined in a total of 252 samples (representing a maximum of c. 20 stratigraphic levels per sampling station) by XRF analysis of 12 g pressed pellets. The partitioning of elements between detrital, hydrous oxide and organic fractions of sediments was established using a sequential extractive procedure based on that developed by Breward and Peachey (1983). This entailed the initial application of 1N HN_4OAc to 1g (wet weight) samples to remove adsorbed/exchangeable metals. Ammonia was then used to extract the organic fraction of the sediment, from which the fulvic and humic components were then separated by HCl precipitation. The inorganic residue was heated in 0.1N $NH_2.OH.HCl$ in 25% v/v HOAc to extract hydrous Fe and Mn oxides. The residuum was then digested in HNO_3+$HClO_4$+HF to liberate metals held in detrital silicates and other residual minerals. The leachates from each stage of the procedure were diluted to an appropriate volume and analysed for 11 elements (Fe, Mn, Al, Co, Cr, Cu, Pb, Zn, V, Ni and Cd) by ICP-ES. Reagent blanks were prepared and simultaneously analysed with each leachate. The procedures and results of granulometric analyses of sediment samples are descibed elsewhere (Rees et al., 1996).

Surficial sediment samples from 6 Mombasa stations (MB1, 5, 20, 23, 27 & 30), plus several sub-surface samples from station MB23 were selected for the determination of petroleum compounds, organochlorines and polycyclic aromatic hydrocarbons (PAH's) by high pressure liquid chromatography (HPLC) and gas chromatography. A hexane solvent was used for extraction in all instances. Surficial samples from stations MB1 and MB23 were scanned to ascertain the concentration of additional organic contaminants (including PCBs) within the matrix using GC mass spectrometry (GCMS).

3.3.2: Metal distribution in surficial sediments:

The distribution of the 10 major oxides and 13 trace elements analysed in surficial sediments (0-2 cm depth in gravity & piston core samples; 0-10 cm depth in grab samples) from all sampling stations is shown in Figs. 31-52, with descriptive statistics and inter-element correlations given in Tables 10-11. The distribution of major oxides suggests that basic lithofacies variations within the inshore and reef-front environments can be explained in terms of the variable mixing of terrigenous and marine biogenic carbonate 'end-members'. Terrigenous detritus (enriched in

Table 10: Descriptive statistics for surficial sediments from Mombasa. All major oxide concentrations are given in %, trace elements in mg/kg.

	SiO2	TiO2	Al2O3	MnO	MgO	Fe2O3	CaO	Na2O	K2O	P2O5	Ni	Cu	Zn
Mean	46.212	.638	11.548	.035	2.016	4.410	8.079	3.759	2.097	.116	19.409	47.023	84.523
Count	44	44	44	44	44	44	44	44	44	44	44	44	44
Minimum	2.930	.008	.230	.005	1.000	.060	.300	1.700	.190	.025	1.000	1.000	3.000
Maximum	64.460	1.223	16.910	.074	3.000	8.340	44.840	10.000	3.330	.390	38.000	1177.000	283.000
# Missing	0	0	0	0	0	0	0	0	0	0	0	0	0
Median	48.705	.684	12.905	.034	2.100	4.950	3.365	2.950	2.285	.110	21.000	18.000	69.500

	Cr	Sn	V	Co	Sr	Zr	Mo	Pb	Ba	Cd	As
Mean	52.682	2.841	76.545	13.159	600.023	337.273	2.977	34.273	361.523	1.534	9.750
Count	44	44	44	44	44	44	44	44	44	44	44
Minimum	.500	1.500	3.000	.500	75.000	1.000	.500	1.000	34.000	1.500	1.000
Maximum	106.000	19.000	163.000	26.000	4118.000	1502.000	5.000	427.000	660.000	3.000	18.000
# Missing	0	0	0	0	0	0	0	0	0	0	0
Median	57.000	1.500	82.000	14.000	233.500	256.000	3.000	21.500	353.000	1.500	10.000

	SiO2	TiO2	Al2O3	MnO	MgO	Fe2O3	CaO	Na2O	K2O	P2O5	Ni	Cu	Zn	Cr	Sn	V	Co	Sr	Zr	Mo	Pb	Ba	Cd	As
SiO2	1.00	.60	.68	.33	-.55	.51	-.89	-.09	.82	-.10	.44	-.08	.14	.51	<0.1	.51	.56	-.84	.53	.49	-.04	.84	-.10	.28
TiO2	.60	1.00	.91	.70	.09	.95	-.84	.36	.85	.06	.93	-.02	.37	.97	.04	.96	.90	-.80	.08	.49	.04	.37	-.06	.51
Al2O3	.68	.91	1.00	.70	.11	.90	-.90	.36	.88	-.09	.89	-.02	.38	.90	-.03	.88	.85	-.86	-.02	.49	.05	.49	-.06	.47
MnO	.33	.70	.70	1.00	.25	.73	-.57	.39	.55	.03	.71	.11	.30	.71	-.01	.68	.68	-.59	-.20	.32	.15	.23	.07	.53
MgO	-.55	.09	.11	.25	1.00	.20	.25	.34	-.17	.02	.28	.15	.19	.20	-.04	.16	.10	.18	-.64	-.12	.16	-.56	.13	.17
Fe2O3	.51	.95	.90	.73	.20	1.00	-.79	.45	.80	.01	.96	.05	.38	.97	-.07	.98	.96	-.76	-.12	.43	.10	.27	.01	.63
CaO	-.89	-.84	-.90	-.57	.25	-.79	1.00	-.28	-.96	.07	-.75	.05	-.32	-.78	-.02	-.77	-.79	.95	-.29	-.56	-.02	-.71	.09	-.44
Na2O	-.09	.36	.36	.39	.34	.45	-.28	1.00	.33	.04	.51	-.03	.30	.39	.06	.38	.40	-.28	-.36	.15	.05	-.12	-.06	.36
K2O	.82	.85	.88	.55	-.17	.80	-.96	.33	1.00	.02	.79	-.03	.36	.81	.03	.81	.78	-.91	.24	.50	.04	.64	-.07	.48
P2O5	-.10	.06	-.09	.03	.02	.01	.07	.04	.02	1.00	<0.1	.16	.49	.07	.83	-.01	-.12	-.04	.40	.12	.26	.04	.13	.25
Ni	.44	.93	.89	.71	.28	.96	-.75	.51	.79	<0.1	1.00	.01	.45	.96	-.02	.95	.90	-.70	-.17	.50	.08	.20	-.04	.55
Cu	-.08	-.02	-.02	.11	.15	.05	.05	-.03	-.03	.16	.01	1.00	.53	.12	.21	-.04	.03	<0.1	-.06	.05	.97	.12	1.00	.14
Zn	.14	.37	.38	.30	.19	.38	-.32	.30	.36	.49	.45	.53	1.00	.48	.61	.30	.27	-.35	.09	.49	.67	.25	.48	.31
Cr	.51	.97	.90	.71	.20	.97	-.78	.39	.81	.07	.96	.12	.48	1.00	.03	.97	.92	-.75	-.05	.45	.17	.29	.07	.54
Sn	<0.1	.04	-.03	-.01	-.04	-.07	-.02	.06	.03	.83	-.02	.21	.61	.03	1.00	-.11	-.18	-.07	.47	.35	.35	.24	.17	.06
V	.51	.96	.88	.68	.16	.98	-.77	.38	.81	-.01	.95	-.04	.30	.97	-.11	1.00	.93	-.73	-.09	.37	<0.1	.25	-.08	.54
Co	.56	.90	.85	.68	.10	.96	-.79	.40	.78	-.12	.90	.03	.27	.92	-.18	.93	1.00	-.75	-.08	.45	.05	.29	<0.1	.56
Sr	-.84	-.80	-.86	-.59	.18	-.76	.95	-.28	-.91	-.04	-.70	<0.1	-.35	-.75	-.07	-.73	-.75	1.00	-.28	-.47	-.07	-.69	.04	-.47
Zr	.53	.08	-.02	-.20	-.64	-.12	-.29	-.36	.24	.40	-.17	-.06	.09	-.05	.47	-.09	-.08	-.28	1.00	.38	-.01	.60	-.06	-.06
Mo	.49	.49	.49	.32	-.12	.43	-.56	.15	.50	.12	.50	.05	.49	.45	.35	.37	.45	-.47	.38	1.00	.16	.45	<0.1	.25
Pb	-.04	.04	.05	.15	.16	.10	-.02	.05	.04	.26	.08	.97	.67	.17	.35	<0.1	.05	-.07	-.01	.16	1.00	.19	.96	.20
Ba	.84	.37	.49	.23	-.56	.27	-.71	-.12	.64	.04	.20	.12	.25	.29	.24	.25	.29	-.69	.60	.45	.19	1.00	.10	.10
Cd	-.10	-.06	-.06	.07	.13	.01	.09	-.06	-.07	.13	-.04	1.00	.48	.07	.17	-.08	<0.1	.04	-.06	<0.1	.96	.10	1.00	.11
As	.28	.51	.47	.53	.17	.63	-.44	.36	.48	.25	.55	.14	.31	.54	.06	.54	.56	-.47	-.06	.25	.20	.10	.11	1.00

Table 11: Pearson correlation matrix showing the inter-relationship between major and trace elements in surficial sediments from Mombasa.

Figs. 31-32: Distribution of SiO_2 and K_2O in surficial sediments of Mombasa

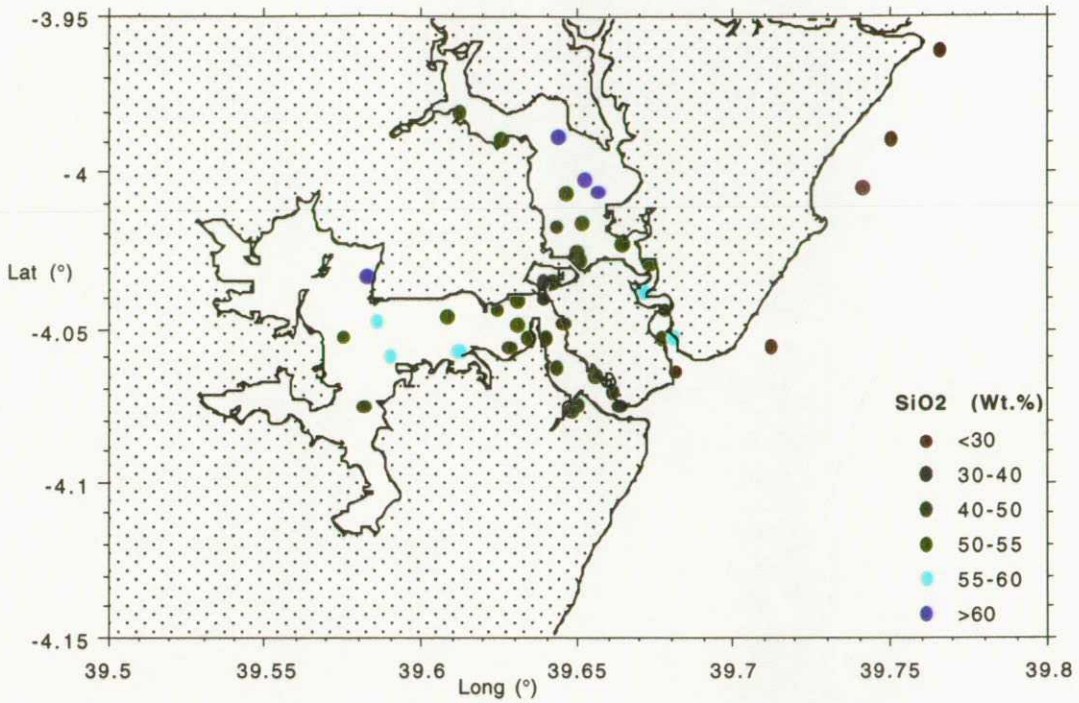

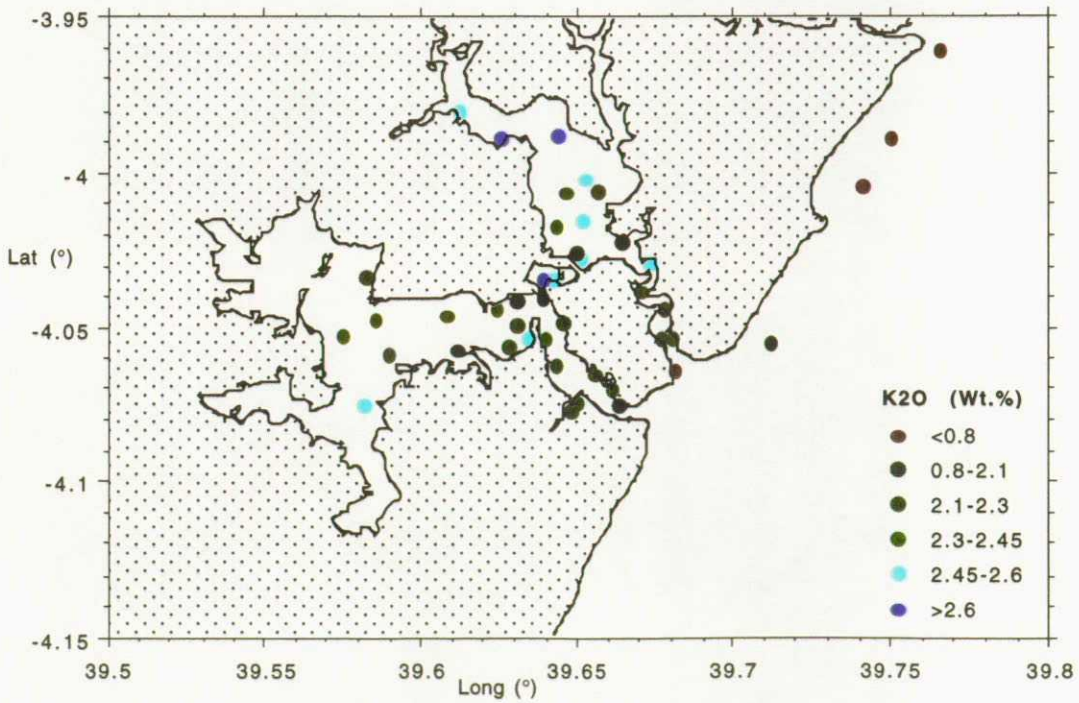

Figs. 33-34: Distribution of P_2O_5 and Al_2O_3 in surficial sediments of Mombasa

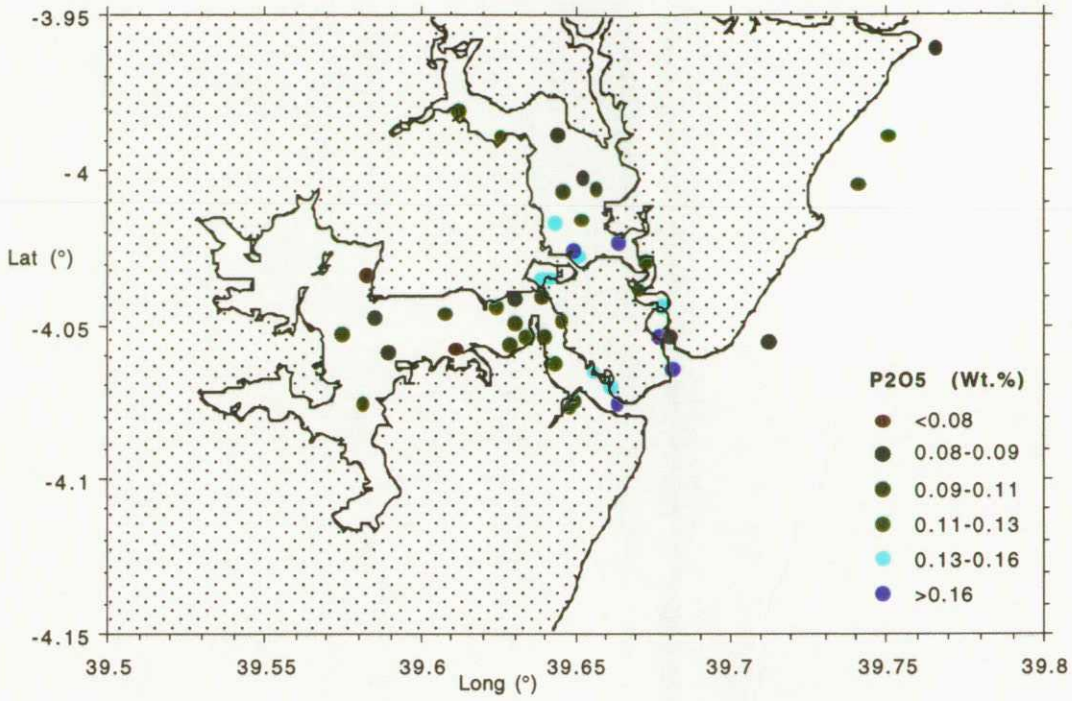

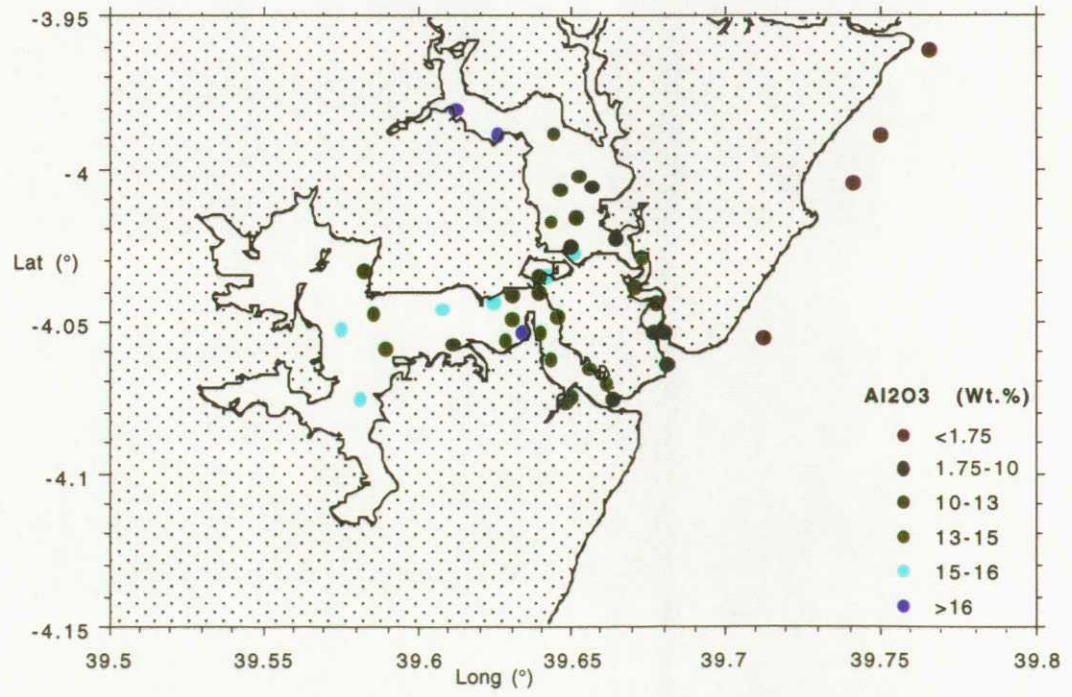

Figs. 35-36: Distribution of TiO_2 and CaO in surficial sediments of Mombasa

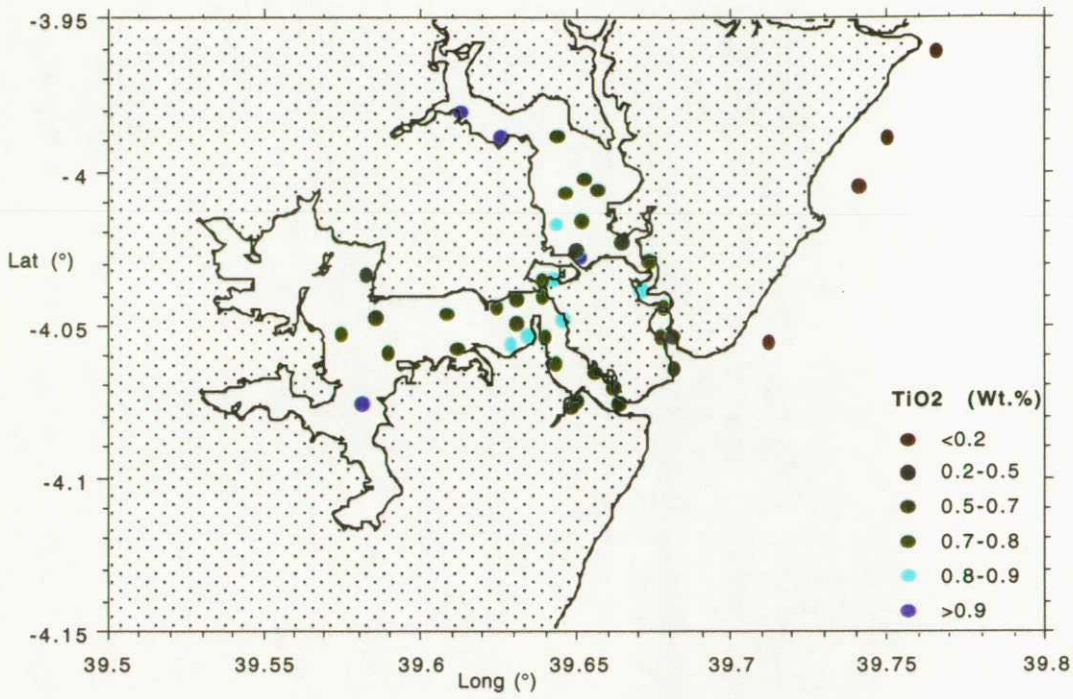

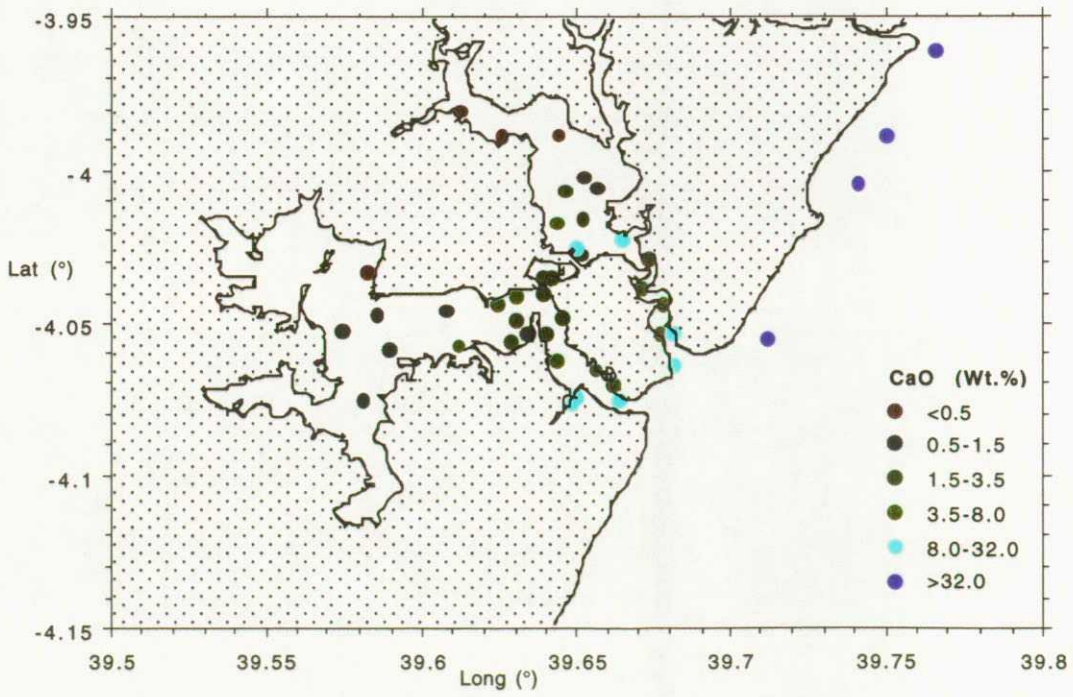

Figs. 37-38: Distribution of MgO and MnO in surficial sediments of Mombasa

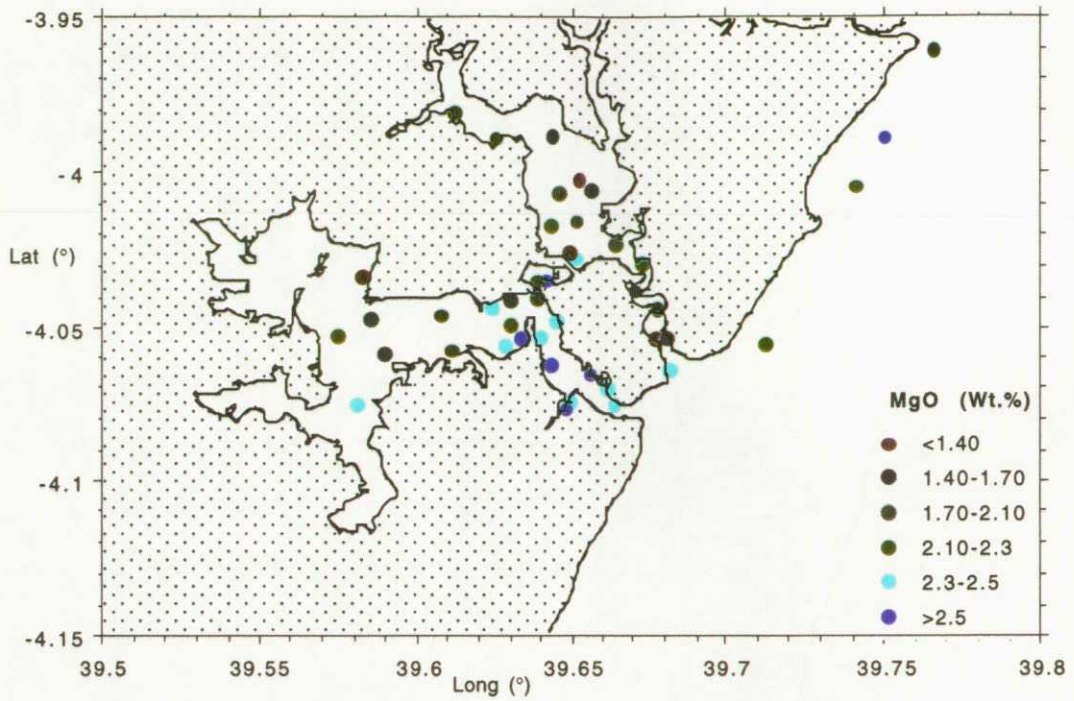

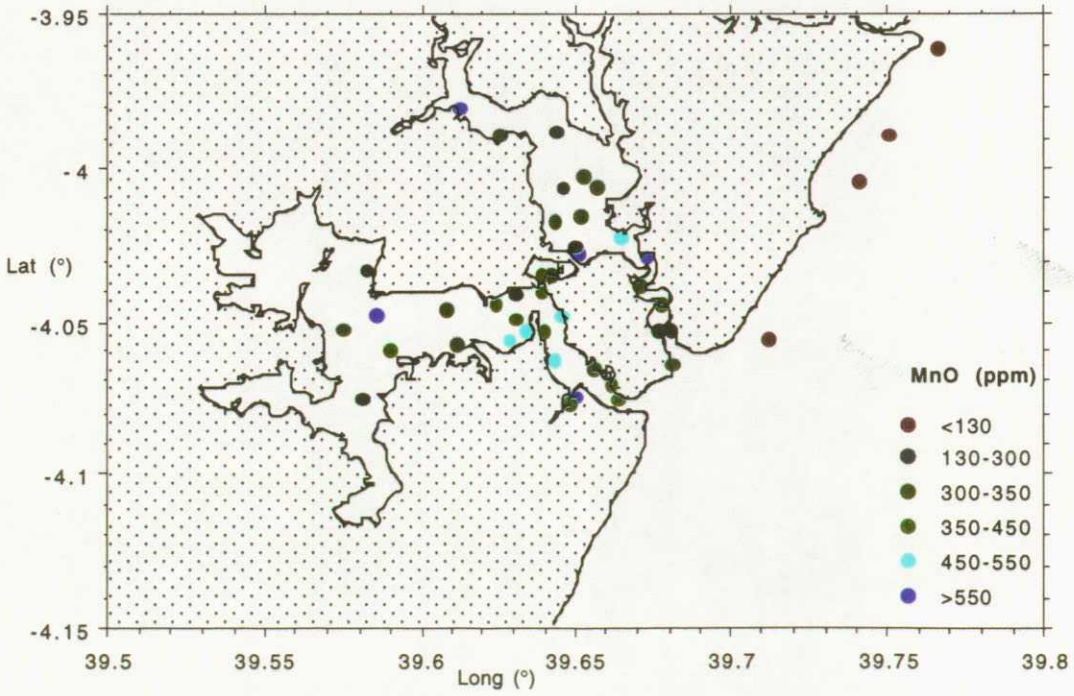

Figs. 39-40: Distribution of Na_2O and As in surficial sediments of Mombasa

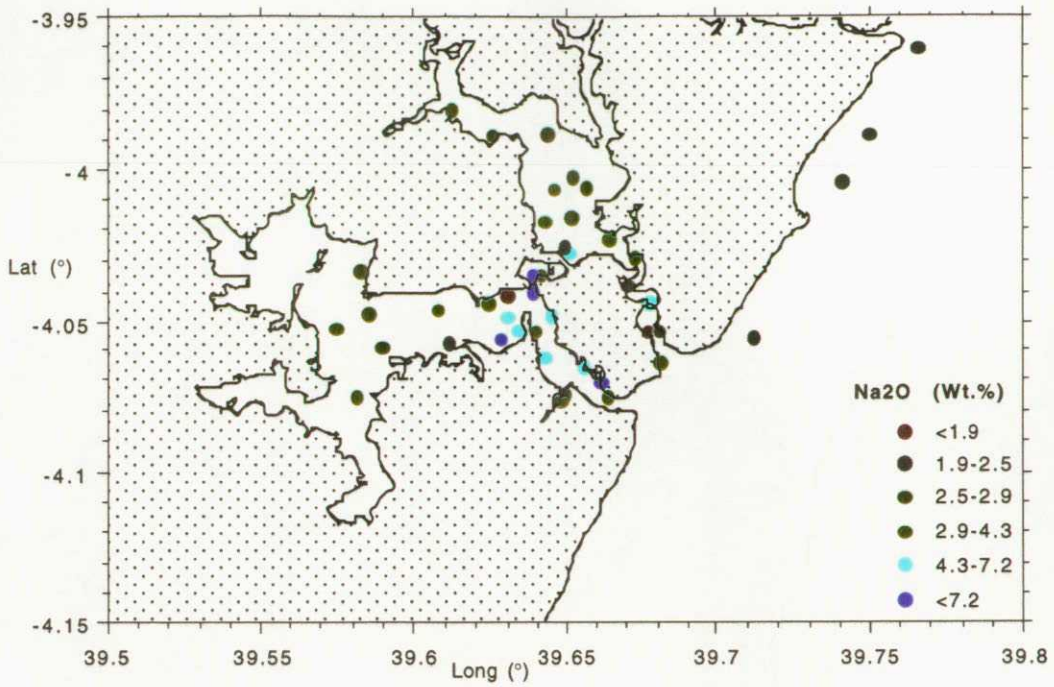

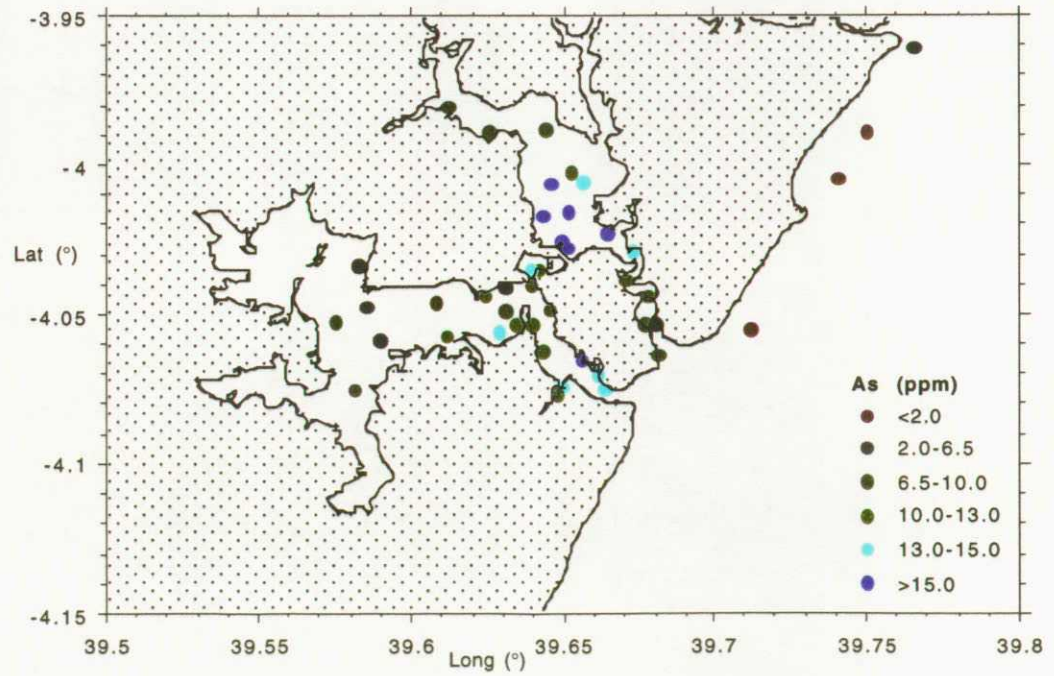

Figs. 41-42: Distribution of Sn and Ba in surficial sediments of Mombasa

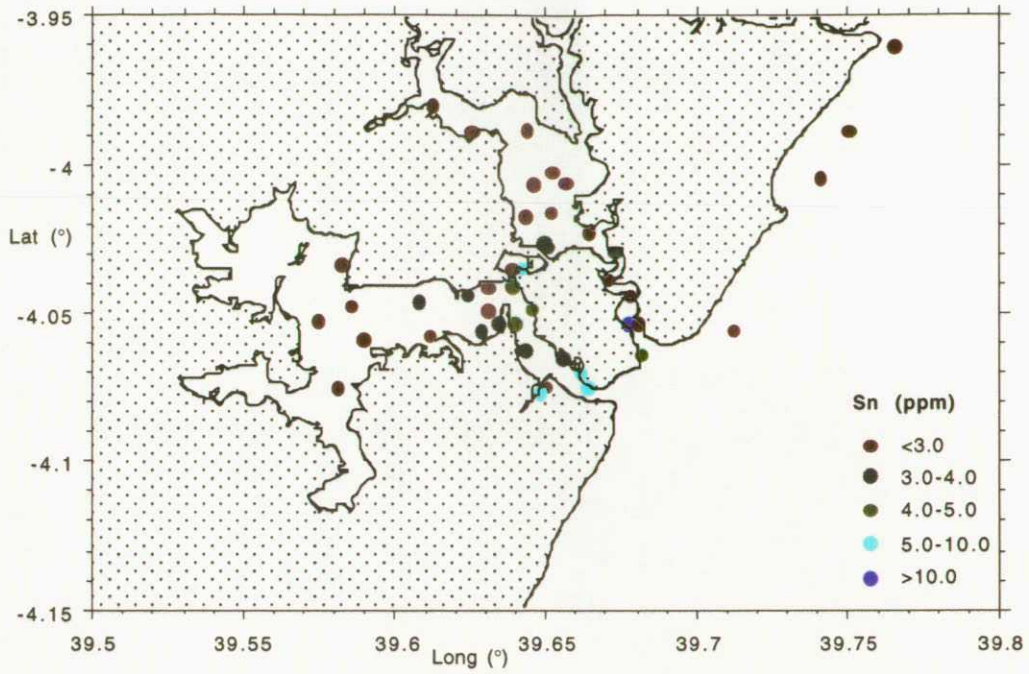

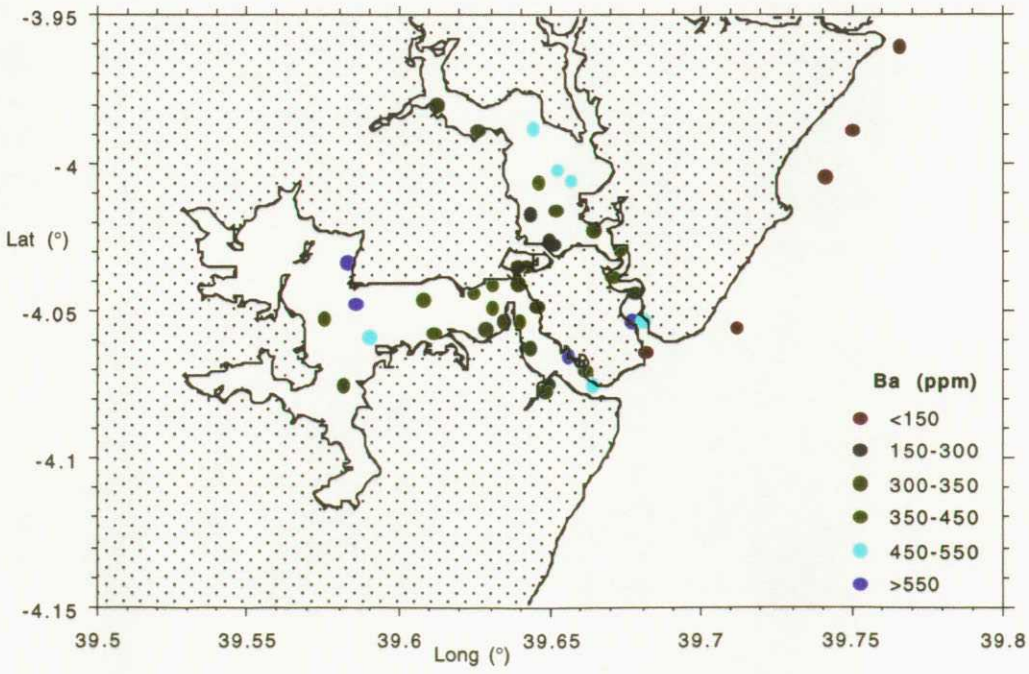

Figs. 43-44: Distribution of Pb and Mo in surficial sediments of Mombasa

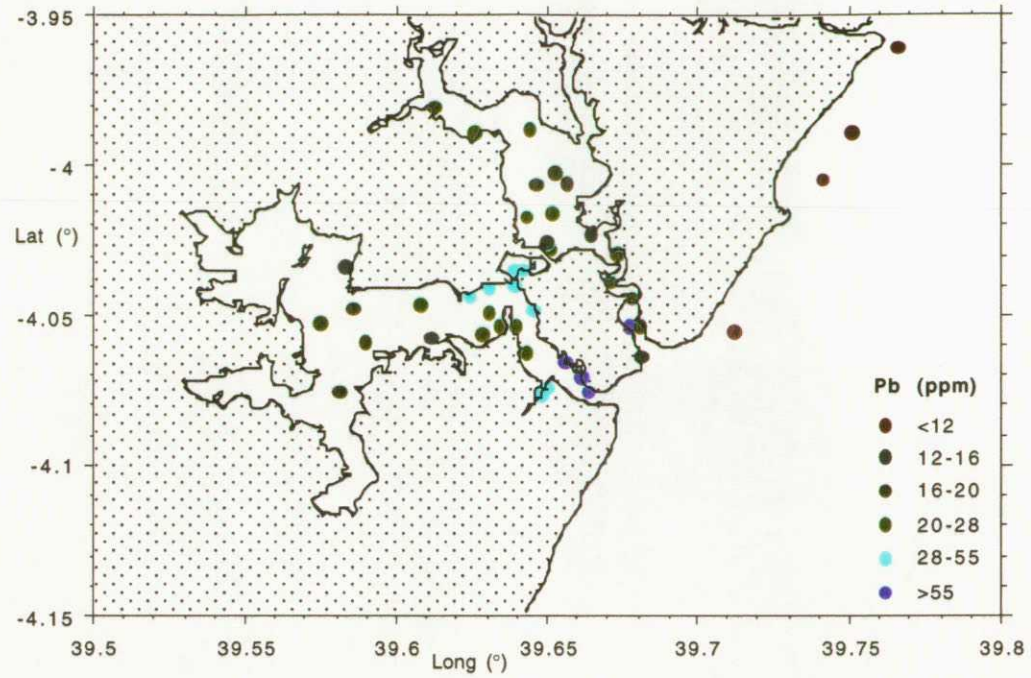

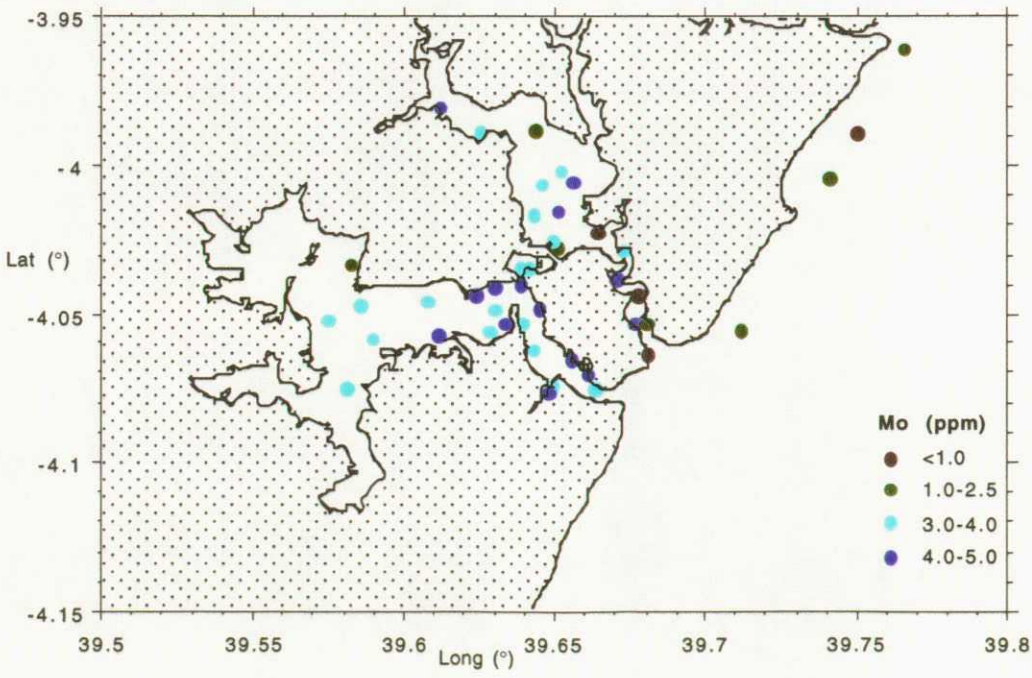

Figs. 45-46: Distribution of Zr and Sr in surficial sediments of Mombasa

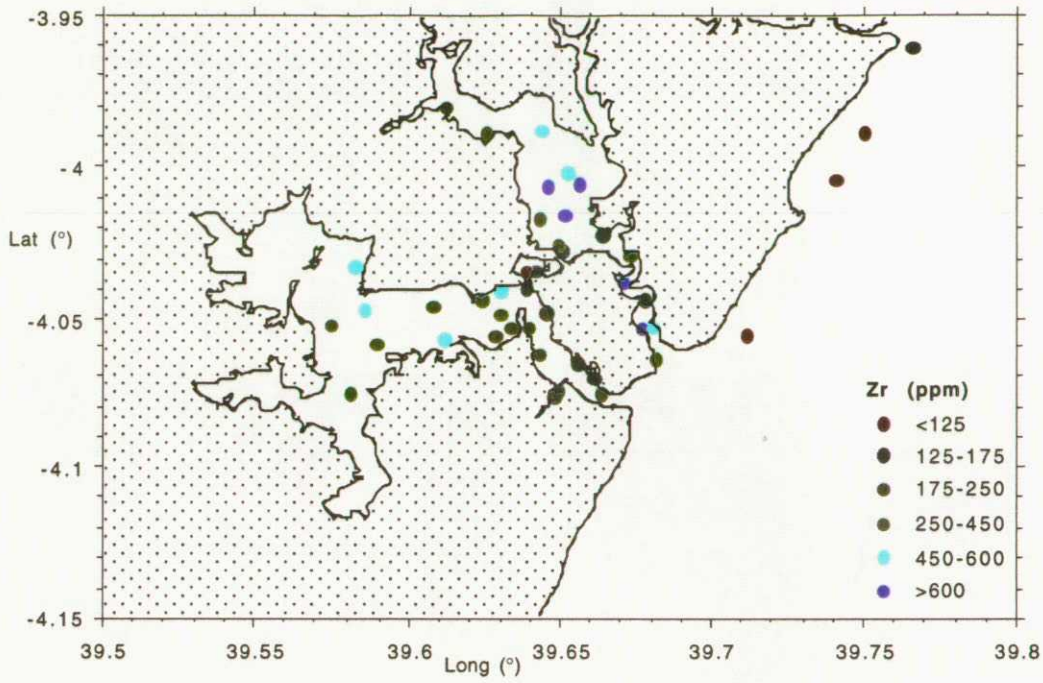

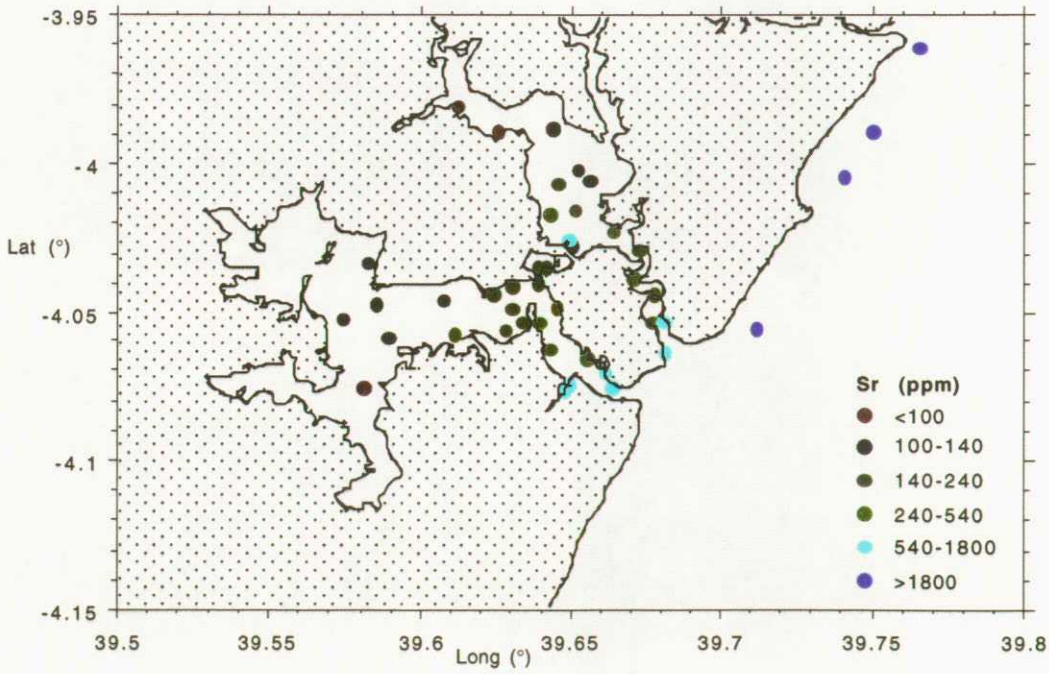

Figs. 47-48: Distribution of Pb and Mo in surficial sediments of Mombasa

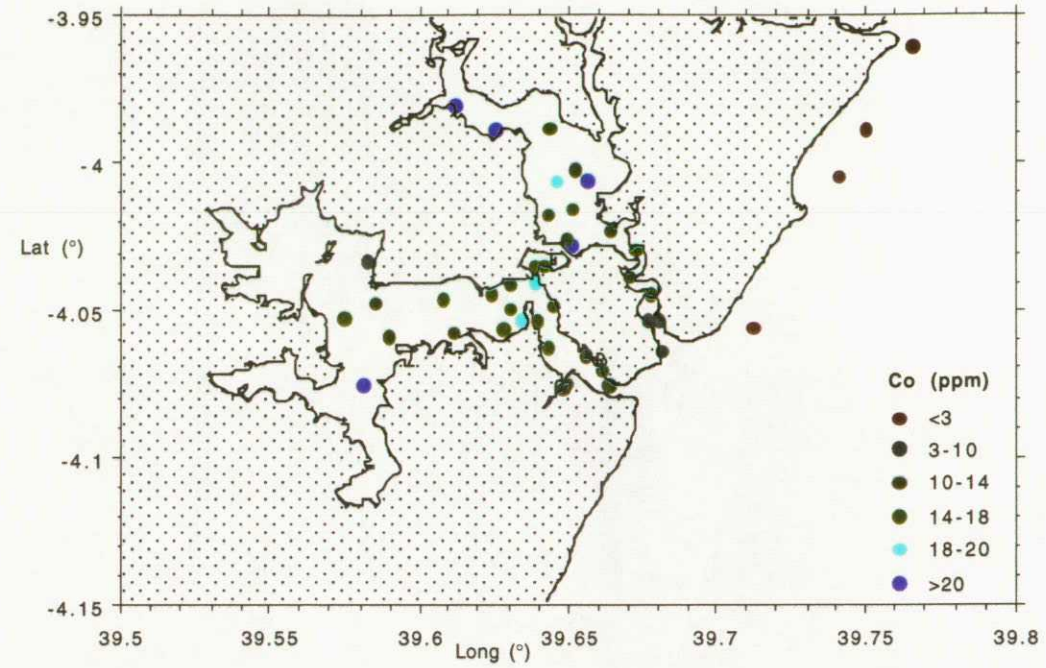

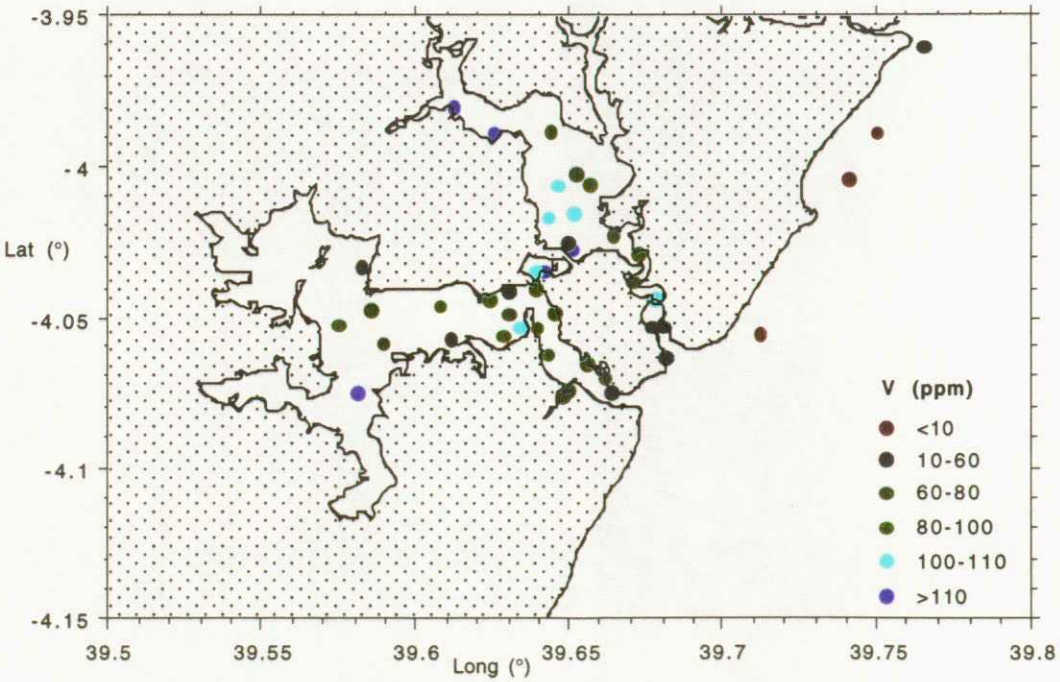

Figs. 49-50: Distribution of Cr and Cu in surficial sediments of Mombasa

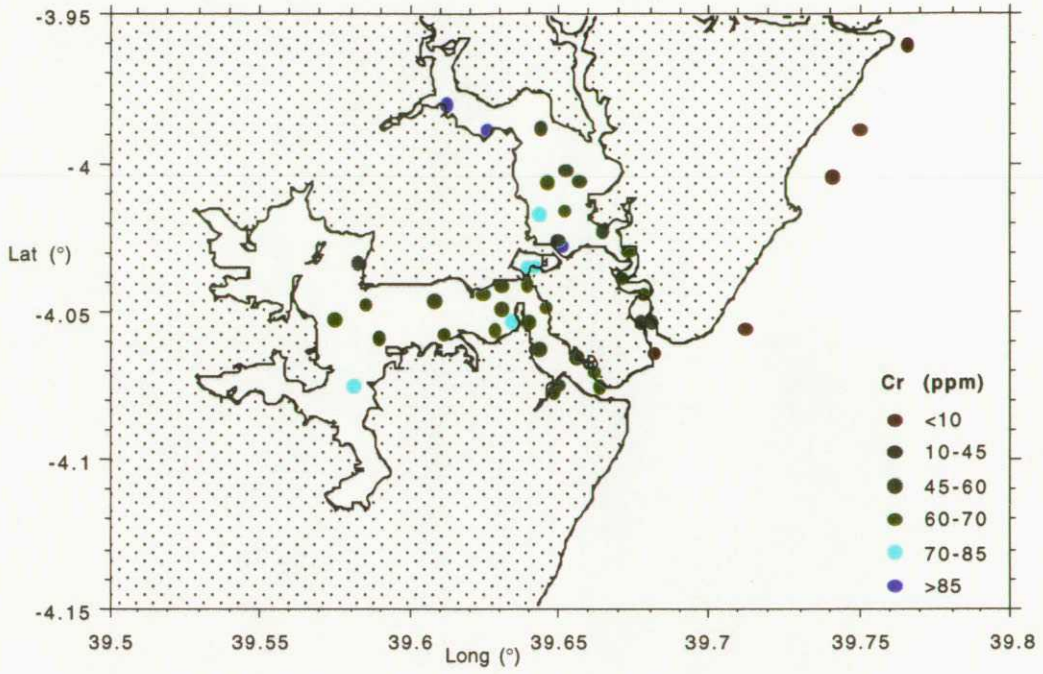

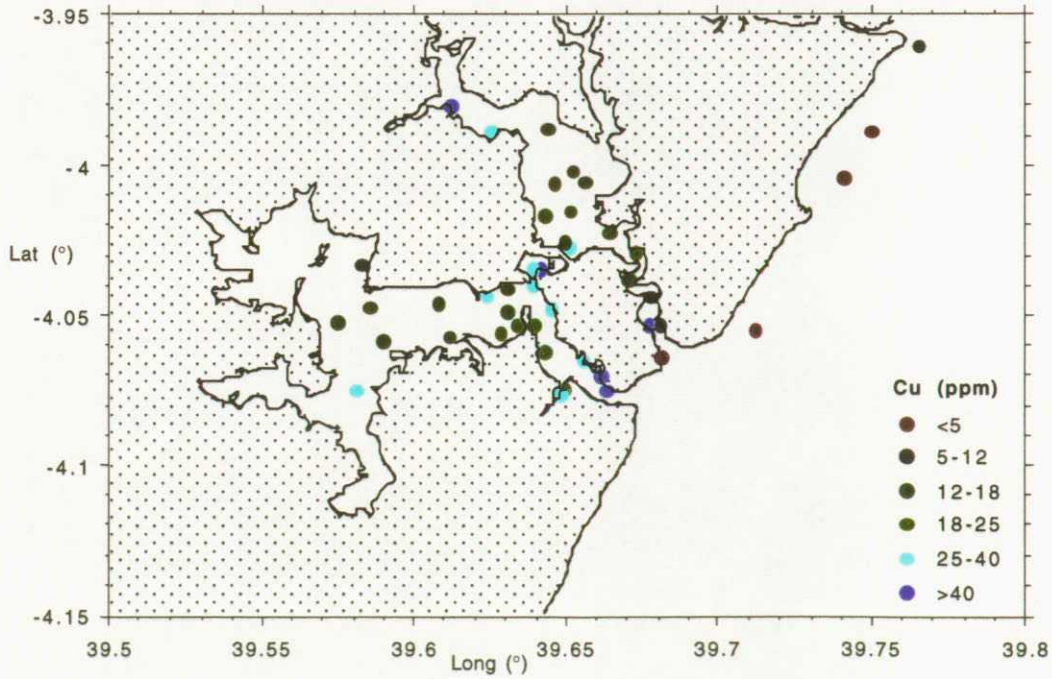

Figs. 51-52: Distribution of Zn and Ni in surficial sediments of Mombasa

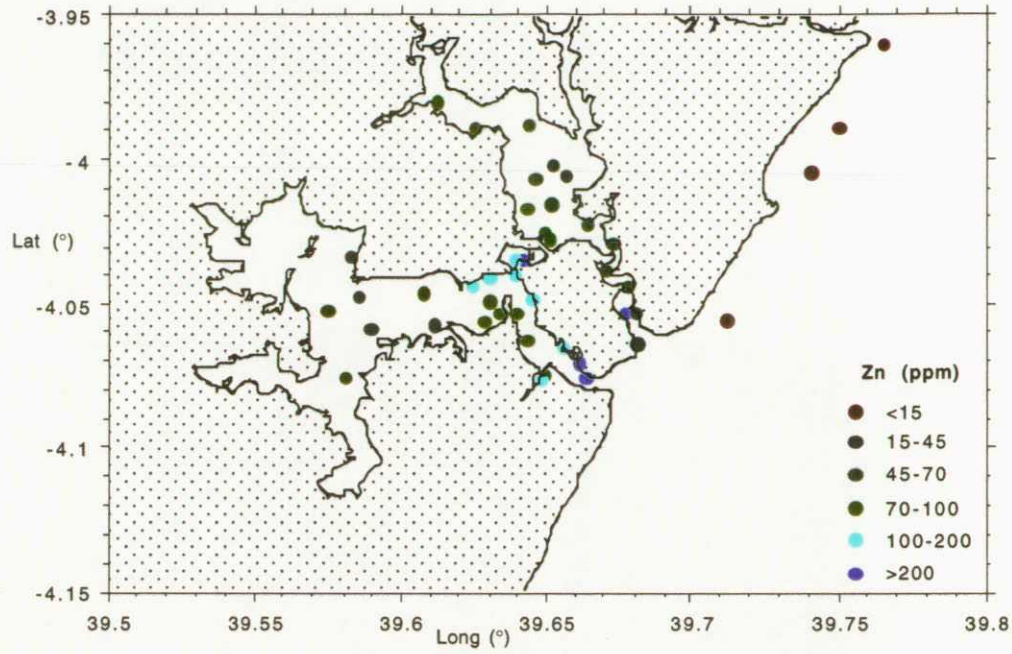

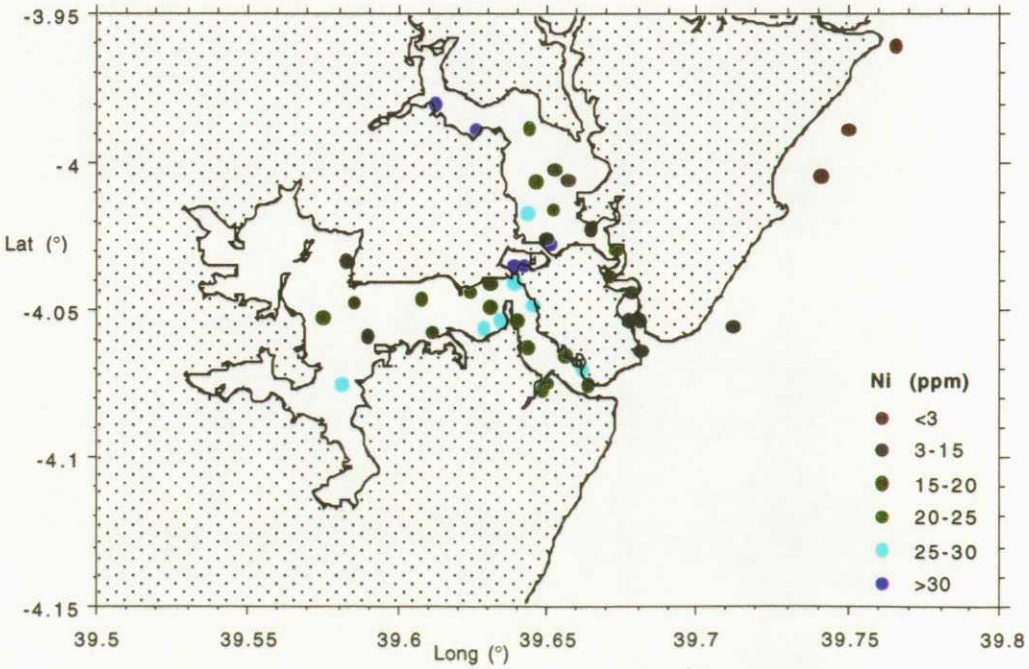

SiO_2, Al_2O_3, TiO_2 and K_2O) is supplied via the Komboni, Tsalu, Mwache and Shimba rivers into Tudor Creek and Port Reitz, and is geochemically predominant in the upper reaches of Tudor Creek. Granulometric sorting of terrestrially-derived detritus in this area has resulted in clear geochemical zonation. Silt-clay sediments characterised up to 15% Al_2O_3 and 2.5% K_2O occupy the low energy marginal settings (including mangrove flats), while the higher energy channel environment extending into central Port Tudor is characterised by coarser sandy sediments (>60% SiO_2). Carbonate sands (characterised by >30% CaO and only trace concentrations of SiO_2 and Al_2O_3) are the dominant lithofacies along the Nyali-Mtwapa reef-front. The transport gradient of this material into the inland waters of Mombasa is portrayed by the sediment CaO content, which declines from >8% at the estuary mouths (lower Mombasa Harbour and Likoni) to 3-8% in upper Mombasa Harbour and Port Kilindini, and <3% in much of Port Tudor and Port Reitz.

Trace element abundances in all Mombasa sediments show a substantial lithological control. Inter-element Pearson correlation coefficients for surficial sediments (Table 11) indicate marked covariance of a first-row transition metal group comprising Ni, Cr, V and Co with Al_2O_3 and TiO_2 ($R > 0.75$). The relationship is primarily controlled by the presence of fine terrestrial clastic material. Disproportionate enrichment of hydrous oxides in such material is indicated by a strong correlation between Al_2O_3 and MnO ($R = 0.70$). These secondary oxides may provide an important carrier of first-row transition metals (e.g. Ni, V, Co) within the matrix. Evidence of an anthropogenic control on the distribution of trace metals in this behavioural group is limited, with the exception of Makupa Creek sites MB 22 and MB23 which display Ni, Cr and V enrichment beyond the levels directly attributable to lithology. The highest concentrations recorded in the entire study area for Ni (43 mg/kg), Cr (112 mg/kg), V (179 mg/kg) and Co (31 mg/kg) are within c. 50% of the global average for marine shales (Ni 80 mg/kg, Cr 100 mg/kg, V 130 mg/kg, Co 20 mg/kg; Krauskopf, 1979).

A strong statistical association with SiO_2 is displayed by Ba and Zr. These elements have a predominantly terrestrial source and are disproportionately enriched (>450 mg/kg) in the quartzose sands which occupy the high energy channel environment of central Port Tudor. Heavy minerals such as barite and zircon are the most likely carrier phases.

A discrete group of heavy metals comprising Pb, Zn and Cu show considerable independence from any lithological or granulometric control, yielding weak or negative correlations with SiO_2, Al_2O_3 and TiO_2 (Cu max. $R = -0.02$, Zn max. $R = 0.38$, Pb max. $R = 0.05$; Table 11) and strong within-group covariability ($R = 0.97$ for Pb vs. Cu, 0.67 for Pb vs. Zn). Anomalous concentrations of these elements (2 SD > mean) are recorded in the lower reaches of Port Kilindini (max. 427 mg/kg Pb, 283 mg/kg Zn, 1177 mg/kg Cu), Makupa Creek (max. 44 mg/kg Pb, 225 mg/kg Zn, 43 mg/kg Cu), the north-eastern shore of Port Reitz (max. 30 mg/kg

Pb, 190 mg/kg Zn and 26 mg/kg Cu) and on the east of Mombasa Island north of Fort Jesus. This distribution is consistent with a predominantly anthropogenic control. Anomalies highlight specific point-sources including Kipevu oil terminal and the adjacent sewage plant (Port Reitz), Kibarani landfill (Makupa Creek) and sewage outfalls from Mombasa Island into Port Kilindini and Mombasa Harbour.

Strontium is closely covariant with CaO (R=0.91) and negatively correlated with most indicators of terrestrial detritus, consistent with the partitioning of Sr into most carbonate matrices by lattice substitution for Ca.

3.3.3: Downcore metal variations:

3.3.3.1: Major oxides: Downcore concentration profiles for major oxides and trace elements at 6 Mombasa coring stations (including sites from Tudor Creek, Port Kilindini, Makupa Creek and Port Reitz) are shown in Figs. 53-58. The fundamental controls on downcore geochemical variations are analogous at all Mombasa coring sites, and the trends evident within these cores can therefore be considered representative of the entire study area.

Textural and mineralogical heterogeneity is evident through the uppermost 20-30 cm of sediment at all stations. Tudor Creek and Port Tudor cores (e.g. MB1 and MB5, Figs. 53-54) show a characteristic downcore transition from predominantly argillaceous clastic sediment to a coarser assemblage of quartzo-feldspathic sand and marine-derived shell fragments, possibly corresponding to lateral migration of a channel. The transition is geochemically reflected by a 20-40% increase in SiO_2, a six-fold increase in CaO, and a negatively correlated adjustment of Al_2O_3, TiO_2 and K_2O concentrations downward of 15-20 cm. Similar antipathetic relationships between the profiles of major oxides carried in quartzose sand (SiO_2) or shelly detritis (CaO) and terrigenous clastic material (Al_2O_3, TiO_2 and K_2O) are evident in cores from Kilindini (e.g. MB20, Fig. 55), Makupa Creek (cores MB22 and MB23, Figs 56-57) and Port Reitz (e.g. MB31, Fig. 58). Reduced concentrations of most major oxides in the uppermost 1-2 cm of sediment (relative to the underlying strata) are evident at the majority of sites and reflect the dilution of inorganic detritus by active organic matter.

In contrast to all other major oxides, the downcore profiles for Mn show no major lithological control. Statistical relationships between Mn and SiO_2, CaO, Al_2O_3, TiO_2 and K_2O in sub-surface profiles are inconsistent (Tables 12-17). Concentrations of Mn characteristically increase progressively through the uppermost 3-6 cm of sediment, consistent with the upward diffusion of Mn^{2+} through anoxic pore-waters, with subsequent precipitation of Mn^{4+} oxides in the aerobic interfacial zone (e.g. Williams et al., 1992).

Figure 53: Downcore distribution of selected major oxides (%) and trace elements (mg/kg) in sediments at Mombasa station MB1.

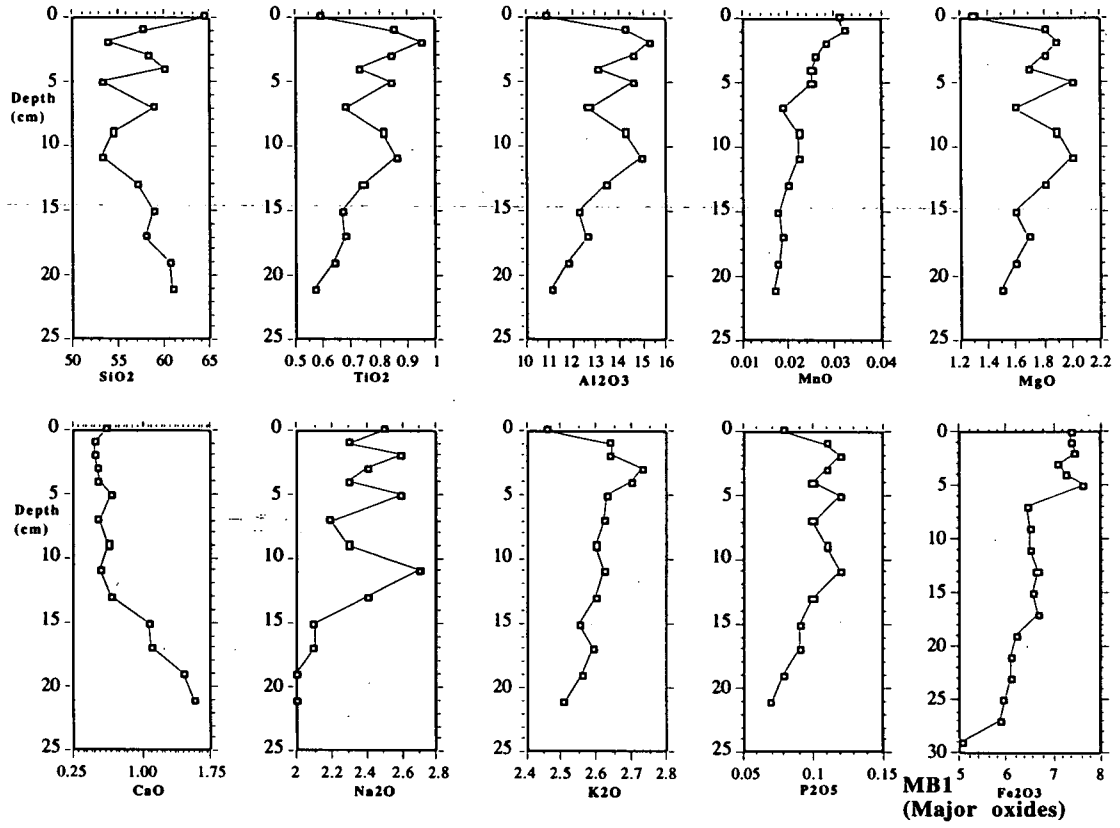

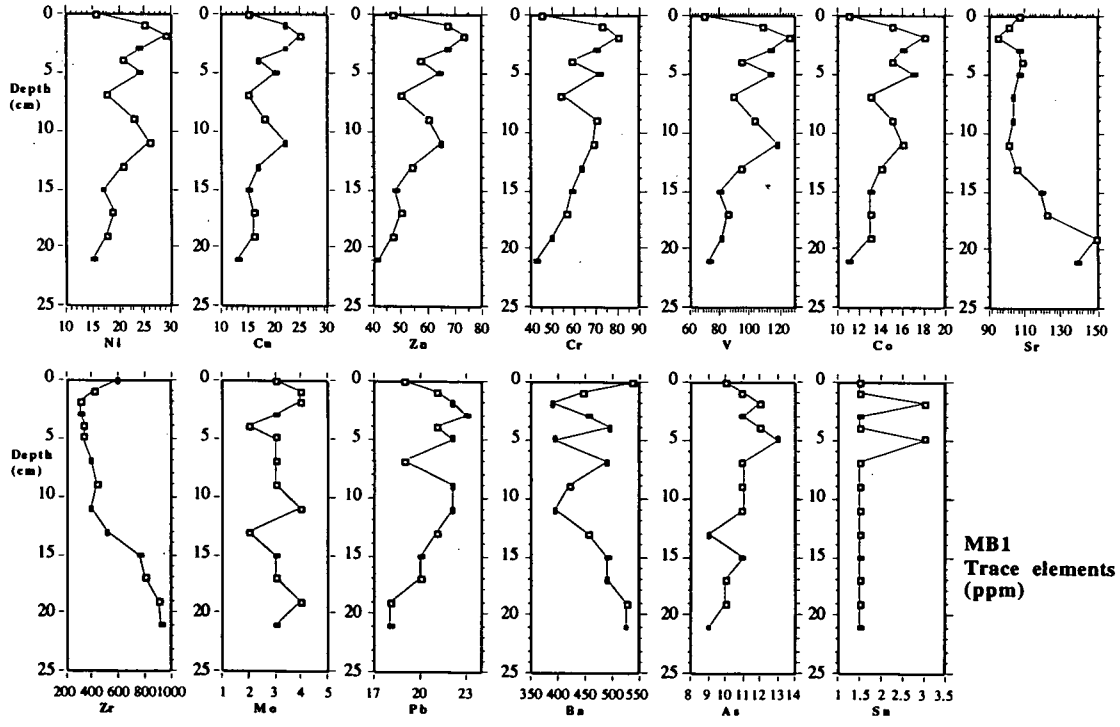

Figure 54: Downcore distribution of selected major oxides (%) and trace elements (mg/kg) in sediments at Mombasa station MB5.

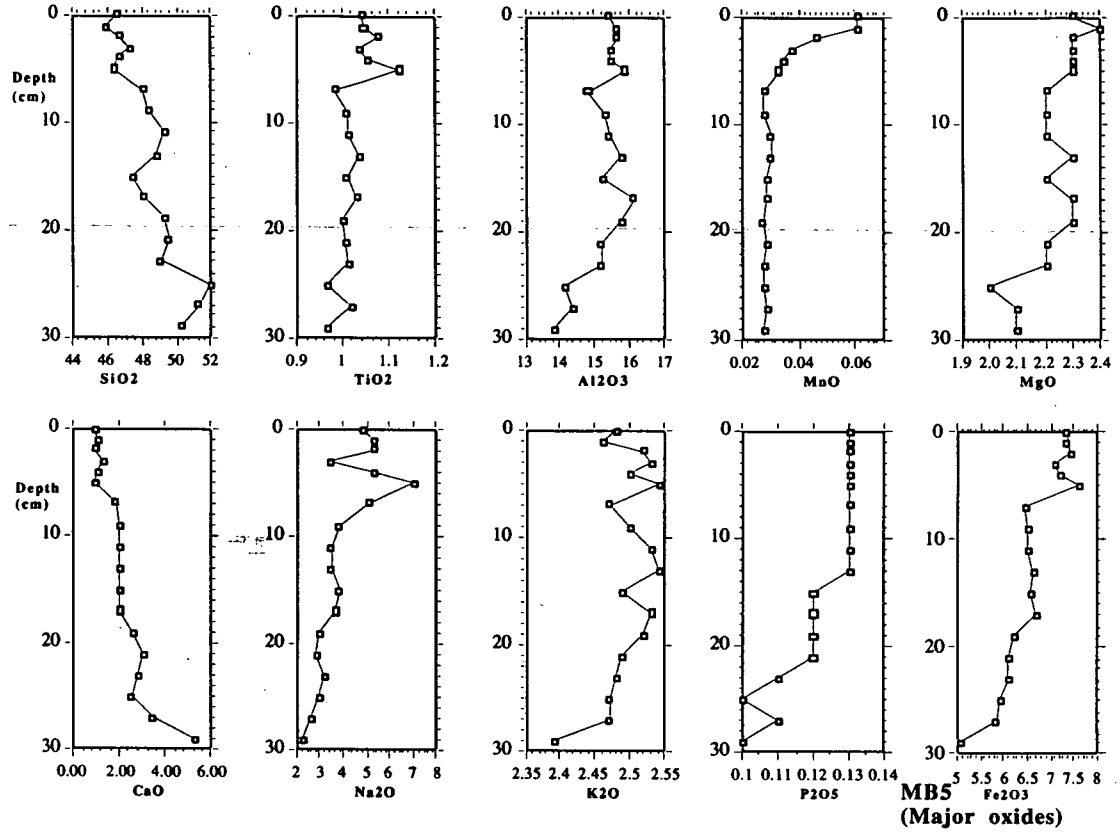

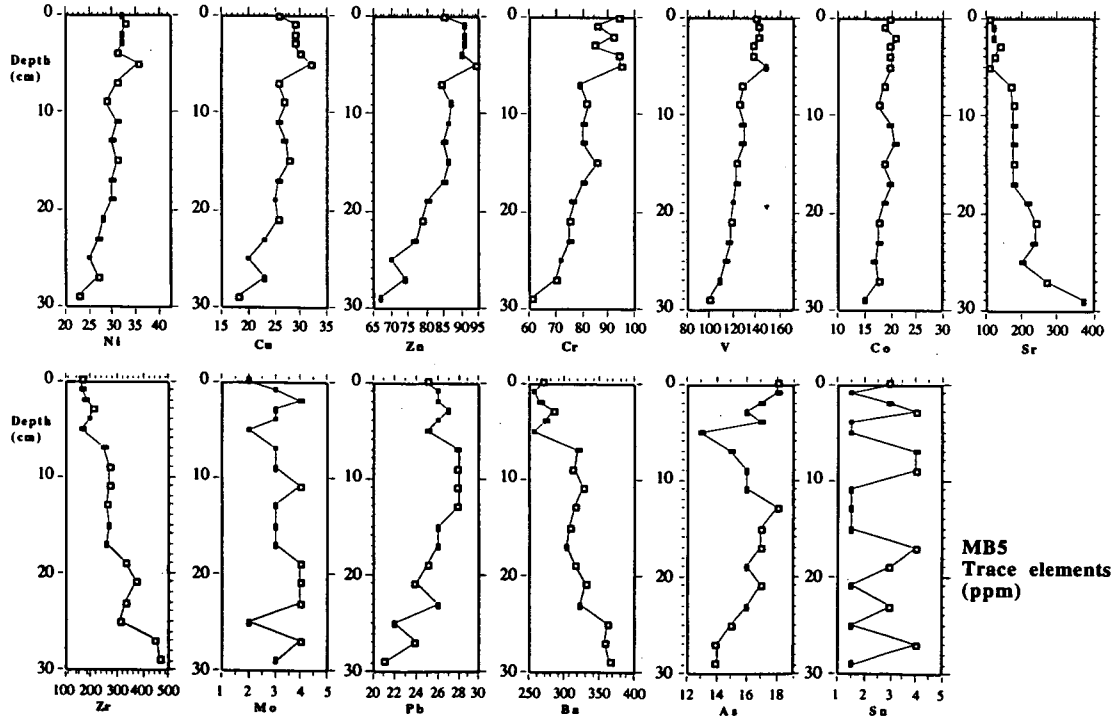

Figure 55: Downcore distribution of selected major oxides (%) and trace elements (mg/kg) in sediments at Mombasa station MB20.

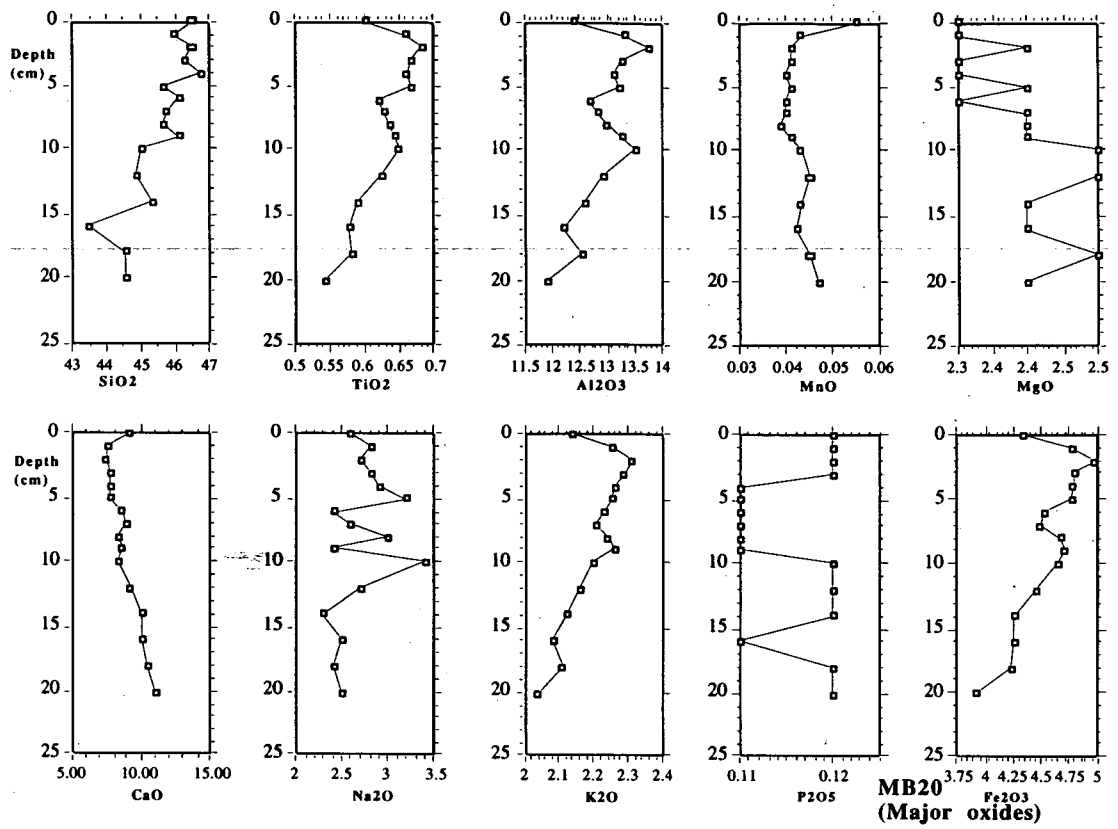

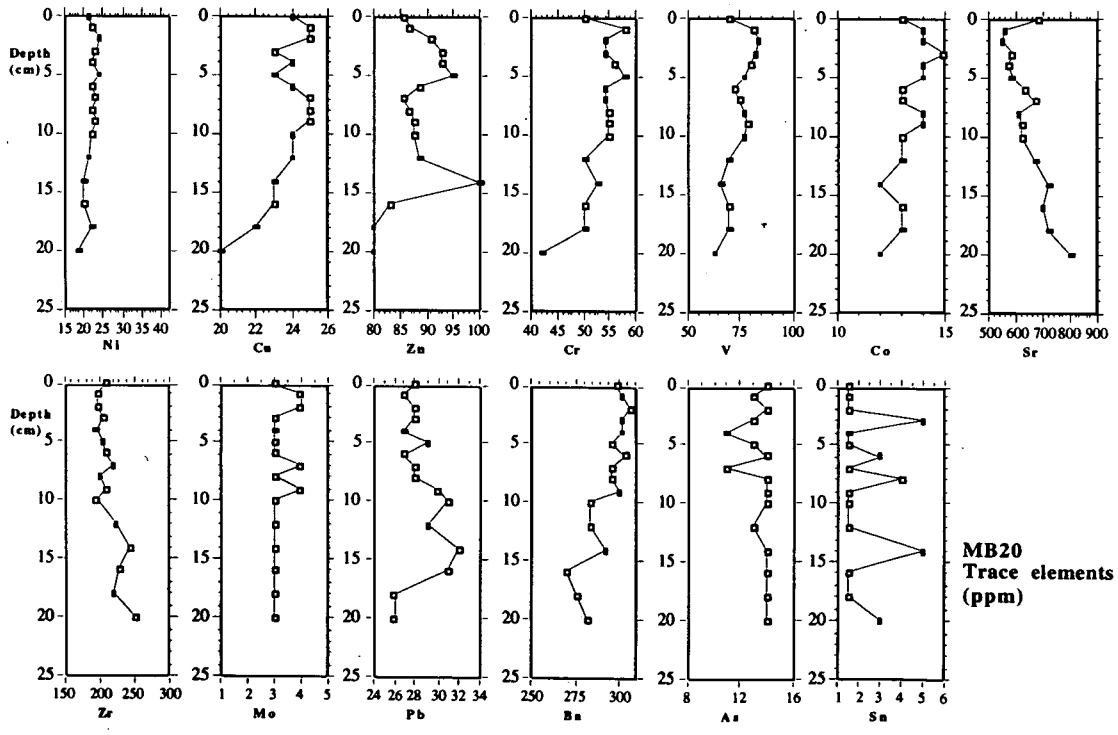

Figure 56: Downcore distribution of selected major oxides (%) and trace elements (mg/kg) in sediments at Mombasa station MB22.

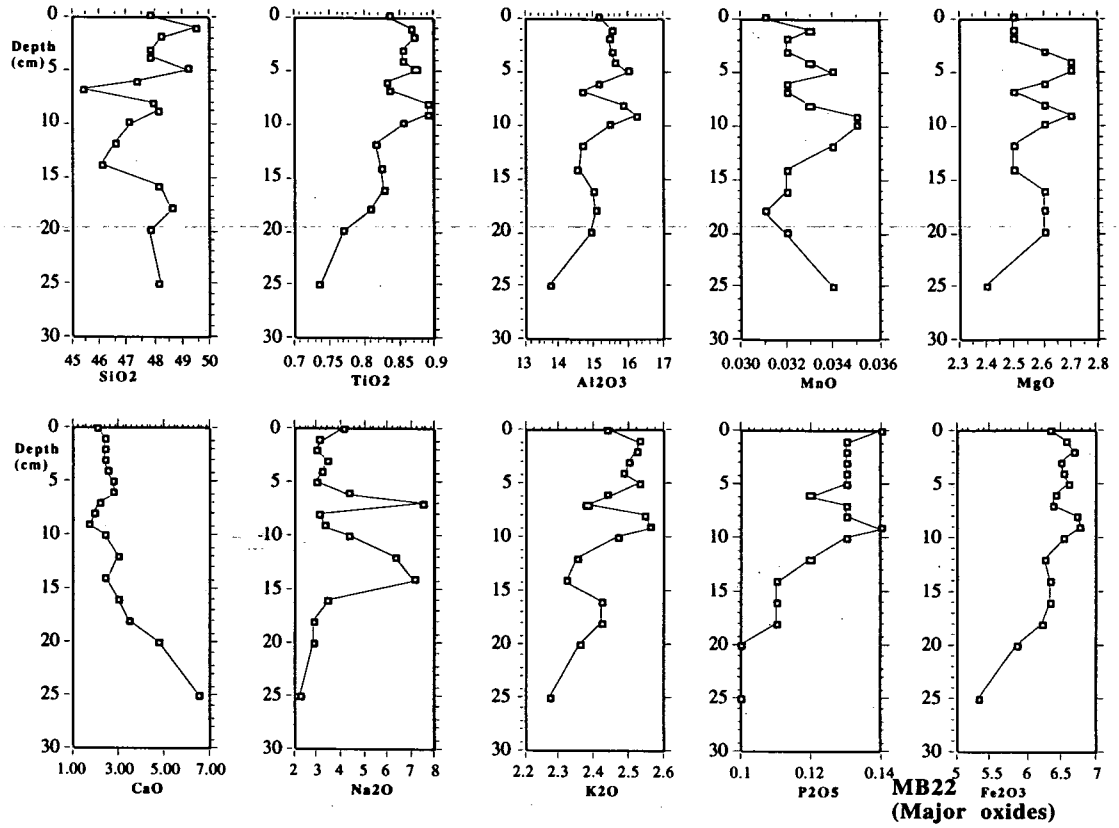

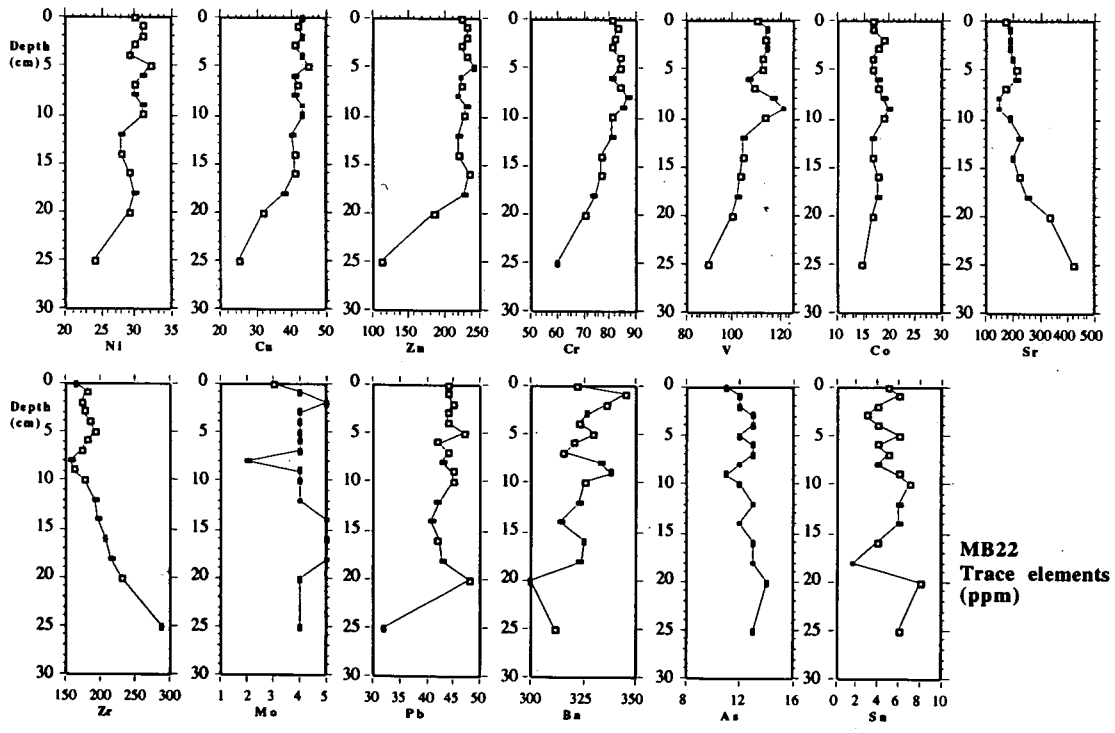

Figure 57: Downcore distribution of selected major oxides (%) and trace elements (mg/kg) in sediments at Mombasa station MB23.

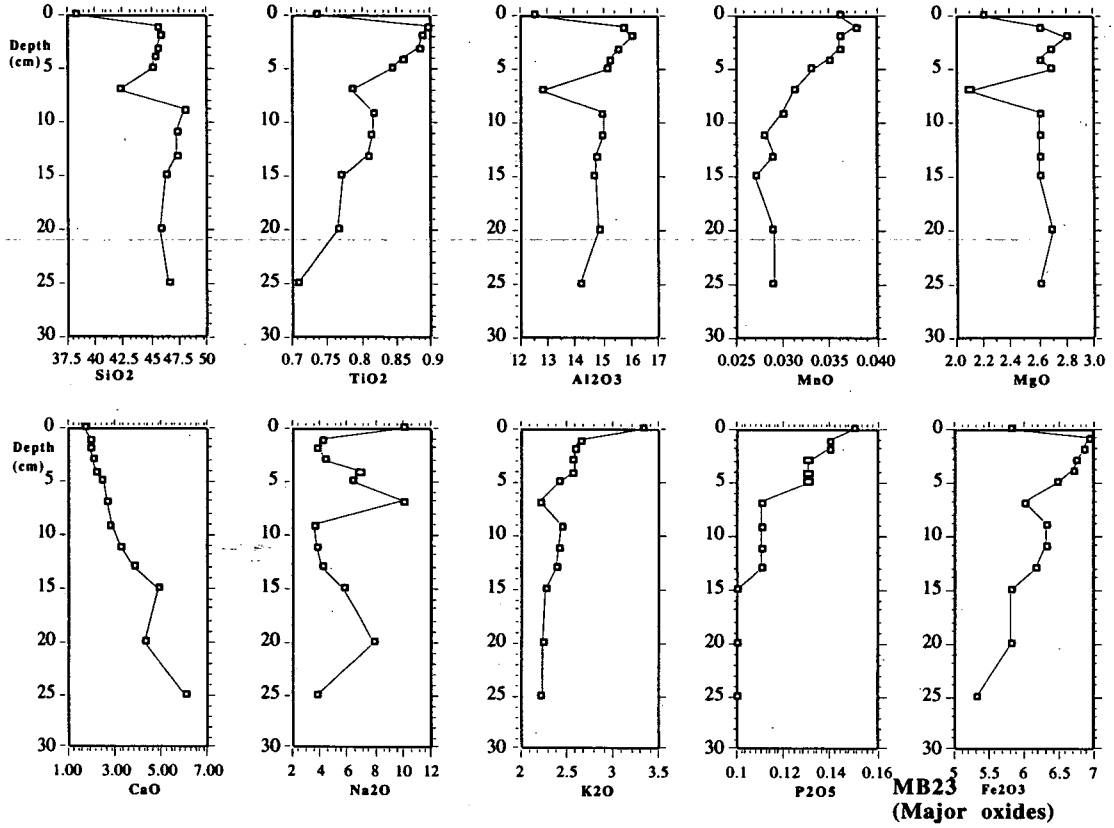

MB23
(Major oxides)

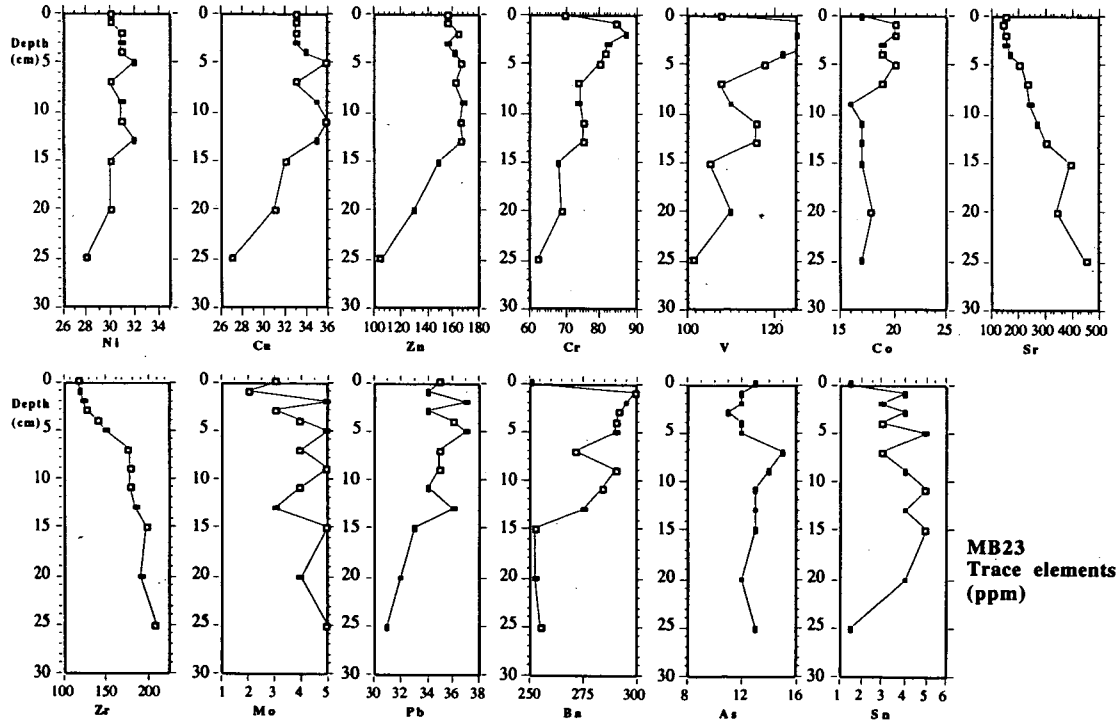

MB23
Trace elements
(ppm)

Figure 58: Downcore distribution of selected major oxides (%) and trace elements (mg/kg) in sediments at Mombasa station MB31.

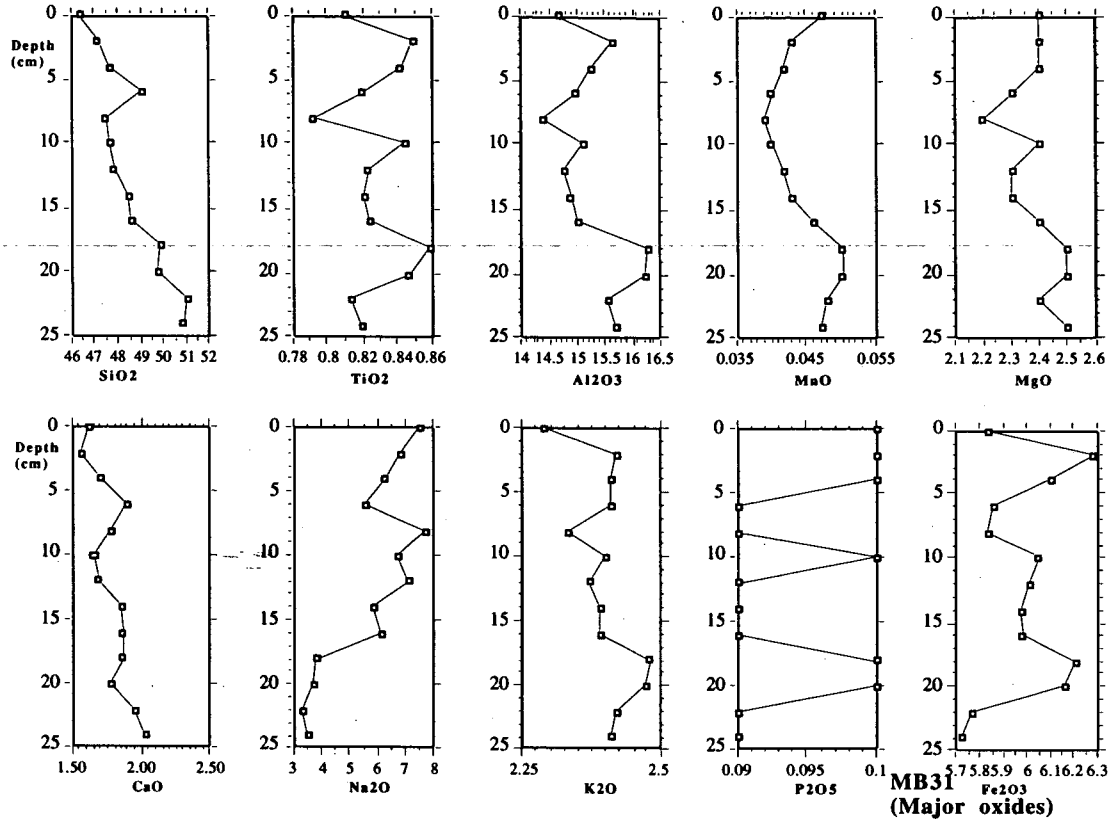

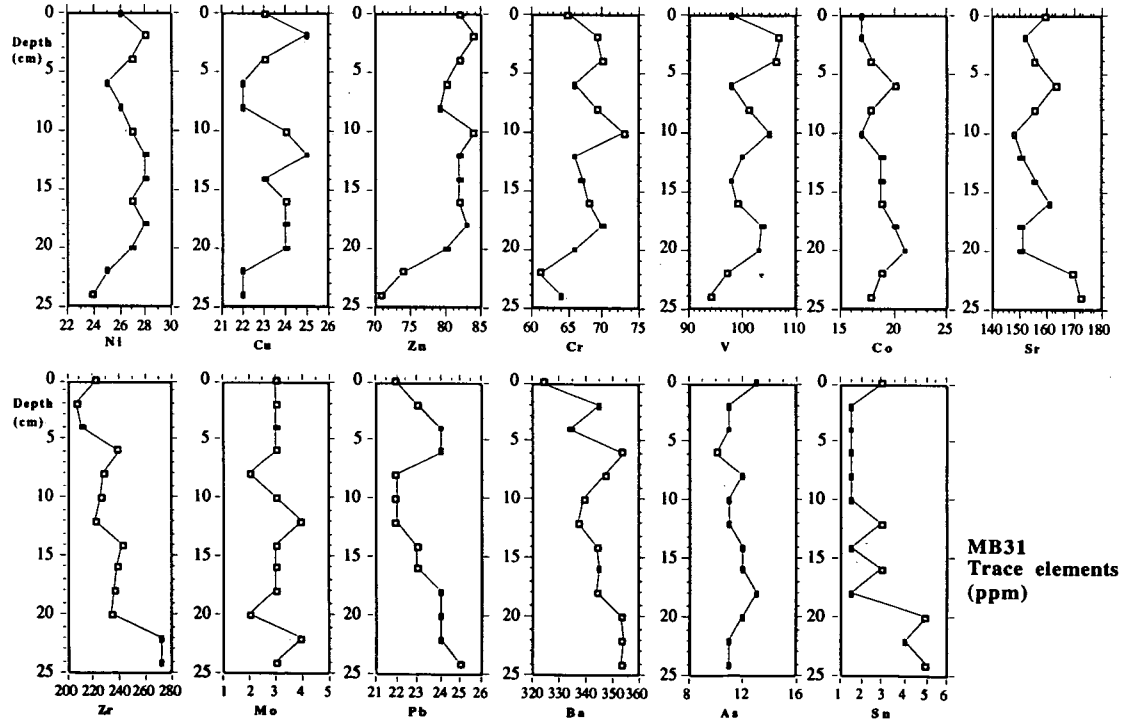

	SiO2	TiO2	Al2O3	MnO	MgO	CaO	Na2O	K2O	P2O5	Ni	Cu	Zn	Cr	V	Co	Sr	Zr	Mo	Pb	Ba	Cd	As	Sn
SiO2	1.00	-.83	-.88	-.01	-.96	.36	-.54	-.50	-.85	-.80	-.68	-.72	-.83	-.85	-.83	.49	.53	-.25	-.73	.96	.09	-.53	-.56
TiO2	-.83	1.00	.99	.47	.88	-.66	.70	.70	.95	.99	.95	.98	.98	.98	.96	-.70	-.77	.34	.89	-.93	-.19	.63	.54
Al2O3	-.88	.99	1.00	.38	.93	-.65	.68	.75	.97	.97	.91	.95	.97	.99	.95	-.69	-.78	.27	.91	-.95	-.20	.62	.49
MnO	-.01	.47	.38	1.00	.11	-.68	.61	.23	.42	.51	.59	.61	.46	.42	.39	-.61	-.60	.21	.44	-.28	-.29	.42	.30
MgO	-.96	.88	.93	.11	1.00	-.43	.55	.67	.89	.86	.75	.80	.87	.90	.89	-.49	-.60	.20	.82	-.94	-.19	.55	.47
CaO	.36	-.66	-.65	-.68	-.43	1.00	-.76	-.55	-.76	-.64	-.61	-.72	-.66	-.63	-.60	.95	.94	.08	-.71	.57	.23	-.55	-.22
Na2O	-.54	.70	.68	.61	.55	-.76	1.00	.30	.76	.72	.71	.73	.64	.70	.67	-.78	-.77	.13	.71	-.73	-.28	.51	.52
K2O	-.50	.70	.75	.23	.67	-.55	.30	1.00	.71	.68	.64	.72	.69	.74	.76	-.45	-.70	-.08	.73	-.55	-.22	.57	.19
P2O5	-.85	.95	.97	.42	.89	-.76	.76	.71	1.00	.92	.86	.93	.94	.95	.93	-.78	-.86	.22	.89	-.94	-.18	.72	.52
Ni	-.80	.99	.97	.51	.86	-.64	.72	.68	.92	1.00	.97	.98	.95	.98	.95	-.67	-.75	.38	.85	-.91	-.29	.60	.54
Cu	-.68	.95	.91	.59	.75	-.61	.71	.64	.86	.97	1.00	.98	.91	.94	.90	-.62	-.70	.49	.81	-.82	-.25	.57	.53
Zn	-.72	.98	.95	.61	.80	-.72	.73	.72	.93	.98	.98	1.00	.96	.97	.94	-.72	-.81	.34	.88	-.87	-.25	.66	.54
Cr	-.83	.98	.97	.46	.87	-.66	.64	.69	.94	.95	.91	.96	1.00	.95	.94	-.71	-.75	.27	.90	-.92	-.08	.63	.53
V	-.85	.98	.99	.42	.90	-.63	.70	.74	.95	.98	.94	.97	.95	1.00	.97	-.65	-.78	.33	.87	-.93	-.26	.65	.56
Co	-.83	.96	.95	.39	.89	-.60	.67	.76	.93	.95	.90	.94	.94	.97	1.00	-.60	-.76	.25	.87	-.90	-.18	.75	.65
Sr	.49	-.70	-.69	-.61	-.49	.95	-.78	-.45	-.78	-.67	-.62	-.72	-.71	-.65	-.60	1.00	.89	.06	-.73	.67	.14	-.50	-.31
Zr	.53	-.77	-.78	-.60	-.60	.94	-.77	-.70	-.86	-.75	-.70	-.81	-.75	-.78	-.76	.89	1.00	.06	-.79	.70	.30	-.69	-.40
Mo	-.25	.34	.27	.21	.20	.08	.13	-.08	.22	.38	.49	.34	.27	.33	.25	.06	.06	1.00	-.01	-.28	-.06	.15	.23
Pb	-.73	.89	.91	.44	.82	-.71	.71	.73	.89	.85	.81	.88	.90	.87	.87	-.73	-.79	-.01	1.00	-.84	-.10	.59	.38
Ba	.96	-.93	-.95	-.28	-.94	.57	-.73	-.55	-.94	-.91	-.82	-.87	-.92	-.93	-.90	.67	.70	-.28	-.84	1.00	.15	-.60	-.61
Cd	.09	-.19	-.20	-.29	-.19	.23	-.28	-.22	-.18	-.29	-.25	-.25	-.08	-.26	-.18	.14	.30	-.06	-.10	.15	1.00	.05	-.11
As	-.53	.63	.62	.42	.55	-.55	.51	.57	.72	.60	.57	.66	.63	.65	.75	-.50	-.69	.15	.59	-.60	.05	1.00	.65
Sn	-.56	.54	.49	.30	.47	-.22	.52	.19	.52	.54	.53	.54	.53	.56	.65	-.31	-.40	.23	.38	-.61	-.11	.65	1.00

Table 12: Pearson correlation matrix showing inter-relationships between major and trace elements in core MB1.

	SiO2	TiO2	Al2O3	MnO	MgO	CaO	Na2O	K2O	P2O5	Ni	Cu	Zn	Cr	V	Co	Sr	Zr	Mo	Pb	Ba	Cd	As	Sn
SiO2	1.00	-.74	-.67	-.65	-.85	.78	-.81	-.33	-.78	-.84	-.83	-.88	-.86	-.89	-.64	.77	.86	.25	-.48	.96	.26	-.41	-.01
TiO2	-.74	1.00	.72	.44	.71	-.72	.79	.60	.65	.83	.84	.80	.82	.82	.72	-.71	-.70	-.15	.33	-.85	-.23	.11	-.06
Al2O3	-.67	.72	1.00	.28	.86	-.73	.50	.82	.75	.78	.79	.81	.71	.73	.84	-.71	-.69	.04	.63	-.76	-.27	.51	.09
MnO	-.65	.44	.28	1.00	.57	-.55	.49	-.07	.43	.48	.36	.44	.56	.63	.35	-.57	-.63	-.28	.05	-.69	-.06	.51	-.06
MgO	-.85	.71	.86	.57	1.00	-.69	.58	.50	.78	.79	.78	.81	.71	.80	.73	-.67	-.72	<0.01	.53	-.87	-.31	.56	.05
CaO	.78	-.72	-.73	-.55	-.69	1.00	-.79	-.65	-.82	-.88	-.85	-.89	-.93	-.95	-.84	1.00	.96	.32	-.61	.87	-.06	-.43	-.07
Na2O	-.81	.79	.50	.49	.58	-.79	1.00	.32	.66	.82	.76	.77	.84	.86	.56	-.79	-.83	-.44	.33	-.83	-.22	.04	-.11
K2O	-.33	.60	.82	-.07	.50	-.65	.32	1.00	.62	.65	.68	.67	.58	.57	.83	-.62	-.52	.08	.63	-.47	.05	.24	.13
P2O5	-.78	.65	.75	.43	.78	-.82	.66	.62	1.00	.86	.87	.92	.81	.86	.82	-.80	-.79	-.05	.80	-.78	-.25	.44	.12
Ni	-.84	.83	.78	.48	.79	-.88	.82	.65	.86	1.00	.93	.94	.89	.93	.81	-.87	-.86	-.21	.59	-.89	-.17	.24	.02
Cu	-.83	.84	.79	.36	.78	-.85	.76	.68	.87	.93	1.00	.97	.89	.90	.80	-.83	-.80	-.10	.63	-.87	-.17	.31	-.02
Zn	-.88	.80	.81	.44	.81	-.89	.77	.67	.92	.94	.97	1.00	.90	.94	.82	-.87	-.88	-.14	.71	-.90	-.14	.37	.06
Cr	-.86	.82	.71	.56	.71	-.93	.84	.58	.81	.89	.89	.90	1.00	.94	.80	-.93	-.92	-.32	.50	-.92	-.12	.39	-.05
V	-.89	.82	.73	.63	.80	-.95	.86	.57	.86	.93	.90	.94	.94	1.00	.80	-.94	-.96	-.31	.55	-.95	-.03	.37	-.04
Co	-.64	.72	.84	.35	.73	-.84	.56	.83	.82	.81	.80	.82	.80	.80	1.00	-.82	-.76	<0.01	.70	-.72	-.12	.49	.11
Sr	.77	-.71	-.71	-.57	-.67	1.00	-.79	-.62	-.80	-.87	-.83	-.87	-.93	-.94	-.82	1.00	.96	.36	-.57	.87	-.08	-.44	-.05
Zr	.86	-.70	-.69	-.63	-.72	.96	-.83	-.52	-.79	-.86	-.80	-.88	-.92	-.96	-.76	.96	1.00	.43	-.54	.91	-.05	-.44	.02
Mo	.25	-.15	.04	-.28	<0.01	.32	-.44	.08	-.05	-.21	-.10	-.14	-.32	-.31	<0.01	.36	.43	1.00	.18	.26	-.34	.10	.18
Pb	-.48	.33	.63	.05	.53	-.61	.33	.63	.80	.59	.63	.71	.50	.55	.70	-.57	-.54	.18	1.00	-.43	-.20	.41	.31
Ba	.96	-.85	-.76	-.69	-.87	.87	-.83	-.47	-.78	-.89	-.87	-.90	-.92	-.95	-.72	.87	.91	.26	-.43	1.00	.16	-.42	.02
Cd	.26	-.23	-.27	-.06	-.31	-.06	-.22	.05	-.25	-.17	-.17	-.14	-.12	-.03	-.12	-.08	-.05	-.34	-.20	.16	1.00	-.15	.07
As	-.41	.11	.51	.51	.56	-.43	.04	.24	.44	.24	.31	.37	.39	.37	.49	-.44	-.44	.10	.41	-.42	-.15	1.00	-.09
Sn	-.01	-.06	.09	-.06	.05	-.07	-.11	.13	.12	.02	-.02	.06	-.05	-.04	.11	-.05	.02	.18	.31	.02	.07	-.09	1.00

Table 13: Pearson correlation matrix showing inter-relationships between major and trace elements in core MB5.

	SiO2	TiO2	Al2O3	MnO	MgO	CaO	Na2O	K2O	P2O5	Ni	Cu	Zn	Cr	V	Co	Sr	Zr	Mo	Pb	Ba	As	Sn
SiO2	1.00	.68	.56	-.10	-.63	-.73	.15	.77	-.08	.59	.53	.49	.54	.63	.55	-.64	-.60	.34	-.28	.96	-.34	.07
TiO2	.68	1.00	.95	-.50	-.23	-.97	.59	.96	-.15	.85	.69	.54	.84	.94	.82	-.96	-.84	.40	.04	.71	-.35	-.13
Al2O3	.56	.95	1.00	-.47	<0.01	-.87	.58	.89	.01	.81	.66	.48	.78	.89	.71	-.89	-.79	.46	.13	.59	-.20	-.15
MnO	-.10	-.50	-.47	1.00	-.01	.46	-.20	-.56	.57	-.48	-.34	-.33	-.57	-.53	-.43	.51	.28	-.25	-.12	-.23	.31	-.18
MgO	-.63	-.23	<0.01	-.01	1.00	.42	.12	-.36	.20	-.08	-.18	-.25	-.26	-.32	-.37	.36	.25	-.10	.30	-.67	.25	-.24
CaO	-.73	-.97	-.87	.46	.42	1.00	-.59	-.95	.22	-.78	-.71	-.49	-.83	-.94	-.83	.98	.88	-.37	.05	-.77	.36	.11
Na2O	.15	.59	.58	-.20	.12	-.59	1.00	.43	-.04	.40	.22	.20	.48	.52	.43	-.56	-.63	-.15	.10	.12	-.21	-.17
K2O	.77	.96	.89	-.56	-.36	-.95	.43	1.00	-.25	.87	.70	.49	.81	.94	.84	-.94	-.82	.46	-.08	.82	-.32	-.01
P2O5	-.08	-.15	.01	.57	.20	.22	-.04	-.25	1.00	-.27	-.31	-.05	-.36	-.19	-.22	.23	.18	-.07	-.07	-.13	.33	.15
Ni	.59	.85	.81	-.48	-.08	-.78	.40	.87	-.27	1.00	.57	.31	.73	.83	.75	-.78	-.75	.48	-.11	.60	-.29	-.23
Cu	.53	.69	.66	-.34	-.18	-.71	.22	.70	-.31	.57	1.00	.28	.73	.67	.48	-.71	-.68	.58	.20	.58	-.25	-.25
Zn	.49	.54	.48	-.33	-.25	-.49	.20	.49	-.05	.31	.28	1.00	.58	.32	.26	-.45	-.18	-.05	.46	.53	-.21	.40
Cr	.54	.84	.78	-.57	-.26	-.83	.48	.81	-.36	.73	.73	.58	1.00	.79	.65	-.86	-.76	.34	.21	.59	-.33	-.08
V	.63	.94	.89	-.53	-.32	-.94	.52	.94	-.19	.83	.67	.32	.79	1.00	.90	-.96	-.88	.48	-.09	.66	-.33	-.15
Co	.55	.82	.71	-.43	-.37	-.83	.43	.84	-.22	.75	.48	.26	.65	.90	1.00	-.84	-.78	.28	-.17	.57	-.26	-.01
Sr	-.64	-.96	-.89	.51	.36	.98	-.56	-.94	.23	-.78	-.71	-.45	-.86	-.96	-.84	1.00	.90	-.38	.02	-.69	.30	.15
Zr	-.60	-.84	-.79	.28	.25	.88	-.63	-.82	.18	-.75	-.68	-.18	-.76	-.88	-.78	.90	1.00	-.25	.14	-.56	.21	.32
Mo	.34	.40	.46	-.25	-.10	-.37	-.15	.46	-.07	.48	.58	-.05	.34	.48	.28	-.38	-.25	1.00	-.06	.44	-.22	-.36
Pb	-.28	.04	.13	-.12	.30	.05	.10	-.08	-.07	-.11	.20	.46	.21	-.09	-.17	.02	.14	-.06	1.00	-.23	.23	.12
Ba	.96	.71	.59	-.23	-.67	-.77	.12	.82	-.13	.60	.58	.53	.59	.66	.57	-.69	-.56	.44	-.23	1.00	-.28	.15
As	-.34	-.35	-.20	.31	.25	.36	-.21	-.32	.33	-.29	-.25	-.21	-.33	-.33	-.26	.30	.21	-.22	.23	-.28	1.00	.22
Sn	.07	-.13	-.15	-.18	-.24	.11	-.17	-.01	.15	-.23	-.25	.40	-.08	-.15	-.01	.15	.32	-.36	.12	.15	.22	1.00

Table 14: Pearson correlation matrix showing inter-relationships between major and trace elements in core MB20

	SiO2	TiO2	Al2O3	MnO	MgO	CaO	Na2O	K2O	P2O5	Ni	Cu	Zn	Cr	V	Co	Sr	Zr	Mo	Pb	Ba	Cd	As	Sn
SiO2	1.00	.17	.43	.08	.29	.14	-.89	.51	.07	.23	-.03	.03	-.06	.14	-.06	.13	.14	-.03	.11	.49	.11	-.19	-.14
TiO2	.17	1.00	.88	.20	.52	-.90	-.01	.90	.85	.79	.88	.79	.93	.96	.72	-.91	-.89	-.26	.57	.80	-.06	-.62	-.20
Al2O3	.43	.88	1.00	.23	.78	-.71	-.33	.96	.73	.83	.73	.71	.79	.90	.68	-.72	-.73	-.27	.72	.69	-.09	-.49	-.14
MnO	.08	.20	.23	1.00	.22	.04	-.10	.19	.20	-.04	<0.01	-.13	.10	.22	.12	.04	.04	-.18	-.09	.28	-.16	-.26	.54
MgO	.29	.52	.78	.22	1.00	-.39	-.31	.62	.32	.57	.47	.54	.49	.53	.48	-.39	-.38	-.07	.61	.23	.09	-.06	-.13
CaO	.14	-.90	-.71	.04	-.39	1.00	-.33	-.69	-.81	-.76	-.95	-.90	-.94	-.88	-.70	1.00	.97	.16	-.59	-.61	.01	.57	.24
Na2O	-.89	-.01	-.33	-.10	-.31	-.33	1.00	-.41	.06	-.06	.27	.22	.24	-.02	.01	-.30	-.28	.12	-.02	-.26	-.07	<0.01	.16
K2O	.51	.90	.96	.19	.62	-.69	-.41	1.00	.77	.80	.69	.65	.76	.90	.66	-.71	-.72	-.30	.59	.82	-.07	-.51	-.24
P2O5	.07	.85	.73	.20	.32	-.81	.06	.77	1.00	.67	.79	.62	.84	.89	.53	-.82	-.86	-.42	.46	.68	-.26	-.70	-.11
Ni	.23	.79	.83	-.04	.57	-.76	-.06	.80	.67	1.00	.81	.84	.79	.79	.68	-.75	-.78	-.08	.83	.57	-.09	-.39	-.15
Cu	-.03	.88	.73	<0.01	.47	-.95	.27	.69	.79	.81	1.00	.95	.92	.83	.59	-.93	-.89	-.04	.64	.61	.04	-.53	-.21
Zn	.03	.79	.71	-.13	.54	-.90	.22	.65	.62	.84	.95	1.00	.85	.75	.61	-.88	-.83	.10	.72	.56	.15	-.36	-.30
Cr	-.06	.93	.79	.10	.49	-.94	.24	.76	.84	.79	.92	.85	1.00	.91	.64	-.94	-.95	-.32	.65	.63	-.10	-.47	-.16
V	.14	.96	.90	.22	.53	-.88	-.02	.90	.89	.79	.83	.75	.91	1.00	.73	-.89	-.90	-.31	.65	.73	-.18	-.61	-.10
Co	-.06	.72	.68	.12	.48	-.70	.01	.66	.53	.68	.59	.61	.64	.73	1.00	-.71	-.72	-.05	.53	.51	.07	-.38	-.23
Sr	.13	-.91	-.72	.04	-.39	1.00	-.30	-.71	-.82	-.75	-.93	-.88	-.94	-.89	-.71	1.00	.97	.20	-.57	-.63	.01	.58	.26
Zr	.14	-.89	-.73	.04	-.38	.97	-.28	-.72	-.86	-.78	-.89	-.83	-.95	-.90	-.72	.97	1.00	.32	-.63	-.58	.13	.56	.19
Mo	-.03	-.26	-.27	-.18	-.07	.16	.12	-.30	-.42	-.08	-.04	.10	-.32	-.31	-.05	.20	.32	1.00	-.05	-.12	.32	.26	-.13
Pb	.11	.57	.72	-.09	.61	-.59	-.02	.59	.46	.83	.64	.72	.65	.65	.53	-.57	-.63	-.05	1.00	.22	-.09	-.14	.10
Ba	.49	.80	.69	.28	.23	-.61	-.26	.82	.68	.57	.61	.56	.63	.73	.51	-.63	-.58	-.12	.22	1.00	.01	-.62	-.28
Cd	.11	-.06	-.09	-.16	.09	.01	-.07	-.07	-.26	-.09	.04	.15	-.10	-.18	.07	.01	.13	.32	-.09	.01	1.00	.17	-.17
As	-.19	-.62	-.49	-.26	-.06	.57	<0.01	-.51	-.70	-.39	-.53	-.36	-.47	-.61	-.38	.58	.56	.26	-.14	-.62	.17	1.00	-.09
Sn	-.14	-.20	-.14	.54	-.13	.24	.16	-.24	-.11	-.15	-.21	-.30	-.16	-.10	-.23	.26	.19	-.13	.10	-.28	-.17	-.09	1.00

Table 15: Pearson correlation matrix showing inter-relationships between major and trace elements in core MB22

	SiO2	TiO2	Al2O3	MnO	MgO	CaO	Na2O	K2O	P2O5	Ni	Cu	Zn	Cr	V	Co	Sr	Zr	Mo	Pb	Ba	As	Sn
SiO2	1.00	.28	.73	-.44	.75	.43	-.84	-.67	-.54	.20	.07	-.06	.08	.15	-.15	.40	.46	.31	-.16	.36	-.16	.55
TiO2	.28	1.00	.75	.61	.46	-.67	-.38	.10	.52	.61	.54	.61	.97	.95	.68	-.72	-.65	-.27	.59	.92	-.51	.42
Al2O3	.73	.75	1.00	.20	.92	-.12	-.75	-.22	.09	.40	.22	.16	.62	.70	.39	-.18	-.20	.06	.17	.68	-.67	.53
MnO	-.44	.61	.20	1.00	-.01	-.81	.11	.68	.93	.14	.12	.28	.71	.73	.68	-.87	-.96	-.49	.44	.53	-.49	-.31
MgO	.75	.46	.92	-.01	1.00	.15	-.74	-.28	-.07	.29	.03	-.10	.34	.43	.20	.09	.01	.25	<0.01	.39	-.71	.45
CaO	.43	-.67	-.12	-.81	.15	1.00	-.22	-.65	-.85	-.52	-.61	-.73	-.79	-.69	-.53	.99	.90	.41	-.72	-.63	.22	<0.01
Na2O	-.84	-.38	-.75	.11	-.74	-.22	1.00	.28	.16	-.14	-.04	.02	-.23	-.33	.11	-.15	-.12	-.14	.07	-.48	.30	-.32
K2O	-.67	.10	-.22	.68	-.28	-.65	.28	1.00	.84	.10	.20	.28	.24	.27	.05	-.65	-.77	-.47	.33	.04	-.24	-.41
P2O5	-.54	.52	.09	.93	-.07	-.85	.16	.84	1.00	.27	.30	.43	.67	.63	.55	-.88	-.97	-.43	.59	.45	-.42	-.27
Ni	.20	.61	.40	.14	.29	-.52	-.14	.10	.27	1.00	.90	.84	.63	.52	.22	-.49	-.31	-.08	.80	.58	-.22	.59
Cu	.07	.54	.22	.12	.03	-.61	-.04	.20	.30	.90	1.00	.94	.56	.43	.12	-.55	-.33	-.14	.76	.58	.02	.59
Zn	-.06	.61	.16	.28	-.10	-.73	.02	.28	.43	.84	.94	1.00	.67	.48	.21	-.68	-.46	-.18	.84	.62	.10	.44
Cr	.08	.97	.62	.71	.34	-.79	-.23	.24	.67	.63	.56	.67	1.00	.93	.75	-.83	-.76	-.28	.71	.89	-.47	.28
V	.15	.95	.70	.73	.43	-.69	-.33	.27	.63	.52	.43	.48	.93	1.00	.70	-.75	-.75	-.50	.48	.84	-.66	.29
Co	-.15	.68	.39	.68	.20	-.53	.11	.05	.55	.22	.12	.21	.75	.70	1.00	-.58	-.61	-.18	.42	.56	-.48	.09
Sr	.40	-.72	-.18	-.87	.09	.99	-.15	-.65	-.88	-.49	-.55	-.68	-.83	-.75	-.58	1.00	.94	.46	-.69	-.67	.30	.03
Zr	.46	-.65	-.20	-.96	.01	.90	-.12	-.77	-.97	-.31	-.33	-.46	-.76	-.75	-.61	.94	1.00	.49	-.55	-.54	.49	.16
Mo	.31	-.27	.06	-.49	.25	.41	-.14	-.47	-.43	-.08	-.14	-.18	-.28	-.50	-.18	.46	.49	1.00	<0.01	-.15	.24	.07
Pb	-.16	.59	.17	.44	<0.01	-.72	.07	.33	.59	.80	.76	.84	.71	.48	.42	-.69	-.55	<0.01	1.00	.60	-.04	.14
Ba	.36	.92	.68	.53	.39	-.63	-.48	.04	.45	.58	.58	.62	.89	.84	.56	-.67	-.54	-.15	.60	1.00	-.31	.35
As	-.16	-.51	-.67	-.49	-.71	.22	.30	-.24	-.42	-.22	.02	.10	-.47	-.66	-.48	.30	.49	.24	-.04	-.31	1.00	-.17
Sn	.55	.42	.53	-.31	.45	<0.01	-.32	-.41	-.27	.59	.59	.44	.28	.29	.09	.03	.16	.07	.14	.35	-.17	1.00

Table 16: Pearson correlation matrix showing inter-relationships between major and trace elements in core MB23

	SiO2	TiO2	Al2O3	MnO	MgO	CaO	Na2O	K2O	P2O5	Ni	Cu	Zn	Cr	V	Co	Sr	Zr	Mo	Pb	Ba	As	Sn
SiO2	1.00	.09	.63	.56	.48	.87	-.95	.65	-.35	-.46	-.37	-.72	-.52	-.45	.60	.55	.87	.16	.80	.78	-.16	.58
TiO2	.09	1.00	.74	.32	.66	-.26	-.30	.76	.71	.55	.64	.46	.48	.70	.19	-.54	-.32	-.02	.29	-.03	.03	-.12
Al2O3	.63	.74	1.00	.72	.85	.25	-.80	.89	.44	.07	.23	-.16	-.05	.26	.43	-.03	.26	-.06	.70	.43	.09	.37
MnO	.56	.32	.72	1.00	.80	.35	-.72	.43	.24	-.05	.09	-.28	-.44	-.19	.41	.23	.43	.04	.49	.15	.53	.65
MgO	.48	.66	.85	.80	1.00	.18	-.67	.60	.52	-.05	.22	-.17	-.08	.11	.16	.10	.25	<0.01	.59	.10	.22	.52
CaO	.87	-.26	.25	.35	.18	1.00	-.74	.33	-.63	-.59	-.63	-.76	-.53	-.71	.52	.73	.91	.10	.70	.70	-.12	.43
Na2O	-.95	-.30	-.80	-.72	-.67	-.74	1.00	-.75	.07	.33	.25	.60	.46	.28	-.60	-.43	-.75	-.09	-.85	-.66	.03	-.58
K2O	.65	.76	.89	.43	.60	.33	-.75	1.00	.24	.18	.23	-.05	.10	.33	.60	-.14	.22	-.03	.69	.58	-.16	.14
P2O5	-.35	.71	.44	.24	.52	-.63	.07	.24	1.00	.40	.46	.53	.50	.75	-.22	-.57	-.58	-.28	-.06	-.46	.32	-.17
Ni	-.46	.55	.07	-.05	-.05	-.59	.33	.18	.40	1.00	.82	.83	.57	.67	.05	-.85	-.66	0.00	-.43	-.39	.34	-.47
Cu	-.37	.64	.23	.09	.22	-.63	.25	.23	.46	.82	1.00	.69	.44	.61	-.03	-.74	-.60	.13	-.37	-.33	.16	-.13
Zn	-.72	.46	-.16	-.28	-.17	-.76	.60	-.05	.53	.83	.69	1.00	.72	.71	-.12	-.85	-.85	-.11	-.58	-.57	.25	-.68
Cr	-.52	.48	-.05	-.44	-.08	-.53	.46	.10	.50	.57	.44	.72	1.00	.77	-.28	-.74	-.67	-.37	-.37	-.34	.10	-.70
V	-.45	.70	.26	-.19	.11	-.71	.28	.33	.75	.67	.61	.71	.77	1.00	-.15	-.80	-.77	-.26	-.22	-.27	.04	-.51
Co	.60	.19	.43	.41	.16	.52	-.60	.60	-.22	.05	-.03	-.12	-.28	-.15	1.00	-.01	.33	-.11	.47	.55	.05	.28
Sr	.55	-.54	-.03	.23	.10	.73	-.43	-.14	-.57	-.85	-.74	-.85	-.74	-.80	-.01	1.00	.78	.26	.53	.38	-.25	.49
Zr	.87	-.32	.26	.43	.25	.91	-.75	.22	-.58	-.66	-.60	-.85	-.67	-.77	.33	.78	1.00	.24	.58	.63	-.10	.59
Mo	.16	-.02	-.06	.04	<0.01	.10	-.09	-.03	-.28	0.00	.13	-.11	-.37	-.26	-.11	.26	.24	1.00	0.00	-.15	-.33	.05
Pb	.80	.29	.70	.49	.59	.70	-.85	.69	-.06	-.43	-.37	-.58	-.37	-.22	.47	.53	.58	0.00	1.00	.61	-.25	.41
Ba	.78	-.03	.43	.15	.10	.70	-.66	.58	-.46	-.39	-.33	-.57	-.34	-.27	.55	.38	.63	-.15	.61	1.00	-.40	.33
As	-.16	.03	.09	.53	.22	-.12	.03	-.16	.32	.34	.16	.25	.10	.04	.05	-.25	-.10	-.33	-.25	-.40	1.00	.03
Sn	.58	-.12	.37	.65	.52	.43	-.58	.14	-.17	-.47	-.13	-.68	-.70	-.51	.28	.49	.59	.05	.41	.33	.03	1.00

Table 17: Pearson correlation matrix showing inter-relationships between major and trace elements in core MB31.

3.3.3.2: Trace metals: Elevated levels (>2 x basal concentrations) of a range of heavy metals including Ni, Cu, Zn, Cr, V, Co and Pb are recorded in the uppermost 5-10 cm of sediment at most sites. In Makupa Creek, the initial increase occurs at a greater depth of c.20 cm. Precise chronologies of metal deposition and flux-rate calculations cannot be derived in the absence of appropriate radiometric data. Rees et al. (1996) have, however, indicated that the contemporary sediment influx to the Mombasa creek systems is negligible, with only an intermittent supply of new material introduced from either seaward or terrestrial sources during severe storm events. Sedimentation rates under this regime are likely to approximate the mean sea-level increment of 1-2 mm/yr, giving a tentative age of 50-100 yrs BP for the 10 cm horizon at most sites. Higher sedimentation rates probably prevail in Makupa Creek due to the influx of unconsolidated detritus from the adjacent landfill. Increments to metal concentrations upward of c. 20 cm depth at this locality could thus be synchronous with similar adjustments at lesser depth elsewhere.

Despite the relative enrichment of potentially toxic metals in sediments deposited in recent decades, there is strong evidence that the control is primarily lithological. The first-row transition metals V, Cr, Co, Ni, Cu, Zn are systematically covariant with TiO_2 (Pearson R coeff. >0.7, Tables 12-17) and, to a lesser extent Al_2O_3, suggesting that concentrations are directly related to the proportion of fine clastic detritus present. A similar (through less systematic) control is evident for Pb, which is strongly correlated (R>0.6) with either TiO_2 or Al_2O_3 and the transition metal suite at most sites. Downcore covariation of Ba and Zr (carried in resistate heavy mineral phases) with SiO_2 is evident in all Tudor Creek, Port Tudor and Port Reitz cores (exemplified by MB1, MB5 and MB31). Profiles for these elements can thus be equated to temporal trends of quartzose sand deposition. In Makupa Creek (MB22 and MB23) and parts of Port Kilindini (e.g. MB20) the distribution of Zr is closely associated with calcareous rather than quartzose detritus.

Statistically significant correlations between Mn and most other first row transition group members (e.g. V, Cr, Co, Ni, Cu, Zn) were observed in 12 Mombasa sediment cores including MB1 (max. R coeff. 0.61), MB3 (max. R coeff. R 0.75), MB4 (max. R coeff 0.97), MB13 (max. R coeff. 0.98), and MB 23 (max. R coeff. 0.73). The relative affinities of individual heavy metals to Mn vary between cores, with no consistent trend apparent. In virtually all instances, however, the association of heavy metals with Mn is weaker than that with major oxide indicators of clastic detrital content. Diagenetic modification of trace metal profiles in the manner reported for many anoxic marine and estuarine sediments elsewhere (e.g. Williams et al., 1992) is not therefore considered significant (see also sections 3.3.4 - 3.3.5).

Anthropogenic impacts on the temporal flux of heavy metals to the inshore sediments of Mombasa have been appraised by normalising the downcore profiles of potential contaminant

elements against major oxides such as Al_2O_3 and TiO_2, the fluxes of which are universally dominated by the lithosphere. Figure 59, illustrates the Al_2O_3-normalised profiles for Ni, Cu, Zn, Cr and V through cores MB1 (Tudor Creek), MB5 (Port Tudor), MB20 (Port Kilindini) and MB22 (Makupa Creek). With the exception of minor profile inflections for Cr, Zn and V

Figure 59: Downcore profiles of heavy metals in selected inshore cores from Mombasa following normalisation against Al_2O_3. Units reflect the factor by which the heavy metal concentration (expressed as mg/kg) exceeds the major oxide abundance (expressed as %).

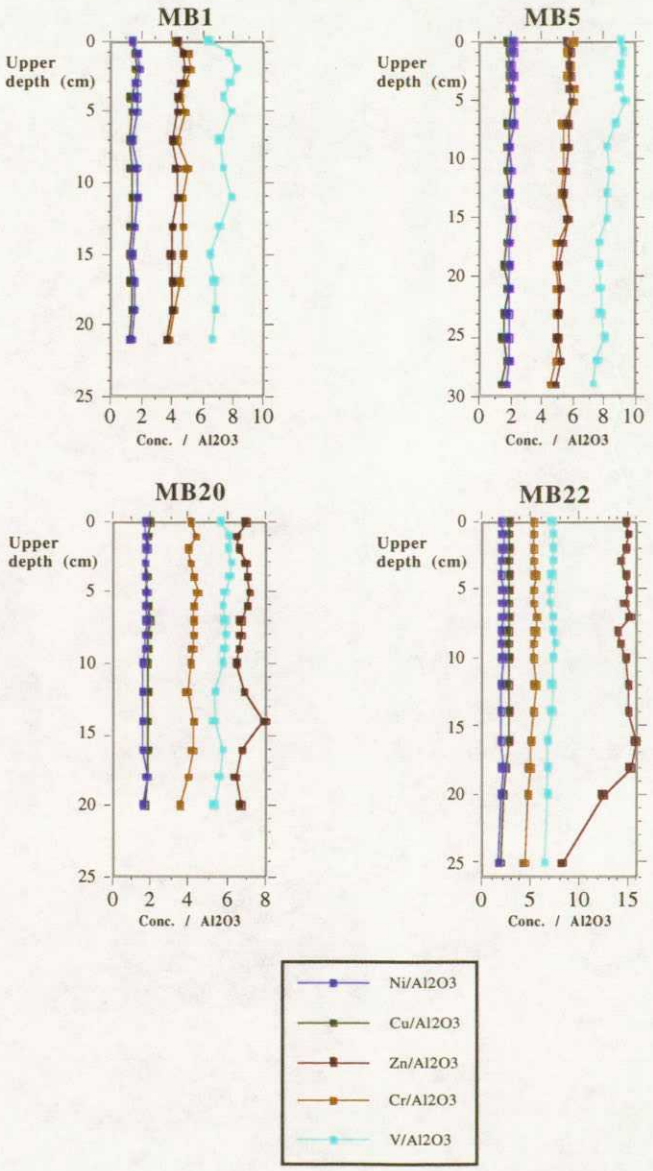

in the uppermost 5 cm of core MB1 and a significant increment of Zn upward of 20 cm in core MB22, the major downcore variations of heavy metal abundance portrayed by the raw data for these cores (Figs. 53-58) are effectively removed. Such trends strongly infer a lack of significant anthropogenic perturbation of the trace metal flux over this period of sedimentation.

3.3.4: Sedimentary partitioning of metals.

The solid-phase partitioning of 11 elements (Fe, Mn, Al, V, Pb, Co, Ni, Cr, Cu, Zn, Cd) in sediment from Makupa Creek was determined through sequential leaching of sub-samples from a 1 m piston core recovered from site MB23 specifically for this purpose in January 1996. All sub-samples were retained wet and unoxidised prior to analysis. The extractive method was based on that of Breward and Peachey (1983), and entailed the addition of (i) NH_4OAc for the dissolution of adsorbed metals, (ii) NH_4 for organically bound phases, (iii) $NH_2.OH.HCl$ for Mn oxides, (iv) Tamms reagent for Fe oxides and (v) aqua-regia for residual phases. The organic matter removed during stage (ii) was subsequently partitioned into fulvic and humic components by HCl precipitation. All leachates were analysed by ICP-AES.

Partitioning trends for 10 elements in 24 sub-samples from Makupa creek piston core MB23 are illustrated in Figures 60-64. Data for Cd are not presented as concentrations in all geochemical fractions fell below the analytical detection limit (1 mg/kg in solid sediment). For all elements the aggregate concentration noted in the six geochemical fractions was found to be low, relative to the corresponding XRF values obtained from an independent site MB23 core (Fig. 57). This discrepancy is ascribed to a low efficiency of metal recovery via the sequential leaching scheme, with estimated recoveries ranging from <35% for Al, to >60% for Cu and Zn. Values of <50% systematically prevail for elements held predominantly in aluminosilicates or other residual phases, as their solubility is strictly limited in the presence of all extractants used.

Adsorbed or exchangeable phases (NH_4OAc extractable) are of negligible significance in the Makupa Creek sediment column. This is consistent with the predominance of anoxic conditions throughout all but the interfacial layer. Up to 7% of the Mn extracted during the leaching sequence was found to be held in this phase, with sub-detection limit concentrations recorded for all other analysed elements. The proportion of total sedimentary metals held in exchangeable form is conventionally regarded as an important determinant of bioavailability (Landner, 1986; Fergusson, 1994). The trends reported for heavy metals in Makupa Creek sediments can therefore be viewed as consistent with a low toxicological risk.

Organo-metallic complexation exerts an important control on the sedimentary retention of Cu (up to 50% total), V (up to 25%) and Zn (up to 10%), with fulvic fractions systematically dominant (c. 80% of the total organic loading). Smaller organically-bound fractions are recorded in the partitioning spectra for Ni, Cr and Mn, with humic compounds dominant in the former two instances. Organic matter is of little significance as a carrier of Al or Mn, and is not represented in the partitioning spectra for Co or Pb.

Figure 60: Partitioning of Cu and Fe between different geochemical fractions of Makupa Creek sediments (station MB23). Note - the downcore (vertical) axis is annotated with respect to sample number not depth. Samples 1-12 were removed at 2 cm resolution fom the uppermost 24 cm, below which 5 cm resolution applies.

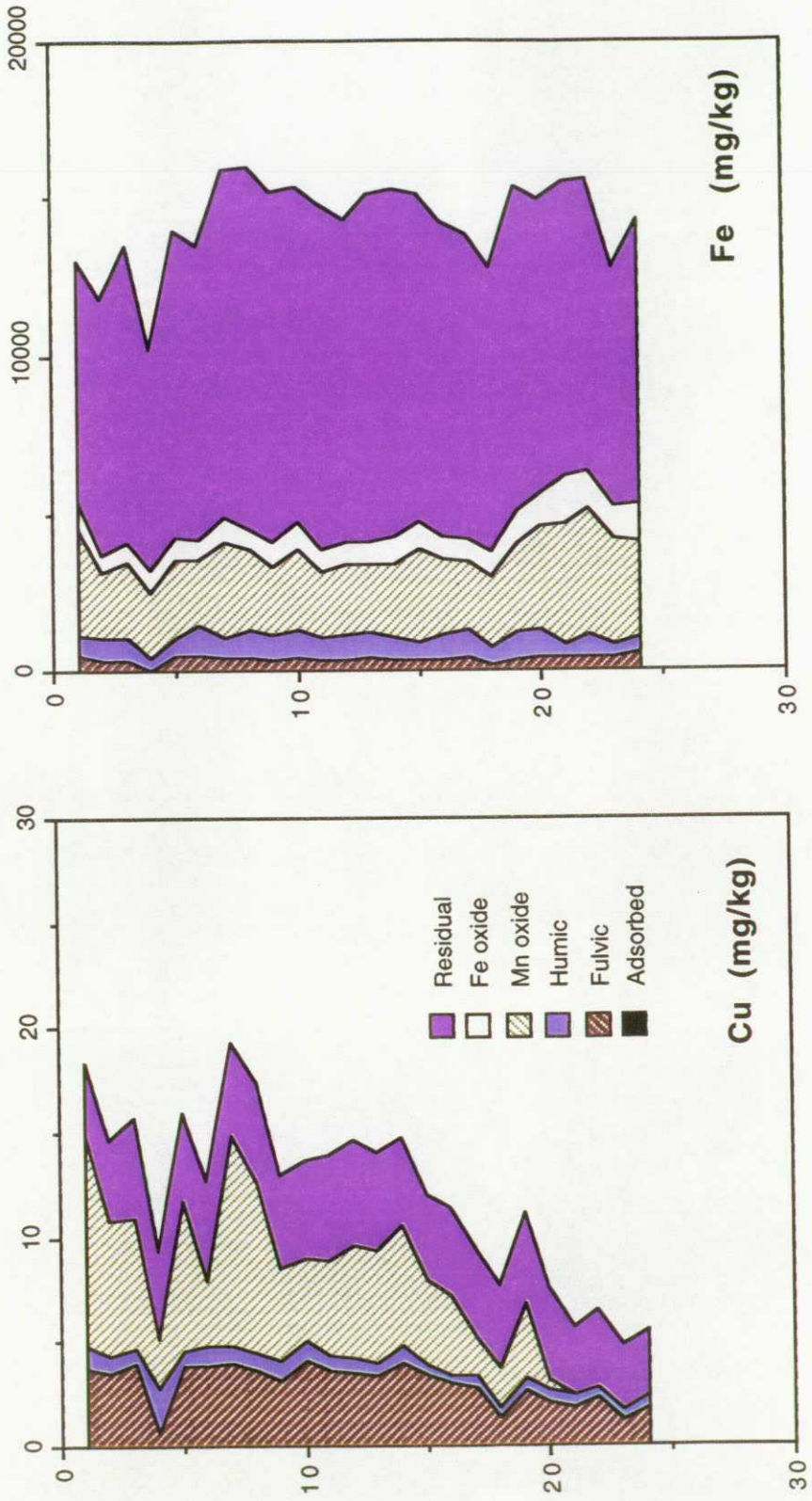

Figure 61: Partitioning of V and Al between different geochemical fractions of Makupa Creek sediments (station MB23). Note - the downcore (vertical) axis is annotated with respect to sample number not depth. Samples 1-12 were removed at 2 cm resolution fom the uppermost 24 cm, below which 5 cm resolution applies.

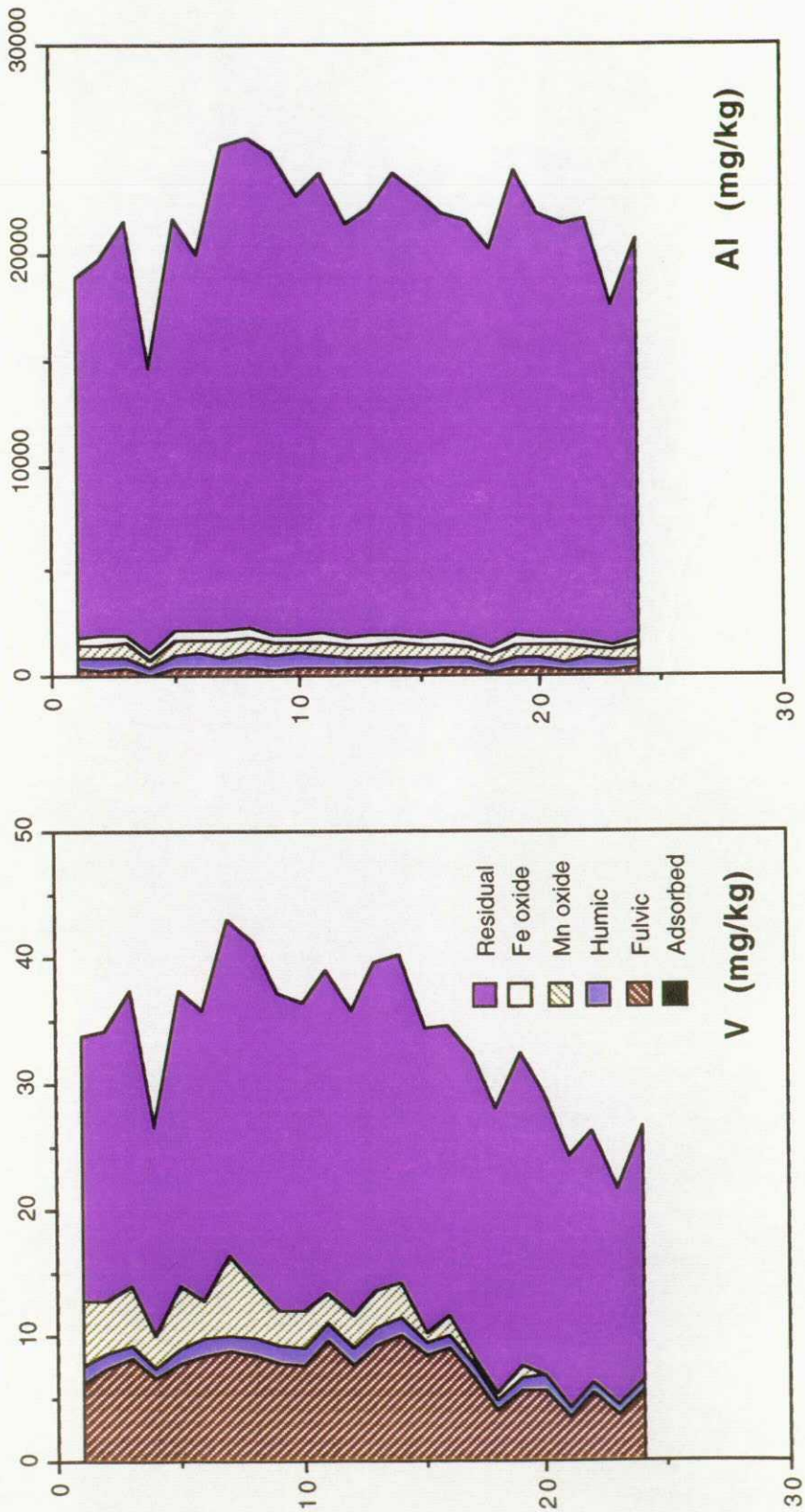

Figure 62: Partitioning of Mn and Ni between different geochemical fractions of Makupa Creek sediments (station MB23). Note - the downcore (vertical) axis is annotated with respect to sample number not depth. Samples 1-12 were removed at 2 cm resolution fom the uppermost 24 cm, below which 5 cm resolution applies.

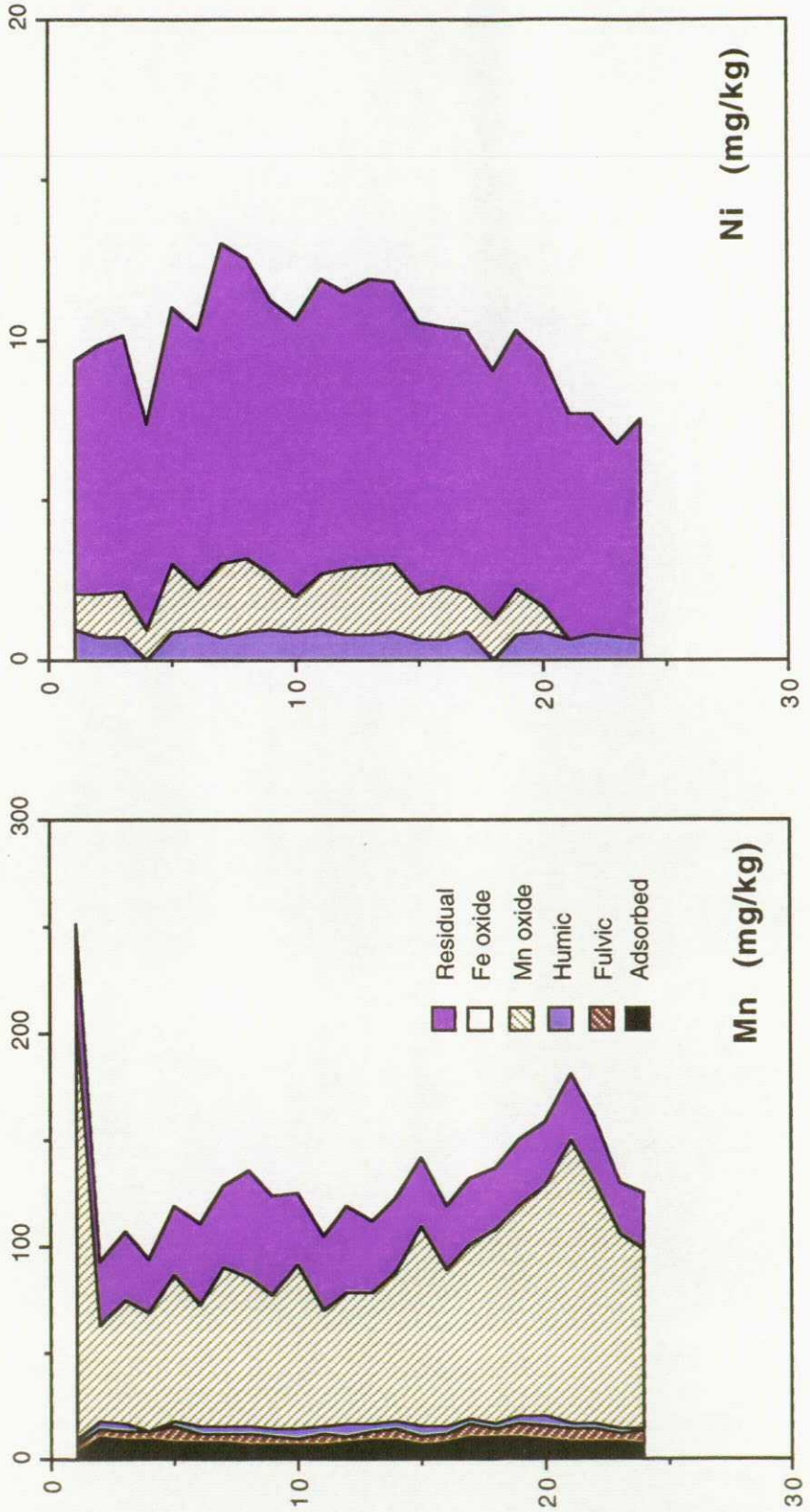

Figure 63: Partitioning of Co and Cr between different geochemical fractions of Makupa Creek sediments (station MB23). Note - the downcore (vertical) axis is annotated with respect to sample number not depth. Samples 1-12 were removed at 2 cm resolution fom the uppermost 24 cm, below which 5 cm resolution applies.

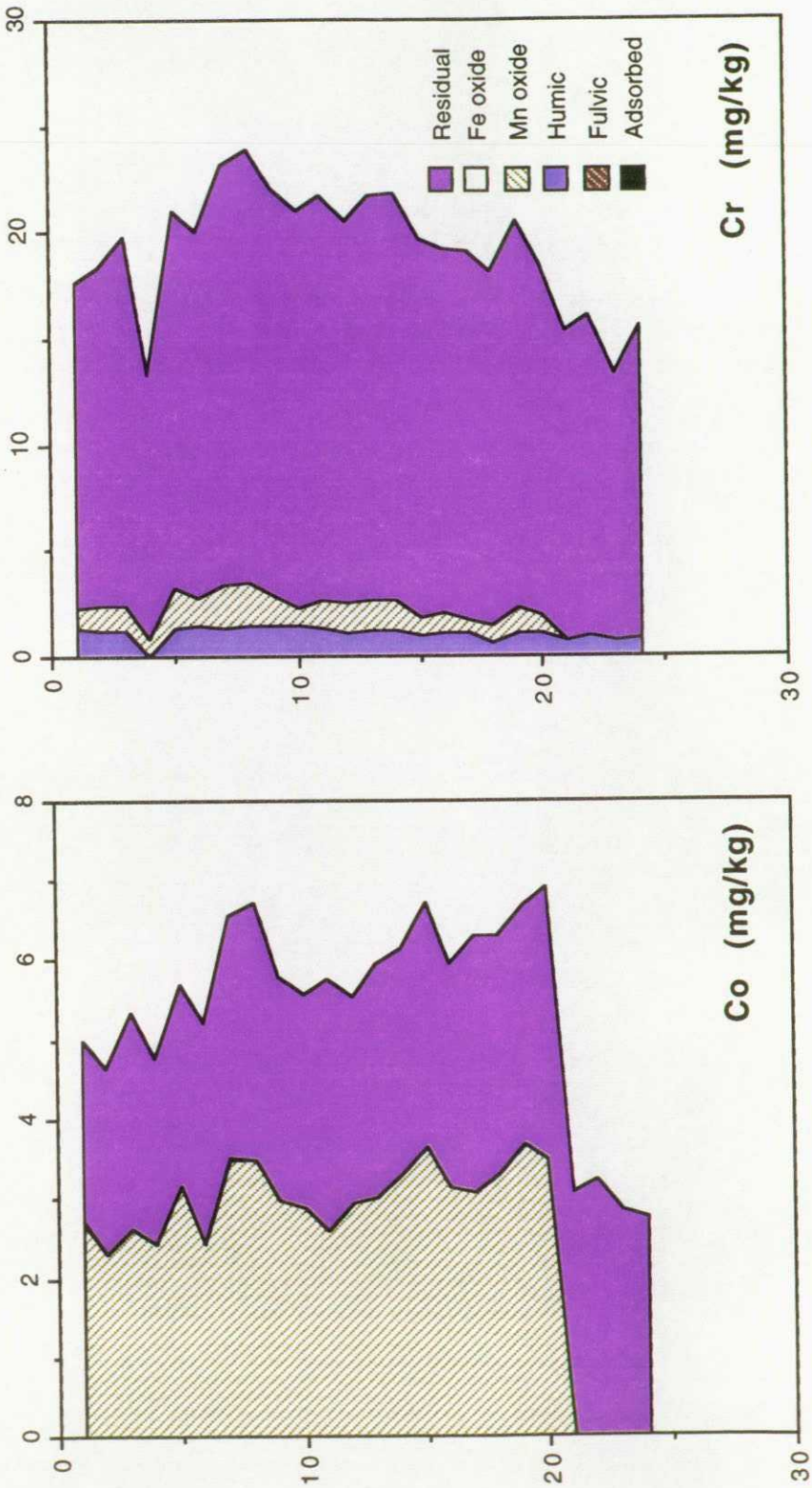

Figure 64: Partitioning of Zn and Pb between different geochemical fractions of Makupa Creek sediments (station MB23). Note - the downcore (vertical) axis is annotated with respect to sample number not depth. Samples 1-12 were removed at 2 cm resolution fom the uppermost 24 cm, below which 5 cm resolution applies.

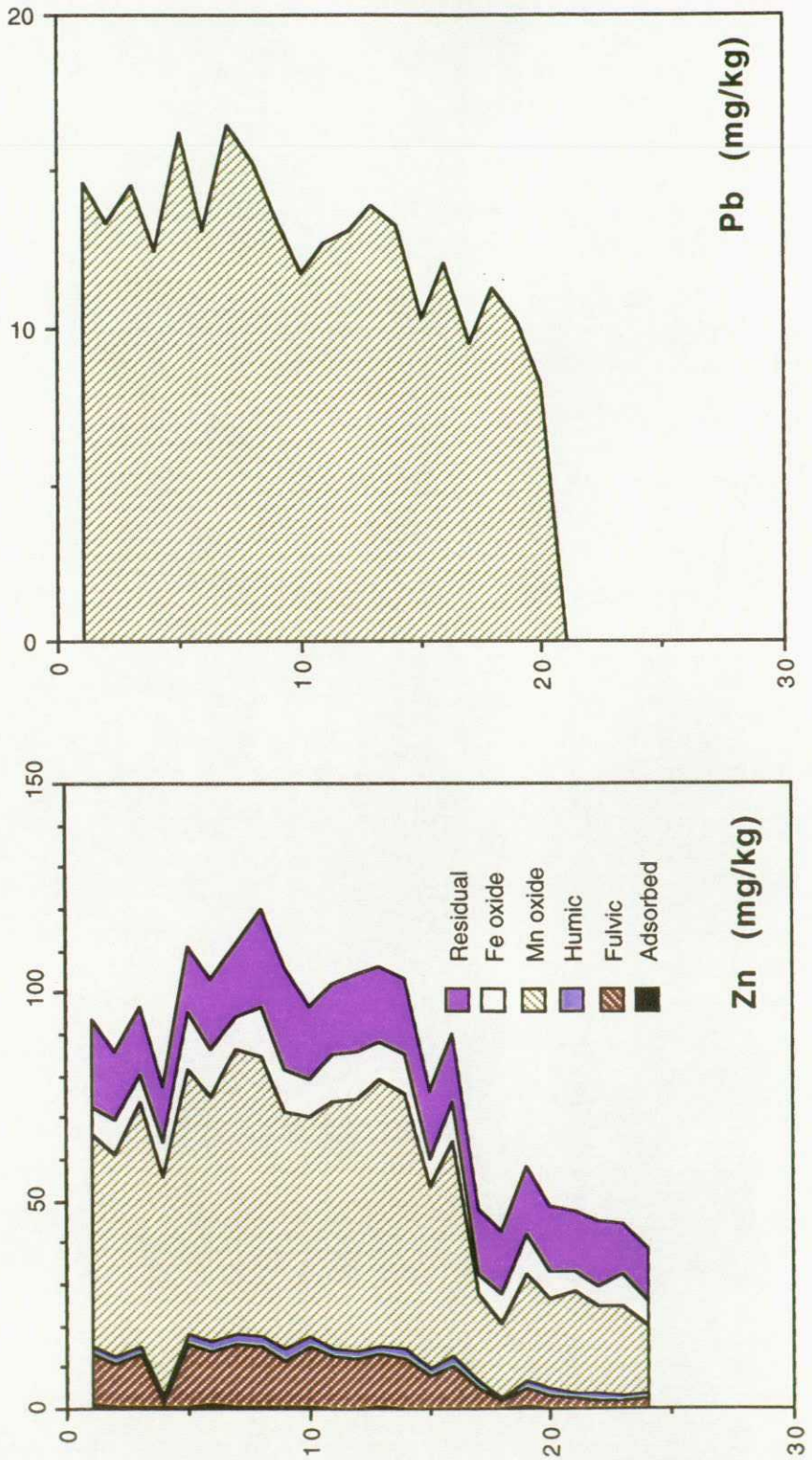

Hydroxylamine hydrochloride extractable phases, interpreted as comprising hydrous Mn-oxides, form the most important carrier of Mn (>50% total) throughout the sediment column, and the predominant host for Zn (c. 60% total), Pb (100% total), Cu (30% total) and Co (50% total) in the uppermost 20 analysed sub-samples (extending to 60 cm core depth). The marked anomaly in the total Mn profile (>200 mg/kg) at the sediment-water interface is largely attributable to hydrous oxides, suggesting active precipitation from the pore-waters above the sediment redoxcline. For Zn, Pb, Cu and Co, the declining presence of Mn-oxides with depth induces distinct downcore concentration gradients within the 'aggregate' profiles of these elements. A high concentration of Fe in this leach relative to the subsequent Tamms reagent stage of the sequence does, however, indicate that poorly- crystalline Fe-oxides or possibly acid-volatile Fe-monosulphides could also contribute. It is notable that the Mn-oxide fraction of the sub-surface sediment almost certainly exists in a state of dis-equilibrium given the anoxic conditions prevailing. These oxides were probably precipitated under aerobic conditions at the sediment-water interface, and are subject to progressive (kinetically constrained) dissolution during burial. This is fully consistent with the declining importance of NH_2.OH.HCl extractable phases noted with increasing depth, and could induce either aqueous mobilisation of liberated heavy metals, or immobilisation as sulphides (see section 3.3.5).

Crystalline Fe-oxides form a minor component of the sediment assemblage, accounting for c. 5% of total Fe, 6% of total Zn and 1.5% of total Mn throughout the sample core. The concentrations of all other elements were found to lie below the analytical detection limit in the Tamms reagent leachate.

Data acquired from the aqua-regia stage of the leaching sequence indicate that aluminosilicates, detrital sulphides and other resistate minerals dominate with respect to the total budgets of Fe (>60%), Al (>85%), V (>50%), Co (>40%), Cr (>85%) and Ni (>70%) at all stratigraphic levels. The low recoveries noted above for many of these elements probably reflects the persistence of additional resistate carriers following aqua-regia digestion, and their dominance may thus be even greater than suggested by the percentages quoted. Irrespective of this potential error, the partitioning trends concur with evidence presented in section 3.3.3.2, that the flux of heavy metals such as V, Cr and Ni is largely lithospheric. Their speciation is such that there is strictly limited potential for post-depositional mobilisation in response to pH/Eh fluctuations or other sedimentary adjustments, and bioavailability will be correspondingly low.

3.3.5: Interactions between sediment and interstitial pore-water.

Interstitial pore-waters were extracted from 9 contiguous sub-samples from the uppermost 18 cm of piston core MB23 within 2 hours of core extrusion using a centrifuge operated at 3000

rpm. All pore-waters were acidified with 1% v/v HNO_3, and were analysed for 9 trace elements (V, Cr, Mn, Co, Ni, Cu, Zn, As, Pb) by ICP-MS. Data for all elements are presented in Table 18.

Table 18: Concentration (µg/l) of selected trace elements in interstitial pore-waters from station MB23.

Depth	V	Cr	Mn	Co	Ni	Cu	Zn	As	Pb
0-2	37	<40	6950	4	20	15	250	<200	<10
3-4	<25	<40	1930	<3	20	10	200	<200	<10
5-6	70	<40	2380	<3	18	43	300	<200	<10
7-8	<25	<40	4300	<3	10	9	100	<200	<10
9-10	45	<40	1550	<3	9	14	200	<200	<10
11-12	<25	<40	1360	<3	19	12	200	<200	<10
13-14	35	290	645	6	200	19	100	<200	<10
15-16	34	<40	485	<3	7	10	<100	<200	<10
17-18	56	<40	521	<3	11	11	100	<200	<10

Ony five elements (Mn, Zn, Ni, Cu &V) were recorded in the pore-waters at adequate concentrations to facilitate any assessment of their dynamic behaviour. Of these, Mn displays a maximum concentration at the sediment-water interface (6.95 mg/l at 0-2 cm), with a pronounced decline (<700 µg/l) downward of 12 cm depth. There is some evidence of a corresponding reduction of Zn concentration in the pore-water (to c. 100 µg/l) at this stratigraphic level. Nickel and Cr show no clear stratigraphic trend, excepting a marked anomaly (200 µg/l and 290 µg/l respectively) at 13-14 cm depth.

Redox measurements of sediment cores (and associated pore-waters) from Makupa Creek have shown aerobic conditions to prevail at the sediment-water interface (Eh >200 mV, possibly extending no further than 1 cm depth) below which the sediment column is strongly anoxic (Eh -100 - -300 mV). In most sedimentary environments, such conditions induce the release of a range of metals into the sub-surface pore-waters through the syn-burial dissolution of hydrous oxides. The operation of this process in Makupa Creek sediments (and probably more widely within the lagoonal waters of Mombasa) is clearly indicated by data presented in section 3.3.4, most notably the downcore loss of NH_2.OH.HCl extractable metals with depth.

In sulphur-poor or sub-oxic systems (ie. those characterised by redox potentials above the SO_4 reduction threshold), trace metals liberated in this manner typically migrate in accordance with the prevailing diffusion gradient, and subsequently precipitate above the redoxcline (e.g. Balistrieri and Murray, 1986; Williams, 1992). Interfacial sediments enriched in toxic metals via this mechanism are environmentally sensitive, as a subsequent release of metals into the water column can be prompted by minor adjustments of pH and Eh, or by physical disturbance. In

sediments hosting active sulphate reduction, metal mobility in the pore-water environment is restricted by in-situ sulphide precipitation. Sulphidic environments can thus provide longer-term sinks for contaminant metals. The pore-water profiles identified in core MB23, coupled with the known abundance of S in the sediment (see section 3.3.6 below) suggest that the latter scenario is most applicable to Makupa Creek. Low dissolved concentrations of elements such as Cu and Ni below 14 cm depth can be considered indicative of the authigenesis of phases such as covellite and millerite. Anomalous concentrations of these elements in the pore-water within a defined zone at 13-14 cm reflect the upper limit of precipitation for these minerals.

3.3.6: Organic contaminants.

3.3.6.1: *GCMS scan*: Analyses of a broad spectrum of potential organic contaminants were undertaken by GCMS, GC-ECD and HPLC for selected Mombasa sediments, following the application of 5 ml of hexane solvent to 1.0 g air-dried sub-samples. A multi-spectral GCMS scan of material from Makupa Creek site MB23 (surficial 5 cm only) was performed to identify the most abundant organic compounds present, from which future analytical work could be rationalised. The hardware comprised a Hewlett Packard series II 5890 gas chromatograph, coupled with a Hewlett Packard 5972 mass-selective detector. Compound identification was carried out using the NIST/EPA/NIH Mass Spectral Database Revision C.00.00 (1992), using a Probability Based Matching (PBM) algorithm.

The generalised GCMS spectrum and corresponding concentration data for Makupa Creek sample MB23-5-6 are shown in Figure 65 and Table 19. A range of light hydrocarbons

Figure 65: GCMS spectrum for surficial sedimen t at Mombasa sampling site MB23. Labels on principal peaks correspond to compounds listed in Table 19.

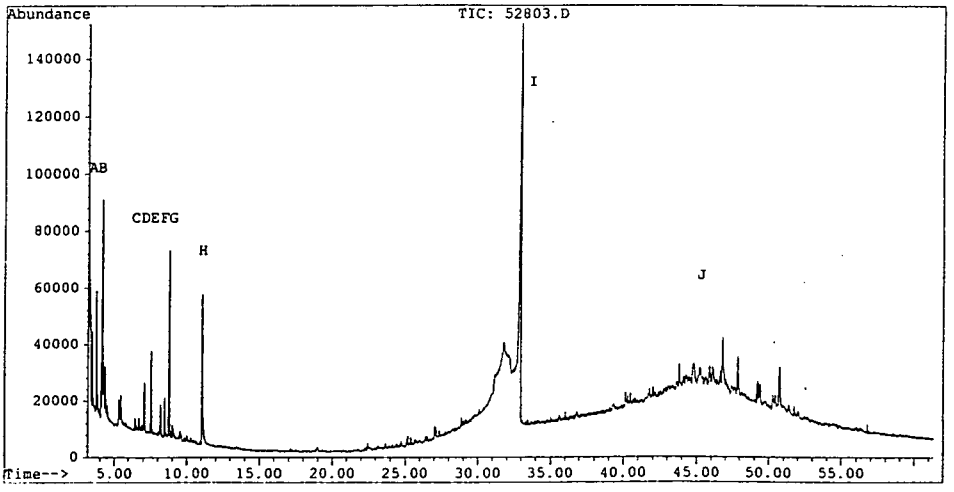

Table 19: GCMS-derived concentration data (mg/kg) for the most abundant compounds in the uppermost 5 cm of Makupa Creek core MB23.

Peak label	Retention time	Compound	CAS-No	Conc. mg/kg
A	3.71	Toluene	108-88-3	12
B	4.13	Hexanone	-	21
C	7.07	Unidentified	-	6.7
D	7.54	Unidentified	-	11
E	8.17	Unidentified	-	4.2
F	8.45	Unidentified	-	5.0
G	8.76	Alkane	-	24
H	11.05	C6 unsat. Keratone	-	31
I	32.9	S8 Sulphur	7704-34-9	1390
J	33.0-60.0	Complex hydrocarbons	-	3600

is represented including anomalous concentrations of toluene (12 mg/kg) and hexanone (21 mg/kg), both probably sourced to Kipevu and Kibarani. A total alkane concentration of 24 mg/kg indicates significant contamination by light crude oil. A wide range of heavier hydrocarbon residues (totalling 3600 mg/kg), almost certainly attributable to the oil-spills of 1988-91, is also recorded. The sulphurous nature of the sediment (noted in section 3.3.5) is confirmed by a major S_8 peak on the GCMS scan (1390 mg/kg).

3.3.6.2: *n-Alkanes.* Alkane compounds consist of a series of straight-chain hydrocarbons which form a major component of crude oil. Their abundance can thus provide a direct indication of petroleum contamination, provided that suitable account is taken of naturally prevailing mechanisms of n-alkane production. Higher plants, for example, produce alkanes in the range C_{27}-C_{33}, while the alkane signatures of light crudes typically encompass compounds from C_{10}-C_{30}, peaking at C_{22}.

Emission peak spectra for n-alkanes in the range C_{11}-C_{34}, acquired by GC analysis of hexane extracts for surficial sediments from sites MB1, MB5, MB20, MB23, MB27 and MB30, (including downcore data for site MB23) are shown in Figure 66. The spectra for individual samples typically fall into two classes. With respect to the surficial sediment suite (Fig. 66a), sites MB1, MB5 and MB20 are clearly distinguished by their high total n-alkane concentration of 15-25 mg/kg (semi-quantitative estimate inferred from peak heights), dominated by compounds in the range C_{13}-C_{17} (>50% total). An additonal peak at C_{20} is evident in the case of

Figure 66: n-Alkane spectra for (a) surficial sediments from five selected Mombasa coring stations and (b) four stratigraphic levels of Makupa Creek core MB23.

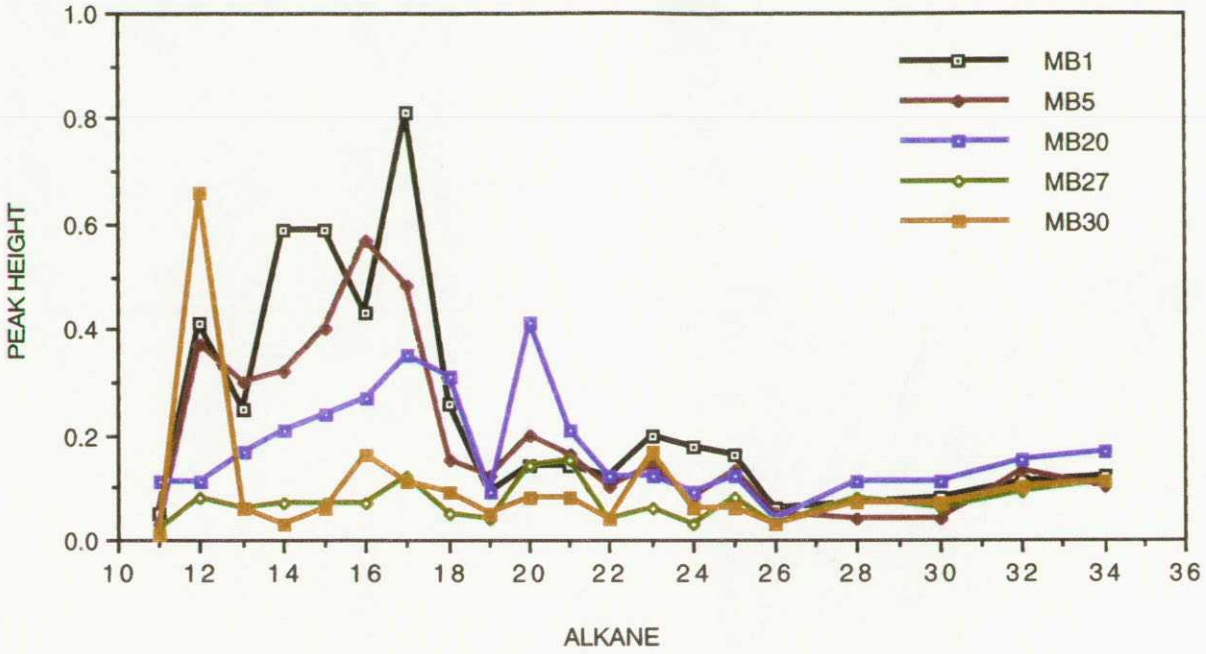

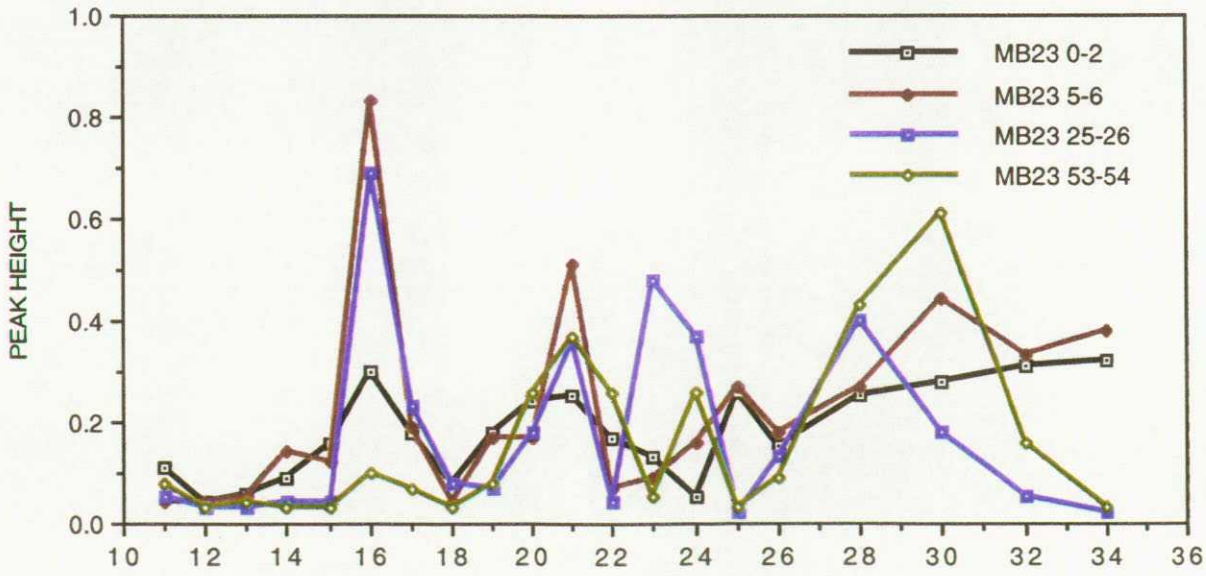

sample MB20. These sites (situated in upper Tudor Creek and western Port Kilindini) are isolated from any clear source of present or historical petroleum contamination and an alkane source cannot readily be identified. Sites MB27 and MB30, situated, in close proximity to the Kipevu oil terminal, are characterised by much lower total alkane loadings (<8 mg/kg). These assemblages show no distinctive fractionation (excepting a C_{12} anomaly in sample MB30) and have signatures uncharacteristic of petroleum derivatives.

Sediments from a range of stratigraphic levels in the Makupa Creek sediment pile (Fig. 66b) are distinguished from those from other sites by their enrichment in heavy n-alkanes (n 26-34). Downcore variations are clearly apparent. Surficial sediments (uppermost 6 cm) show greatest enrichment in the alkane range n-32-34, while more deeply buried sediments (below 25 cm) display dual peaks at n-16 and n 28-30. None of these signatures can be ascribed to petroleum derivatives, suggesting that crude oil spillages into Makupa Creek during the late 1980s have exerted no long-term sedimentary impact. The heavy alkane enrichment of recent sediments is, however, consistent with particulate or solute transport of organic waste products from the Kibarani landfill.

3.3.6.3: *Polycyclic aromatic hydrocarbons.* Polycyclic aromatic hydrocarbons (PAHs) are fused ring structures which form through pyrolysis of organic matter and oil maturation. The concentration of 16 PAH compounds in sediments from 6 Mombasa sampling sites, including two stratigraphic levels (0-2 cm, 45-46 cm) of Makupa Creek core MB23, was ascertained by HPLC analysis following hexane solvent extraction. Data for these compounds (Table 20) indicate that concentrations are universally low, with aggregate PAH levels of <1 mg/kg. At sites such as MB30 and MB23 where substantial oil spills have been recorded during the past decade, the occurrence of such low concentrations is surprising. Low molecular weight compounds such as naphthalene may have been ineffectively incorporated into the sediment as a consequence of their high solubility. With regard to the heavier members of the analysed suite, an unusually high rate of biodegradation is inferred.

3.3.6.4: *Organochlorines.* Data for organochlorines including pesticides such as DDT with with known persistence and bioaccumulation potential were acquired by GC analysis of samples from 6 Mombasa coring stations, following hexane solvent extraction. With the exception of a single anomaly for DDT (0.46 mg/kg) at Tudor Creek site MB5, all samples yielded values of <0.1 mg/kg for the following compounds:- DDE, DDT, dieldrin, alpha-endosulphan, beta-endosulphan, endrin, alpha HCH, beta HCH, hexachlorobenzene and trifluralin. The influx and retention of pesticides in the inshore waters of Mombasa can, therefore be concluded to be negligible.

Table 20: Polycyclic aromatic hydrocarbon concentrations in surficial sediments from six sampling sites. All data relate to samples extending from 0-5 cm depth, except station MB23 for which two stratigraphic levels were analysed.

Sample No.	MB1	MB5	MB20	MB27	MB30	MB23/96 0-2	MB23/96 45-46
Sample weight (g)	21.261	25.955	16.82	30.03	29.995	8.033	13.527
PAH (ug/g)							
1 Naphthalene	<0.03	<0.02	<0.03	<0.02	<0.02	<0.06	<0.04
2 Acenaphthylene	<0.03	<0.02	<0.03	<0.02	<0.02	<0.06	<0.04
3 Acenaphthene	<0.03	0.04	<0.03	<0.02	<0.02	<0.06	<0.04
4 Fluorene	<0.01	<0.01	<0.02	<0.01	<0.01	<0.03	<0.02
5 Phenanthrene	0.04	<0.01	<0.02	<0.01	0.03	0.03	<0.02
6 Anthracene	0.12	<0.01	0.12	0.05	<0.01	<0.03	0.10
7 Fluoranthene	0.02	<0.01	<0.02	<0.01	0.01	<0.03	<0.02
8 Pyrene	0.06	<0.01	<0.02	<0.01	0.03	<0.03	0.02
9 Chrysene	0.16	0.09	<0.02	<0.01	<0.01	<0.03	<0.02
10 Benz(a)anthracene	0.23	0.01	<0.02	<0.01	<0.01	0.07	<0.02
11 Benz(b)fluoranthene	0.12	<0.01	<0.02	<0.01	<0.01	0.03	0.02
12 Benz(k)fluoranthene	<0.01	<0.01	<0.02	0.03	<0.01	<0.03	<0.02
13 Benz(a)pyrene	0.04	0.03	<0.02	<0.01	<0.01	<0.03	<0.02
14 Dibenz(ah)anthracene	0.11	<0.02	0.12	<0.02	<0.02	<0.06	<0.04
15 Indeno(123-cd)pyrene	0.10	<0.02	<0.03	<0.02	<0.02	<0.06	<0.04
16 Benz(ghi)perylene	0.10	<0.02	<0.03	<0.02	<0.02	<0.06	<0.04

4: SUMMARY AND CONCLUSIONS.

4.1: Impact of urban and industrial development.

Empirical data depicting the historical (notably pre-industrial) abundance of heavy metals and hydrocarbons in sediments and inshore waters are unavailable for Mombasa. Any estimation of the impact of urban and industrial expansion on ambient contaminant concentrations in these media must therefore be regarded as tentative. Data acquired for 48 inshore-lagoonal and reef-front monitoring sites in this study, however, provide unequivocal evidence that the extent of perturbation to date remains relatively limited. Critical observations supporting this conclusion include:-

1: With the exception of Pb, median trace metal concentrations in the inshore waters of Mombasa are within the range reported globally for open oceanic waters, and are low relative to most urbanised estuarine settings (Fergusson, 1994). While Pb, Zn and Cd anomalies do occur, their locations are spatially unrelated to known contaminant sources. Elevated concentrations of

these elements in water along the reef-front between Nyali and Mtwapa remain, however, inadequately explained, and an anthropogenic influence cannot be specifically discounted.

2: With the exception of Pb, Zn and Cu, all major and trace elements (including Si, K, P, Al, Fe, Mn, Ti, Ca, Mg, Na, Sn, Ba, Pb, Mo, Zr, Sr, Co, Cr, Ni) analysed in surficial sediments around Mombasa display distributional patterns contolled by lithological or sedimentological factors, with no clear anthropogenic overprint. With regard to Pb, Zn and Cu, sediment anomalies are spatially confined, usually to the immediate vicinity of documented point-sources (including Kibarani disposal site, Kipevu oil terminal, Likoni ferry crossing and domestic sewage outfalls on the eastern side of Mombasa Island). Substantial dispersion trains have not been identified at any of these localities.

3: The concentrations of organochlorines, PAHs and alkanes recorded in surficial sediments at all Mombasa sampling sites are extremely low (often falling below analytical detection limits). The n-alkane spectra for both surficial and sub-surface sediments show no clear evidence of the presence of petroleum derivatives.

4: After normalisation against TiO_2 or Al_2O_3 (thus largely removing downcore lithological influences), heavy metal profiles in sediment cores from most Mombasa sampling sites (including potentially perturbed localities such as Makupa Creek) show little clear evidence of increased contaminant deposition in recent decades. Pore-water and metal partitioning studies of selected cores suggest that post-depositional mobilisation of trace metals and consequent diagenetic alteration of the profiles has been limited. The credibility of these sediment-based metal deposition chronologies does, however, require further validation. The extent to which metal concentration gradients have been destroyed by bioturbation requires particular scrutiny. It also remains possible that increasing metal fluxes have occurred during recent decades, but have been disguised by a simultaneous increase in mass sedimentation. Detailed Pb^{210} chronologies provide the only reliable basis for resolving such uncertainties.

4.2: Mechanisms of contaminant dispersal and degradation.

The limited degeneration of inshore/nearshore sediment and water quality attributable to urban and industrial activity in Mombasa is striking, given the magnitude of annual discharges which indisputably prevail. In addition to the suspended solid influx derived from sewage (>3500 t/yr), stormwater runoff (>9000 t/yr) and routine industrial activities (>20000 t/yr; Munga et al., 1994), the Mombasa creeks have been subject to at least two significant oil-spills in the past decade, the geochemical effects of which are now difficult to detect. Such trends indicate that the system has physical, hydrodynamic and biogeochemical attributes which promote contaminant dilution, dispersal and/or degradation, an understanding of which may assist in

predicting the dynamics and fates of contaminants in inshore and nearshore marine settings elsewhere. Three regulatory mechanisms have been identified as particularly critical with respect to the inhibition of contaminant accumulation:-

1: The hydrodynamic regime is fundamental to the sediment and water quality of the Mombasa creeks. Water residence-times range from approximately two tidal-cycles (ie. 24 hrs) in the central channels of Port Kilindini and Mombasa Harbour, to >2 weeks in the mangroves of upper Port Reitz. Significantly, it is the former areas (plus Makupa Creek) into which urban and industrial discharges are predominantly introduced. Unsorbed metals, dissolved organics and low mass/density particulates (with sedimentation times exceeding c. 24 hr) are thus effectively removed from the system, maintaining a low ambient water concentration and minimal sedimentary accumulation. To maintain water and sediment quality in the future, major contaminant discharges into the landward sectors of Port Reitz, Tudor Creek and other areas of impeded water-circulation should be prohibited.

2: Acute salinity gradients or fronts, such as characterise the zone of saline-freshwater mixing in most estuarine settings were not encountered during the September 1995 and January 1996 LOCS surveys of Mombasa due to the negligible fluvial discharges entering Port Reitz and Tudor Creek. These salinity fronts are instrumental in inducing the flocculation of Fe (plus co-precipitated trace metals) and dissolved humic complexes. Their absence within the main body of any Mombasa creek or lagoon may thus preclude a commonly important mechanism of contaminant sedimentation and environmental retention.

3: Rapid and efficient biodegradation of petroluem hydrocarbons is clearly inferred from low concentration of n-alkanes and PAHs recorded in sediment cores from localities known to have been impacted by oil spills during the past decade. Such rates can be explained only as a function of a high ambient temperature, coupled with a conducive microbial population. Detailed research into the precise controls on biodegradation of petroleum hydrocarbons in the Mombasa inshore environment warrants a high future priority.

It requires emphasis that all conclusions drawn regarding the limited impact of anthropogenic discharges on sediment and water quality around Mombasa relate to a specific and incomprehensive range of contaminants (metals, organochlorines, PAHs and alkanes). The occurrence of pronounced cultural impacts on water and sediment quality with respect to coliform bacteria (as documented by Norconsult, 1975) are not in dispute. From visual observations made during sampling, eutrophication of both the inshore and reef-lagoon environment, and increasing sediment anoxia in areas prone to high organic loadings (e.g. Makupa Creek and Port Reitz in the vicinity of the sewage outfall near Kipevu) may also constitute hazards warranting immediate assessment and mitigation.

4.3: Mombasa contamination in an international context.

Although the impact of recent industrial expansion on the geochemical signatures of nearshore sediments around Mombasa is apparently limited, comparative assessments of metal data against values reported for over 60 estuarine and marine settings in West Africa, the Indian sub-continent, Europe, the USA and central America (Fergusson, 1994) suggest that ambient concentrations exceed those typically associated with pristine sites. Using Pb and Cd for exemplification, mean and maximum values reported in this study (34 & 427 mg/kg Pb, 1.5 & 3.0 mg/kg Cd) are analogous to those recorded in the urbanised/industrialised environments of New York harbour (25-370 mg/kg Pb, 0.5-4.0 mg/kg Cd, Carmody et al., 1973), San Francisco Bay (9-174 mg/kg Pb, 0.5-3.3 mg/kg Cd, Bradford and Luoma, 1980), Puget Sound (max Pb 114 mg/kg, Skei and Paus, 1979) and Poole Harbour (50-190 mg/kg Pb, Boyden, 1975). The high natural background for heavy metals in the inshore lagoonal sediments of Mombasa can be directly ascribed to the presence of organic-rich Jurassic shales, inherently enriched with elements such as Pb, Zn, Cu, Cd, Co, Cr, Ni and V (Krauskopf, 1979), within much of the catchment hinterland. This metal-rich detrital influx may, in part, account for the lack of a clear sedimentary pollution chronology in the sediment, providing a matrix within which any subtle variations of anthropogenic input are indiscernible.

Despite the high background metal concentrations described, the total loading of potentially toxic elements remains substantially lower than reported for many perturbed coastal settings, for which Fergusson (1994) has documented concentrations of Pb ranging from 1000 - 10,000 mg/kg (e.g. Rio Tinto estuary and Sorfjord), with Cd frequently exceeding 100 mg/kg (e.g. Derwent estuary, Corpus Christi). Formal sediment quality criteria remain to be finalised by most national and international regulatory authorities. However, the mean Cu, Zn and Cd concentrations recorded in Mombasa sediments fall within the 'target' (Cu 25 mg/kg, Zn 180 mg/kg, Cd 0.8 mg/kg)) or 'standard' (Cu 70 mg/kg, Zn 750 mg/kg, Cd 4 mg/kg) guidelines proposed in a Draft Criteria Document at an International Sediment Quality Forum in 1992 (Van Veen and Strotelder, 1988). 'Limit' values proposed in this document are substantially higher (Cu, 400 mg/kg, Zn 2500 mg/kg, Cd 30 mg/kg) and are exceeded at only one Mombasa sampling site (Cu only).

Previous pollution studies of the inshore waters of Mombasa (e.g. Oteko, 1987) have utilised Gazi, a smaller creek on the Kenya coast approximately 50 km to the south, as a non-industrialised analogue of the Mombasa creeks and hence a valid control-site for assessing the geochemical impact of urbanisation. Analyses of surficial sediment collected during a visit to Gazi by BGS and KMFRI personnel in January 1996 have confirmed that concentrations of Pb, Zn, Cu, Cd, Ni and Cr are up to an order of magnitude lower than reported for the Port Tudor,

Kilindini and Port Reitz systems of Mombasa. The value of Gazi as a pre-industrial analogue of the Mombasa creeks is, however, extremely doubtful. While the geological setting is broadly comparable, the surficial lithofacies encountered at Gazi comprised coarse quartzose sands in the mid-reaches of the creek, grading to carbonate sand in the seaward reaches. A scour channel extends across almost the entire width of the creek in many localities, and the deposition of fine clastic sequences, such as predominate around Mombasa, is effectively precluded.

4.4: A geochemical baseline for the Mombasa coast.

In establishing the limited degeneration of water, SPM and sediment quality so far induced by anthropogenic activities around Mombasa, the datasets compiled in this study provide a valuable baseline against which the effects of future urban and industrial expansion can be evaluated. The need for such baselines in environmental management is increasingly recognised internationally, forming the impetus for global data collation exercises such as the IGCP Global Geochemical Mapping Programme (IGCP 360) and the IOC/UNEP Global Inventory for Pollution in the Marine Environment (GIPME). An integrated marine environmental monitoring capacity in East Africa (incorporating Kenya, Mozambique, Comoros, Reunion, Magagascar, Mauritius, Seychelles, Somalia and Tanzania) is currently being established under project EAF/6 of the UNEP Action Plan for the Protection, Management and Development of the Marine and Coastal Environment of the East African Region (coordinated by UNEP OCA/PAC, Nairobi). At present, however, the Mombasa coast of Kenya is probably unique with respect to the volume of geochemical baseline data available.

In Mombasa, as in all LOCS case-study locations, the establishment of an appropriate system for integrating geochemical, sedimentological and oceanographic data with a wider range of environmental and socio-economic datasets is vital to maximise the utility of LOCS outputs in future coastal-zone management (CZM). The generation of such a system for Mombasa has been greatly assisted by the development under UNEP OCA/PAC project EAF/6 of a GIS for the Kenya coast, holding information on over 80 human and environmental variables including land use, industrial, recreational and fisheries activities. Integration of the LOCS and EAF/6 databases into a single GIS, accessed and interrogated using ARCVIEW, has been achieved by BGS, in close liaison with UNEP and KMFRI (for details see Williams et al., 1996). The integrated system provides a powerful decision-support tool for CZM, with a particular capacity for highlighting conflicts of nearshore marine resource use (e.g locations in which contaminant discharges impact on marine recreation, commercial fishing or aquaculture activities).

It is anticipated that the contaminant database and GIS now established for Mombasa and administered by KMFRI will be extended periodically through the incorporation of new contaminant survey data. If utilised effectively, the Mombasa GIS may serve as a valuable

model for marine environmental monitoring and data management throughout (and beyond) the East African region.

5: ACKNOWLEDGEMENTS

All field surveys undertaken by BGS in Mombasa were supported both logistically and scientifically by staff of the Kenya Marine and Fisheries Research Institute. Particular thanks are due to Mr K K Kairu, Kenyan coordinator of the LOCS programme, and Mr A C Yobe, principal scientific counterpart. Data from the EAF/6 database was provided for BGS use by courtesy of UNEP OCA/PAC and KMFRI. Special thanks are extended to Mr D Van Speybroek for kindly assisting in the digital transfer of this information, and for the provision of useful advice and guidance to BGS staff working in Kenya. Data processing and statistical analysis was assisted by Dr Richard Herd. Funding for all work carried out under the LOCS project was provided by the UK ODA (Environment Division) under R&D contract R6191.

6: REFERENCES:

Badarudeen, A., Damodaran, K.T., Sajan, K. and Padmalal, D. 1996: Texture and geochemistry of the sediments of a tropical mangrovee ecosystem, southwest coast of India. Environmental Geology 27: 164-169.

Balistrieri, L. S., and J. W. Murray, 1986: The surface chemistry of sediments from the Panama Basin: The influence of Mn oxides on metal adsorption: Geochimica et Cosmochimica. Acta 50, 2235-2243.

Bradford, W.L. and Luoma, S.N. 1980: Some perspectives on heavy metal concentrations in shellfish and sediment in San Francisco Bay, California. In. Baker, R.A. Ed. Contaminants and Sediments: Ann Arbor Science. 501-532.

Breward, N and Peachey, D. 1983: The development of a rapid scheme for the elucidation of the chemical speciation of elements in sediments. Science of the Total Environment, 29, 155-162.

Boyden, C.R: 1975. Distribution of some trace metals in Poole Harbour, Dorset. Marine Pollution Bulletin. 6, 180-187.

Carmody, D.J., Pearce, J.B. and Yasso, W.E. 1973: Trace metals in sediments if New York Bight. Marine Pollution Bulletin. 4, 132-135.

Carruthers, R M. 1985. Report on geophysical studies relating to the coastal aquifer of the Mombasa district, Kenya. British Geological Survey Regional Geophysics Research Group Report 85/4.

Caswell, P V. 1953. Geology of the Mombasa-Kwale area. Report 24, Geological Survey of Kenya.

Caswell, P V. 1956. Geology of the Kilifi-Mazeras area. Report 34, Geological Survey of Kenya.

Fergusson, J.E. 1994: The heavy elements: chemistry, environmental impact and health effects. Pergamon Press, 614 p.

Krauskopf 1979: Handbook of geochemistry. McGraw Hill, 510 p.

Landner, L. 1986: Speciation of metals in water, sediment and soil systems. Speinger Verlag, 189 p.

Munga, Yobi, Owili and Mwaguni 1994. Assessment of land-based sources of marine pollution along the Kenyan coast. Draft report prepared for FAO, KMFRI, Mombasa.

Norconsult. 1975: Mombasa water pollution and waste disposal study. Republic of Kenya Ministry of Local Government.

Oteko, D. 1987: Analysis of some major and trace metals in the sediments of Gazi, Makupa and Tudor creeks of the Kenya coast. A comparative investigation of the anthropogenic input levels. Unpublished MSc thesis, Free University of Brussels.

Rais-Assa, R. 1988. Stratigraphy and geodynamics of the Mombasa Basin (Kenya) in relation to the genesis of the proto-Indian Ocean. Geological Magazine, Vol. 125, 141-147.

J G Rees, T M Williams, M Nguli, K K Kairu and A C Yobe: 1996. Contaminant transport and storage in the estuarine creek systems of Mombasa, Kenya. British Geological Survey, Overseas Geology Series Technical Report WC/96/42.

Skei, J. and Paus, P.E. 1979: Surface metal enrichment and partitioning in a dated sediment core from a Norwegian fjord. Geochemica et Cosmochmica Acta. 43, 239-246.

Van Veen, R.J. and Strotelder, P.B.M. 1988: Research on contaminated sediments in the Netherlands. In Wolf, K., Van de Brink, W.J. and Colon, F.J (Eds). Contaminated soil. 1263-1275. Academic. Publ.

Williams, T.M. 1992: Diagenetic metal profiles in the recent sediments of a Scottish freshwater loch. Environmental Geology and Water Sciences, 20, 117-124.

Williams, T M, Mackenzie, A C, and Rees, J G. 1996. A Geographic Information System (GIS) for envionmental management of the Mombasa coast, Kenya. British Geological Survey Technical Report WC/97/41.